



Knot homologies and generalized quiver partition functions

Tobias Ekholm^{1,2} · Piotr Kucharski^{3,4,5}  · Pietro Longhi⁶

Received: 13 January 2022 / Revised: 16 August 2023 / Accepted: 9 October 2023
© The Author(s) 2023

Abstract

We introduce generalized quiver partition functions of a knot K and conjecture a relation to generating functions of symmetrically colored HOMFLY-PT polynomials and corresponding HOMFLY-PT homology Poincaré polynomials. We interpret quiver nodes as certain basic holomorphic disks in the resolved conifold, with boundary on the knot conormal L_K , a positive multiple of a unique closed geodesic, and with their (infinitesimal) boundary linking density measured by the adjacency matrix of the generalized quiver. The basic holomorphic disks that are quiver nodes appear in a certain $U(1)$ -symmetric configuration. We propose an extension of the quiver partition function to arbitrary, not $U(1)$ -symmetric, configurations as a function with values in chain complexes. The chain complex differential is trivial at the $U(1)$ -symmetric configuration, under deformations the complex changes, but its homology remains invariant. We also study recursion relations for the partition functions connected to knot homologies. We show that, after a suitable change of variables, any (generalized) quiver partition function satisfies the recursion relation of a single toric brane in \mathbb{C}^3 .

✉ Piotr Kucharski
piotr.kucharski@mimuw.edu.pl

Tobias Ekholm
tobias.ekholm@math.uu.se

Pietro Longhi
longhip@phys.ethz.ch

¹ Department of Mathematics, Uppsala University, Box 480, 751 06 Uppsala, Sweden

² Institut Mittag-Leffler, Aurav. 17, 182 60 Djursholm, Sweden

³ Walter Burke Institute for Theoretical Physics, California Institute of Technology, Pasadena, CA 91125, USA

⁴ Faculty of Physics, University of Warsaw, ul. Pasteura 5, 02-093 Warsaw, Poland

⁵ Institute of Mathematics, University of Warsaw, ul. Banacha 2, 02-097 Warsaw, Poland

⁶ Institute for Theoretical Physics, ETH Zurich, 8093 Zurich, Switzerland

Keywords Quiver · Holomorphic disks · Knot · Conormal Lagrangian · HOMFLY homology

Mathematics Subject Classification 57K18 · 57K14 · 53D42

Contents

1	Introduction and summary
2	Background
2.1	Knot polynomials and homologies
2.2	Observed relations between knots and quivers
2.3	Physics and geometry of knots and quivers
2.4	Omega-background and refined indices
3	Generalized quivers and HOMFLY-PT homology
3.1	Geometry and combinatorics of multiply-wrapped basic disks
3.2	Holomorphic curves viewed as BPS generators
3.3	M2-branes wrapping holomorphic curves
3.4	R-charge, homological degree, and self-linking
3.5	HOMFLY-PT homology and geometric deformations
3.6	Unlinking and multiple disks
4	Recursion relations for generalized quiver partition functions
4.1	Non-commutative variables
4.2	A-polynomials for generalized partition function
4.3	The toric brane property
5	Homology structure encoded in the quiver
5.1	Redundant pairs and \mathfrak{sl}_1 pairs
5.2	Knot homologies in toric brane variables: a new grading
5.3	Traces of a spectral sequence of symmetrically colored knot homologies
6	Examples with multiply-wrapped basic disks
6.1	The line in real projective 3-space
6.2	The knot 9_{42}
A	Inductive derivation of the q -multinomial identity
B	A stronger conjecture on refinement
B.1	The knot 9_{42}
B.2	The knot 10_{132}
C	Comparing $T[L_K]$ and $T[Q]$ in view of knot homology
	References

1 Introduction and summary

Polynomial knot invariants such as the Jones and HOMFLY-PT polynomials, originally defined combinatorially, have been interpreted and further explained from physical and geometric points of view. In physics the invariants appear through quantum field theory (Chern–Simons theory) [1], topological strings and M-theory in combination with the conifold transition [2], and in geometry through Gromov–Witten counts of bare curves [3, 4]. Many polynomial knot invariants admit categorifications, where the polynomial is expressed as the (graded) Euler characteristic of a chain complex associated to the knot, with homology which is a knot invariant. The first example is

Khovanov's categorification of the Jones polynomial [5]. Connections between categorified knot invariants and BPS states in the physical theories underlying the original knot polynomials have been proposed, see, e.g., [6, 7].

Following [8, 9], we study connections between knot invariants and quivers as in [10, 11], where the motivic generating function of a quiver gives the generating series for HOMFLY-PT polynomials from the perspective of BPS counts. Here quiver nodes are basic BPS states, their interactions are governed by the quiver arrows, and the interacting nodes generate the whole spectrum. Geometrically, basic BPS states correspond to M2-branes wrapping basic holomorphic disks in the resolved conifold with boundary on an M5-brane wrapping the knot conormal, and the quiver adjacency matrix encodes boundary linking data.

The main theme of this paper is a conjectural extension of the correspondence between knot invariants and quivers to the categorified level. The extension involves new types of quiver nodes that geometrically correspond to certain 'stretched' (non-embedded near the boundary) holomorphic disks. More precisely, we define a *generalized quiver* Q as an finite oriented graph in which each vertex i has a positive integral *multiplicity* μ_i and each arrow $i \rightarrow j$ carries a sign.¹ If $N_{ij} \in \mathbb{Z}$ denotes the number of signed arrows from i to j , then the *adjacency matrix* of Q is given by

$$C_{ij} = \begin{cases} N_{ij} & \text{if } \mu_i \neq \mu_j, \\ \frac{1}{\mu} \cdot N_{ij} & \text{if } \mu_i = \mu_j = \mu. \end{cases} \quad (1.1)$$

In this paper we focus on symmetric generalized quivers (for which $C_{ij} = C_{ji}$), associate variables x_i to the generalized quiver nodes $i = 1, 2, \dots, m$, and their partition function as follows.

Definition 1.1 The partition function of symmetric generalized quiver Q is

$$P_Q(\mathbf{x}; q) = \sum_{\mathbf{d}} (-1)^{\sum_i C_{ii} \mu_i d_i} q^{\sum_{i,j} C_{ij} (\mu_i d_i)(\mu_j d_j)} \prod_{i=1}^m \frac{x_i^{d_i}}{(q^{2\mu_i}; q^{2\mu_i})_{d_i}}, \quad (1.2)$$

where \mathbf{d} ranges over all dimension vectors in $\mathbb{N}Q_0$ (i.e., the lattice with basis given by the set of vertices of Q).

Definition 1.1 is the starting point for our conjecture on HOMFLY-PT homology and a refinement of the partition function (1.2) will be discussed in the main text.

Consider a knot K and its conormal L_K in the resolved conifold. We conjecture that it (after degeneration onto the unknot conormal) admits a $U(1)$ -symmetry and that there is a finite number of basic disks that we label $1, \dots, m$. We view these disks as generalized quiver nodes, where the multiplicity of a node is the multiplicity of the boundary of the corresponding basic disk. Attaching data for the normal bundles of the basic disks give a quiver adjacency matrix C_{ij} . Here, for $i \neq j$, C_{ij} is the infinitesimal mutual linking (a relative framing). In particular C_{ij} is integral if

¹ We consider signed oriented edges, where negative signature may arise from a choice of large negative framing.

$\mu_i \neq \mu_j$. For $\mu_i = \mu_j = \mu$, C_{ij} is $\frac{1}{\mu} \cdot N_{ij}$, where N_{ij} is the self- or mutual-linking, depending on whether $i = j$ or $i \neq j$. This defines a symmetric generalized quiver Q associated to K . Let $\log x$ be the positive generator of $H_1(L_K)$ and let $\log a^2$ denote homology class of \mathbb{CP}^1 in the resolved conifold. Let the homology class of the generalized disk i be $\mu_i \log x + a_i \log a$ and its invariant self-linking (or 4-chain intersection far from the boundary) be q_i .

Conjecture 1.2 *Let Q be a symmetric generalized quiver. If we substitute*

$$x_i = x^{\mu_i} q^{q_i - C_{ii}\mu_i} a^{a_i} \quad \text{for } i = 1, 2, \dots, m$$

then the generalized quiver partition function $P_Q(\mathbf{x}; q)$ equals the generating function of the Gromov–Witten invariants counting generalized holomorphic curves, or equivalently the generating function of the symmetrically colored HOMFLY-PT polynomials of K .

Remark 1.3 The change of framing operation, counterpart to changing variables $x \rightarrow x(-y)^f$ with $f \in \mathbb{Z}$ in the augmentation curve, is given by the usual shift of the linking matrix $C_{ij} \rightarrow C_{ij} + f$, both for diagonal and off-diagonal elements, in the partition function.

Remark 1.4 Equation (1.2) completes and corrects [8, Conjecture 1.1] as follows. There, a μ times around generator in framing zero was assumed to be an embedded disk that contributes $(x^\mu; q^2)_\infty$ to the partition function. Its contribution to the refined partition function was not specified as can be seen already on level d . One would have to explain how the contribution $\frac{x^\mu}{(q^2; q^2)_1}$ implied by the proposal of [8] would be promoted to a linear combination of $\frac{x^\mu}{(q^2; q^2)_\mu}$ with coefficients in $\mathbb{N}[q, t]$. In our new framework, the basic object is different: it is an embedded disk outside, completed by a multiply covered disk inside. Its level- μd contribution to the partition function is now $\frac{x^{\mu d}}{(q^{2\mu}; q^{2\mu})_d}$. On the refined level denominators in (1.2) must once again be enhanced to $(q^2; q^2)_{\mu d}$. Once again this involves taking linear combinations of different basic disks with coefficients in $\mathbb{N}[q, t]$. We do not determine those combinations completely, but discuss various possibilities and related evidence in the main text and the appendix.

Equation (1.2) differs from the proposed knots-quivers correspondence of [10, 11] in several ways. Because of their denominators, they are not quiver partition functions, nor are they characters of a cohomological Hall algebra [12, 13]. Nevertheless, both expressions reflect the idea that the whole spectrum of BPS states is generated by a finite set of basic objects, interacting in a certain way. The basic objects may be viewed as nodes of a generalized quiver, whose adjacency matrix encodes their interactions. The main difference with the knots-quivers correspondence of [10, 11] is that we allow for nodes with $\mu > 1$ and with new denominators.

We list some arguments that show that some properties of our proposed partition function are necessary:

1. In any quiver-like description, nodes with $\mu > 1$ are necessary, see [8] and the examples in Sect. 6.

2. A basic disk wrapping μ -times around L_K contributes to the multi-cover formula with q^2 replaced by $q^{2\mu}$. See Sect. 3.1 for motivation and Sect. 6 for examples. This leads to replacing denominators $(q^2; q^2)_{d_i}$ in (2.6) by $(q^{2\mu_i}, q^{2\mu_i})_{d_i}$ in (1.2).
3. Poincaré polynomials of knot homologies seem to agree with the refinement of vortex Hilbert spaces, as discussed in Sect. 3.2 where denominators of $x^{\mu d}$ correspond to contributions from standard vortices, $(q^2, q^2)_{\mu d}$. The change of variables then requires multiplication and division by the finite polynomial: $(q^2, q^2)_{\mu d} / (q^{2\mu_i}, q^{2\mu_i})_{d_i}$.

In connection with 2, we also consider refinement. The correction introduced in the numerator by $(q^2, q^2)_{\mu d} / (q^{2\mu_i}, q^{2\mu_i})_{d_i}$ should arise from a similar correction by polynomials in (q, t) with positive coefficients, where negative signs in the original expression come from (odd) powers of t . Algebraically, there are several possibilities, and we explore some of them for the specific case $\mu = 2$. Our proposal is based on the passage from Bott to Morse localization in (3.34). We check it in concrete calculations of colored superpolynomials for knots 9_{42} and 10_{132} in Sect. 6 and “Appendix B”.

We also make predictions for the general structure of HOMFLY-PT homology colored by symmetric representations with r boxes. We view the generators of colored HOMFLY-PT homology in the r -th symmetric representation as equivariant vortices of vorticity r in the theory $T[L_K]$, see Sect. 3. The connection between quiver nodes and equivariant vortices is somewhat involved: a basic curve on a knot conormal with boundary that wraps r times around the circle in the conormal gives 2^{r-1} generators in the r -th symmetrically colored homology. At level $r = 1$ every generator corresponds to a node of the generalized quiver. The quiver partition function describes a tower of contributions from $r = 1$ generators to all higher levels with $r > 1$, which is completely determined by homology data of these nodes and their mutual linking. Knowing the structure of these contributions from level 1 to level 2 allows to separate them from the genuinely new generators that appear on level 2. We continue in this way inductively: taking out contributions from all nodes of levels $< r$ allows us to identify the genuinely new generators on level r . We verify the claim about homology contributions of level r generators against several proposals for categorification of knot invariants for the knots 9_{42} and 10_{132} for $r = 2$, see Sect. 6 and “Appendix B”. Further structures appear when we deform away from the $U(1)$ -symmetric configuration. Here, the pure level r generators generate a chain complex of ‘Bott-equivariant’ vortices, see (3.35), which are transformed by chain homotopy under deformation. The homology of the level r generators is non-vanishing only for finitely many r and, together with linking data, it recovers the usual $U(1)$ -symmetric HOMFLY-PT homology.

In Sect. 3, we also consider deformations that break the $U(1)$ symmetric configuration and propose an extension of the generalized quiver partition function. We first show that the moduli spaces of stretched basic disks can be carried along generic 1-parameter families of complex structures that remain stretched near the Lagrangian, so that these moduli spaces together with linking information suffices to compute the refined partition function. We also perform a bifurcation analysis of such deformations. We generalize the quiver partition function to a function with values in chain complexes and show that at any generic parameter in a generic path of deformations

there are differentials on these chain complexes with homology that remains invariant. (It should be mentioned that this does not lead to any closed formula for the differential at generic moments, but shows that a differential that gives the right homology exists.) Here, for higher symmetric colorings, the chain complexes correspond to certain subspaces of the homology which nevertheless contain sufficient information to recover all of the homology, see Sect. 3.5.2 for details.

Generating series for knot polynomials satisfy polynomial recursion relations. Geometrically, such relations originate from counts of punctured holomorphic curves at infinity with boundary on the knot conormal and asymptotic to Reeb chords at punctures, see [4, 14]. From the viewpoint of the quiver or the basic disks without punctures, the recursion relation is generated by similar relations localized around individual basic disks. This leads to an algebraic description of the ensemble of basic disks in terms of non-commutative variables, see [9]. In Sect. 4 we take this further and show that after a suitable change of non-commutative variables the recursion relation of *any* quiver is the recursion relation of the basic toric brane in \mathbb{C}^3 . We generalize this simple recursion relation to include also the new basic curves discussed above and look at the implications of such a relation for both knot polynomials and their categorifications. As the toric brane has a unique embedded holomorphic disk ending on it, this universal relation to the toric brane is in line with $U(1)$ -symmetric configurations of knot conormals, where all holomorphic curves have boundaries which are multiples of a unique simple closed geodesic.

In the light of the conjectured connection between HOMFLY-PT homology and generalized quivers, one might expect that structures in one of the theories are reflected in the other. We first consider structures in HOMFLY-PT homology that we expect originate from the geometry of the basic disks in the $U(1)$ -symmetric configuration. There are \mathfrak{sl}_N differentials d_N [15], which act on the HOMFLY-PT homology with resulting homology being \mathfrak{sl}_N Khovanov–Rozansky homology. The \mathfrak{sl}_1 homology is very simple, it has rank one for every knot (in reduced normalization). In Sect. 5 we conjecture that this structure is reflected on the level of generalized quivers and that the quiver of a knot can be obtained from one ‘spectator’ node and a quiver of half the size of the original quiver together with a ‘universal disk’ that comes from the closed sector and carries the same grading of the \mathfrak{sl}_1 -differential d_1 . The application of the multi-cover skein unlinking operation of [9] to a basic once-around disk and the universal disk gives a pair of generators connected by d_1 . This pair corresponds to two holomorphic curves which differ by a unit of winding around the base \mathbb{CP}^1 of the resolved conifold, where the heavier disk can be viewed as a bound state of the lighter and the universal disk. The connection between reduced and unreduced homologies seems to be reflected in the structure of the generalized quiver in a similar way.

As already mentioned, the form of generalized quiver partition functions that we introduce for multiply wrapped basic disks is conjectural. We check it against the few available (also conjectural) results for knot homologies of 9_{42} and 10_{132} , and it goes without saying that further tests are important. In particular, calculations of colored knot homologies of knots with more than eight crossings would provide support or indicate possible changes to our conjecture. In this context we point out that our conjecture has both a structural and a technical aspect. The structural aspect says that the

Fig. 1 The framed skein relation

$$P(\overline{\times}) - P(\overleftarrow{\times}) = (q - q^{-1}) P(\overline{\cup}) P(\overleftarrow{\cup})$$

$$P(\overline{\smile}) = a P(\overline{\mid}) \quad P(\overleftarrow{\smile}) = a^{-1} P(\overleftarrow{\mid})$$

$$P(\bigcirc) = 1$$

basic generalized holomorphic disks (generalized quiver nodes) and their boundary linking densities (weighted quiver arrows) contain all information about symmetrically colored HOMFLY-PT homology. The technical aspect gives the ‘change of variables’ for extracting this information. It is thus possible that the structural part is the correct, even if the technical part needs modification. As discussed above, there are knots for which standard quiver partition functions cannot reproduce HOMFLY-PT homologies and, therefore, a generalization is needed. Our proposal is in a sense a minimal extension, compatible with available data and with the geometry of holomorphic curves under SFT-stretching.

2 Background

In this section we review earlier results on knot polynomials and knot homologies and their connections to quivers and (refined) curve counting. This is the starting point for our study in later sections.

2.1 Knot polynomials and homologies

If $K \subset S^3$ is a framed knot, then its framed *HOMFLY-PT polynomial* $P(K; a, q)$ [16, 17] is a two-variable polynomial that can be calculated from a knot diagram (a projection of K with over/under information at crossings and framing given by the projection direction) via the framed skein relation, see Fig. 1.

The polynomial is an invariant of framed knots up to framed isotopy. The standard HOMFLY-PT polynomial of a knot is the framed HOMFLY-PT of that knot when equipped with the framing for which its self-linking number vanishes. For $a = q^2$, the HOMFLY-PT reduces to the Jones polynomial $J(K; q)$ [18], and for $a = q^N$ to the \mathfrak{sl}_N Jones polynomial $J_N(K; q)$ [19].

More generally, the *colored* HOMFLY-PT polynomials $P_R(K; a, q)$ are similar polynomial knot invariants depending also on a representation R of the Lie algebra $\mathfrak{u}(N)$. In this setting, the original HOMFLY-PT corresponds to the standard representation. Also the colored version admits a diagrammatic description: it is given by a linear combination of the standard polynomial of certain satellite links of K . From the physical point of view, the colored HOMFLY-PT polynomial with $a = q^N$ is the expectation value of the knot viewed as a Wilson line in $U(N)$ Chern–Simons gauge theory on S^3 .

[1]. In order to simplify the notation, we will write the HOMFLY-PT polynomial also when we refer to the more general colored version.

HOMFLY-PT polynomials also have an interpretation in terms of open topological string or holomorphic curve counts. Physically, $P(K; a, q)$ can be interpreted as the partition function of open topological string of the Lagrangian conormal of the knot after transition from T^*S^3 to the resolved conifold, where $q = e^{g_s}$ and a is the Kähler parameter in the resolved conifold [2]. From the mathematical point of view, this results from invariant counts of open holomorphic curves by the values of their boundaries in the skein module of the Lagrangian, see [3, 4].

We next consider knot homologies. Khovanov [5] introduced a knot invariant which is a far-reaching generalization of the Jones polynomial. To any knot K he associated a doubly-graded chain complex, the homology of which is a knot invariant and such that the Jones polynomial arises as its (graded) Euler characteristic:

$$J(K; q) = \sum_{i,j} (-1)^j q^i \dim \mathcal{H}_{i,j}^{\mathfrak{sl}_2}(K). \quad (2.1)$$

In this sense $\mathcal{H}_{i,j}^{\mathfrak{sl}_2}(K)$ is a categorification of $J(K; q)$. Khovanov–Rozansky homology, which categorifies the \mathfrak{sl}_N polynomial, was defined in [20]:

$$J_N(K; q) = \sum_{i,j} (-1)^j q^i \dim \mathcal{H}_{i,j}^{\mathfrak{sl}_N}(K). \quad (2.2)$$

In this paper we focus mostly on HOMFLY-PT homology [21], which is a categorification of the (original) HOMFLY-PT polynomial:

$$P(K; a, q) = \sum_{i,j,k} (-1)^k a^i q^j \dim \mathcal{H}_{i,j,k}(K). \quad (2.3)$$

The corresponding Poincaré polynomial then provides a t -refinement of HOMFLY-PT polynomial called the *superpolynomial* [15]:

$$P(K; a, q, t) = \sum_{i,j,k} a^i q^j t^k \dim \mathcal{H}_{i,j,k}(K), \quad (2.4)$$

with $P(K; a, q, -1) = P(K, a, q)$. Categorifications of colored HOMFLY-PT polynomials were considered in [7], where it was conjectured that there exists a colored HOMFLY-PT homology, which is invariant under isotopy and such that

$$\begin{aligned} P_R(K; a, q) &= \sum_{i,j,k} (-1)^k a^i q^j \dim \mathcal{H}_{R;i,j,k}(K), \\ P_R(K; a, q, t) &= \sum_{i,j,k} a^i q^j t^k \dim \mathcal{H}_{R;i,j,k}(K). \end{aligned} \quad (2.5)$$

There are also colored Khovanov ($\mathcal{H}_R^{\mathfrak{sl}_2}$) and Khovanov–Rozansky ($\mathcal{H}_R^{\mathfrak{sl}_N}$) homologies, which categorify $J_R(K; q)$ and $J_{N,R}(K; q)$, respectively. We point out that there are many constructions of colored HOMFLY-PT and \mathfrak{sl}_N homologies. They do not always give the same results and some work only in special cases (e.g., for Λ^r representations), see [22–28] and references therein. Here we focus on symmetric representations $R = S^r$, corresponding to Young diagrams with a single row of r boxes, and we will write P_r and \mathcal{H}_r instead of P_{S^r} and \mathcal{H}_{S^r} to simplify the notation. (For example, \mathcal{H}_1 will denote the original HOMFLY-PT homology corresponding to the standard representation.)

2.2 Observed relations between knots and quivers

In [10, 11], knot polynomials were related with representations of quivers. A quiver Q is an oriented graph with a finite number of vertices connected by finitely many signed arrows. We denote the set of vertices by Q_0 and the set of arrows by Q_1 . A *dimension vector* for Q is a vector in the integral lattice with basis Q_0 , $\mathbf{d} \in \mathbb{N}Q_0$. We number the vertices of Q by $1, 2, \dots, m = |Q_0|$. A quiver representation with dimension vector $\mathbf{d} = (d_1, \dots, d_m)$ is the assignment of a vector space of dimension d_i to the node $i \in Q_0$ and of a linear map $\gamma_{ij}: \mathbb{C}^{d_i} \rightarrow \mathbb{C}^{d_j}$ to each arrow from vertex i to vertex j . The *adjacency matrix* of Q is the $m \times m$ integer matrix with entries C_{ij} equal to the algebraic number of arrows from i to j . A quiver is symmetric if its adjacency matrix is.

Quiver representation theory studies moduli spaces of stable quiver representations (see, e.g., [29] for an introduction to this subject). While explicit expressions for invariants describing those spaces are hard to find in general, they are quite well understood in the case of symmetric quivers [12, 13, 30]. Important information (such as the intersection homology Betti numbers of the moduli space of all semi-simple representations of Q of dimension vector \mathbf{d} , see [31, 32]) about the moduli space of representations of a symmetric quiver with trivial potential is encoded in the *motivic generating series* defined as

$$\begin{aligned} P_Q(\mathbf{x}; q) &= \sum_{d_1, \dots, d_m \geq 0} (-q)^{\sum_{1 \leq i, j \leq m} C_{ij} d_i d_j} \prod_{i=1}^m \frac{x_i^{d_i}}{(q^2; q^2)_{d_i}} \\ &= \sum_{\mathbf{d}} (-q)^{\mathbf{d} \cdot \mathbf{C} \cdot \mathbf{d}} \frac{\mathbf{x}^{\mathbf{d}}}{(q^2; q^2)_{\mathbf{d}}}, \end{aligned} \quad (2.6)$$

where the denominator is the so called q -Pochhammer symbol:

$$(z; q^2)_r = \prod_{s=0}^{r-1} (1 - zq^{2s}). \quad (2.7)$$

We will often refer to $P_Q(\mathbf{x}; q) = P_Q(x_1, \dots, x_m; q)$ as the quiver partition function. We point out that the quiver representation theory involves the choice of an element,

the potential, in the path algebra of the quiver and that the trivial potential is the zero element.

A correspondence between knots and quivers proposed in [10, 11] associates quivers to knots by equating the motivic generating series with the generating series of superpolynomials or HOMFLY-PT generating series in the variable x :

$$\begin{aligned} P_K(x, a, q, t) &= \sum_{r=0}^{\infty} \frac{P_r(K; a, q, t)}{(q^2; q^2)_r} x^r, \\ P_K(x, a, q) &= \sum_{r=0}^{\infty} \frac{P_r(K; a, q)}{(q^2; q^2)_r} x^r. \end{aligned} \quad (2.8)$$

More precisely, the most basic version of the correspondence states that for each knot K there exist a symmetric quiver Q and integers $\{a_i, q_i\}_{i \in Q_0}$, such that

$$P_K(x, a, q) = P_Q(\mathbf{x}; q) \quad \text{for } x_i = x a^{a_i} q^{q_i - C_{ii}}. \quad (2.9)$$

The refined version conjectures the bijection between Q_0 and the set of generators of \mathcal{H}_1 , which fixes (a_i, q_i, t_i) to be (a, q, t) -degrees of respective generators:

$$P_K(x, a, q, t) = P_Q(\mathbf{x}; q) \quad \text{for } x_i = x a^{a_i} q^{q_i - C_{ii}} (-t)^{t_i}. \quad (2.10)$$

For $t = -1$, this equation reduces to (2.9), following the relation between the superpolynomials and HOMFLY-PT polynomials.

The correspondence between knot invariants and quivers stated above was proved for all 2-bridge knots in [33] and for all arborescent knots in [34] but *it does not hold* for all knots, e.g., the knot 9_{42} gives a counterexample, see Sect. 6. We will discuss a modification of the correspondence below that includes new types of nodes.

2.3 Physics and geometry of knots and quivers

2.3.1 $3d \mathcal{N} = 2$ gauge theories

The physics around the knots-quivers correspondence is a duality between two $3d \mathcal{N} = 2$ theories: one associated to the knot and denoted $T[L_K]$, and the other associated to the quiver and denoted $T[Q]$, see [8].

The theory associated to the knot K , which we denote $T[L_K]$, arises from M-theory over the resolved conifold X with a single M5-brane wrapping the conormal Lagrangian of the knot L_K [2]:

$$\begin{aligned} \text{space-time} : \quad & \mathbb{R}^4 \times S^1 \times X \\ & \cup \quad \quad \quad \cup \\ \text{M5} : \quad & \mathbb{R}^2 \times S^1 \times L_K. \end{aligned} \quad (2.11)$$

In general $T[L_K]$ does not admit a simple Lagrangian description, but its vortex partition function is known to count M2-branes wrapping embedded holomorphic curves ending on L_K .

In contrast, $T[Q]$ is easier to describe: the gauge group is $U(1)^{\times Q_0}$ and there is one charged chiral for each $U(1)$ factor. Interactions among the different sectors are mediated by (mixed) Chern–Simons couplings, encoded by the quiver adjacency matrix. The quiver variables x_i encode exponentiated Fayet–Iliopoulos couplings. The partition function of vortices again counts M2-branes wrapping embedded holomorphic disks. But in this case there are only $|Q_0|$ of them that are linked according to the adjacency matrix. Here, all other holomorphic curves are branched covers of the basic embedded disks which after perturbation are counted in the $U(1)$ -skein of the Lagrangian projected to homology and linking [3, 9]. The duality with $T[L_K]$ is encoded by the change of variables (2.9).

An important distinction to keep in mind is that while $T[Q]$ has a simple Lagrangian description, $T[L_K]$ is closer to knot homology, see Appendix C. Indeed, its vortex partition function equals the generating series of colored HOMFLY-PT polynomials:

$$\begin{aligned} P_K(x, a, q) &= \sum_{r=0}^{\infty} \frac{P_r(K; a, q)}{(q^2; q^2)_r} x^r = \sum_{r \geq 0} Z_r^{\text{vortex}}(a, q) x^r \\ &= Z^{\text{vortex}}(x, a, q). \end{aligned} \quad (2.12)$$

The coefficient $Z_r^{\text{vortex}}(a, q)$ is a character for the moduli space \mathcal{M}_r of r vortices, see [2, 35]. It takes the form $Z_r^{\text{internal}}(a, q)/(q^2; q^2)_r$ since schematically $\mathcal{M}_r \simeq \mathcal{M}_r^{\text{internal}} \times (\mathbb{C}^r/S_r)$, where the second factor parametrizes positions of r vortices in the plane, and generates the denominator, see (3.34) below. Therefore, $Z_r^{\text{internal}}(a, q)$ is a polynomial whose coefficients correspond to net counts (with signs, including cancellations) of cohomology generators of $\mathcal{M}_r^{\text{internal}}$. Passing to categorification, this polynomial corresponds to an index for the Hilbert space arising from quantization of $\mathcal{M}_r^{\text{internal}}$, which serves as a model for $\oplus_{i,j,k} \mathcal{H}_{r;i,j,k}(K)$.

2.3.2 Basic holomorphic curves

In the previous subsection we saw that $T[L_K]$ arises from M-theory as the effective theory on the surface of the M5-brane and that its BPS particles originate from M2-branes ending on the M5. From the symplectic geometric point of view, BPS states correspond to generalized holomorphic curves with boundary on the Lagrangian submanifold L_K .

We recall the definition of generalized holomorphic curves in the resolved conifold X with boundary on a knot conormal $L_K \subset X$ (as defined in [8, 14]) from the skeins on branes approach to open curve counts in [3]. The key observation in [3] is that the count of bare curves (i.e., curves without constant components) counted by the values of their boundaries in the skein module remains invariant under deformations. The count of such curves also requires the choice of a 4-chain C_K with $\partial C_K = 2L_K$. Intersections of the interior of a holomorphic curve and the 4-chain contribute to the framing variable a in the skein module. For generalized curves there is a single brane on L_K , which leads to $a = q$. Then, the map from the skein module to ‘homology class and linking’

is well-defined and thus counting curves this way, less refined than the $U(1)$ -skein, also remains invariant. In $L_K \simeq S^1 \times \mathbb{R}^2$ one can define such a map that depends on the choice of a framing of the torus at infinity. More precisely, one fixes bounding chains for the holomorphic curve boundaries that agree with multiples of the longitude at infinity and replace linking with intersections between curve boundaries and bounding chains. In [14] an explicit construction of such bounding chains and compatible 4-chain C_K from a certain Morse function of L_K was described and shown to give invariant curve counts in 1-parameter families.

Consider now holomorphic disks with boundary in the basic homology class. Such disks are generically embedded and can never be further decomposed under deformations. Assuming, in line with [36, 37], that all actual holomorphic curves with boundary on L_K lie in neighborhoods of such holomorphic disks attached to the conormal, it would then follow that all generalized holomorphic curves are combinations of branched covers of the basic disks. Using the multiple cover formula the count of generalized curves then agrees with the quiver partition function with nodes at the basic disks and with arrows according to linking and additional contributions to the vertices given by 4-chain intersections.

From this point of view, the theory $T[Q]$ can be thought of as changing the perspective, starting from a neighborhood of the Lagrangian in its cotangent bundle and attaching small neighborhoods of the basic holomorphic disks along curves near the central S^1 . The resulting neighborhood is then determined up to symplectomorphism by the framed link of the boundaries of the disks attached. In this paper we will extend the collection of basic holomorphic curves to include certain non-standard disks that are not embedded. Such curves have boundary that wraps the homology generator of the conormal several times, but are not combinations of curves going once around that generator. As we will discuss below, the most basic such curves are not embedded disks: an embedded disk that goes d times around is expressed as d such basic holomorphic curves. We give a conjectural picture of the contribution from holomorphic curves in a neighborhood of such basic curves to the partition function, also on the refined level. From the quiver point of view, these curves could perhaps be considered as a new type of ‘orbifold’ quiver nodes, see Sect. 3.1.2 for the underlying geometry.

2.4 Omega-background and refined indices

Having reviewed the geometric and physical features of the quiver-like description of knot invariants in the context of topological strings, we now turn to the question of refinement. We begin with a review of well-known facts about refinement in the context of closed topological string theory. We then give a brief description of the counterpart for the open sector for a knot conormal L_K from the point of view of the theory $T[L_K]$. In Sect. 3.3 we discuss the extension of refinement to the open string sector further, reviewing and clarifying the role of a certain $U(1)$ symmetry and its interpretation in the context of branes wrapping knot conormal Lagrangians.

2.4.1 Closed string sector

One of the motivations leading to refined topological strings was the explicit evaluation of partition functions of 4d $\mathcal{N} = 2$ gauge theories via localization [38, 39]. These gauge theories may be engineered by type IIA string theory on a Calabi–Yau threefold X times \mathbb{R}^4 , denoted $T_{4d}[X]$. This construction may be further viewed as a circle compactification of M-theory on $X \times S^1_\beta \times \mathbb{R}^4$, which engineers a 5d theory $T_{5d}[X]$. The eight supercharges of $\mathcal{N} = 2$ SUSY in 4d transform as spinors under $SO(4) \simeq SU(2)_L \times SU(2)_R$, and are further charged under a $U(1) \times SU(2)_I$ R-symmetry. This $U(1)$ is often anomalous and we will ignore it. Supercharges transform under $SU(2)_L \times SU(2)_R \times SU(2)_I$ as $(\tilde{Q}^I_\alpha, Q^I_\alpha) = (2, 1; 2) \oplus (1, 2; 2)$.

If $S^1 \times \mathbb{R}^4$ is replaced by an \mathbb{R}^4 -bundle over S^1 with holonomy $g \in SO(4)$, in order to preserve some supersymmetry one can turn on a non-trivial R-symmetry background as follows [40]. Via the identification $SO(4) \simeq SU(2)_L \times SU(2)_R$, we may split $g = (g_L, g_R)$. One can turn on a holonomy g_I of $SU(2)_I$ for the rank-2 R-symmetry bundle when going around S^1 , in particular one can set $g_I = g_R$. It is then natural to consider the diagonal subgroup $SU(2)_d \subset SU(2)_R \times SU(2)_I$. Supercharges transform under $SU(2)_L \times SU(2)_d$ as

$$(2, 1; 2) \rightarrow \underbrace{(2, 2)}_{\tilde{Q}_\mu}, \quad (1, 2; 2) \rightarrow \underbrace{(1, 1)}_{\tilde{Q}} \oplus \underbrace{(1, 3)}_{\tilde{Q}_{\mu\nu}}. \quad (2.13)$$

There is a distinguished supercharge \tilde{Q} , which is invariant under the S^1 holonomy for any choice of (g_L, g_R) .

Next we restrict to a specific choice of bundle, the so-called Omega-background, see [39] for an in-depth description. In this case the holonomies g_L, g_R are restricted to $U(1)_L \times U(1)_R$ subgroups. Notably, this implies that one only needs a $U(1)_I$ subgroup of $SU(2)_I$ to perform a topological twist. This fact will be important later when introducing branes. After twisting, the holonomy group is then $U(1)_L \times U(1)_d$, and acts by rotations $(g_L, g_d) = (e^{\epsilon_1 + \epsilon_2}, e^{\epsilon_1 - \epsilon_2})$ of $\mathbb{R}^4 \sim \mathbb{R}^2_{\epsilon_1} \oplus \mathbb{R}^2_{\epsilon_2}$. Thanks to this restriction there are actually two conserved supercharges in the Omega-background.

To understand this, let us choose a basis for spinors in which $J^3_{L,R}$ are diagonal. Doing the same for $SU(2)_I$, the eight supercharges of the 4d theory have charges

$$\underbrace{\left(\pm \frac{1}{2}, 0; \pm \frac{1}{2}\right)}_{\tilde{Q}^I_\alpha} \oplus \underbrace{\left(0, \pm \frac{1}{2}; \pm \frac{1}{2}\right)}_{Q^I_\alpha} \quad \text{under } U(1)_L \times U(1)_R \times U(1)_I, \quad (2.14)$$

where signs are chosen independently. With the topological twist, one may preserve the following two linear combinations:

$$\tilde{Q}_\pm \sim \left(0, \pm \frac{1}{2}; \mp \frac{1}{2}\right), \quad (2.15)$$

where now the *signs are correlated*. In fact, under $U(1)_L \times U(1)_d$ both of these transform as $(0, 0)$.² As already hinted by our parametrization of (g_L, g_d) in terms of ϵ_1, ϵ_2 , $J_{L,R}^3$ are diagonal/anti-diagonal combinations of $J_{1,2}$, the latter being generators of rotations in $\mathbb{R}_{\epsilon_1}^2 \oplus \mathbb{R}_{\epsilon_2}^2$. The surviving supercharges therefore transform as

$$\begin{aligned} \tilde{Q}_+ : \left(\frac{1}{2}, \frac{1}{2}; -\frac{1}{2} \right), \quad \tilde{Q}_- : \left(-\frac{1}{2}, -\frac{1}{2}; \frac{1}{2} \right) \\ \text{under } U(1)_1 \times U(1)_2 \times U(1)_I. \end{aligned} \quad (2.16)$$

Note that $\tilde{Q}_- = \tilde{Q}_+^\dagger$. Taking into account that our conventions for R-charges are opposite to those of [41], we can readily identify these supercharges with \tilde{Q}_r, \tilde{Q}_l there, respectively.

Note that $[F, \tilde{Q}_\pm] = \pm \tilde{Q}_\pm$ with $F = 2(J_L^3 + J_R^3)$ ensures that $\{\tilde{Q}_\pm, (-1)^F\} = 0$. Reducing the theory along $\mathbb{R}_{\epsilon_1}^2 \oplus \mathbb{R}_{\epsilon_2}^2$ gives a $\mathcal{N} = 2$ quantum mechanics on S^1 , where $\{\tilde{Q}_+, \tilde{Q}_-\} \sim H$ and $[\tilde{Q}_\pm, H] = 0$. It is well-known that \tilde{Q}_+ cohomology only gets contributions from groundstates with $H = 0$, due to cancellations among bosons and fermions for all excited states. Deformations of the theory may lead some excited states to become groundstates, or vice versa, however the count of bosonic ($F \in 2\mathbb{Z}$) minus fermionic ($F \in 2\mathbb{Z} + 1$) groundstates remains invariant. Witten index $\text{Tr}(-1)^F e^{-\beta H}$ coincides with the invariant difference of dimensions of spaces of groundstates $\dim \mathcal{H}_{(0)}^B - \dim \mathcal{H}_{(0)}^F$ [42]. By construction \tilde{Q}_\pm are invariant under J_L^3 , and $J_R^3 + J_I^3$, therefore one may introduce additional grading on the whole Hilbert space (both groundstates and excited states), preserving cancellations induced by the twisting $(-1)^F$ in the trace. This leads to the following for the 5d theory [38]:

$$Z(\epsilon_1, \epsilon_2) = \text{Tr}_{\mathcal{H}[T_{5d}]} (-1)^F e^{-(\epsilon_1 - \epsilon_2)J_L^3 - (\epsilon_1 + \epsilon_2)(J_R^3 + J_I^3)}. \quad (2.17)$$

Although this index will not be an object of primary interest for us, we will use it as a point of contact to match with conventions of [41]. If we turn off R-symmetry and only rotate \mathbb{R}^4 , one readily sees that $J_1 = J_L^3 + J_R^3$ and $J_2 = -J_L^3 + J_R^3$ are the generators of rotations of $\mathbb{R}_{\epsilon_1}^2$ and $\mathbb{R}_{\epsilon_2}^2$, respectively. We then identify $S_1, S_2, S_R, e^{-\epsilon_1}, e^{-\epsilon_2}$ from [41] with $J_1, J_2, -J_I^3, q, t^{-1}$ in the present paper. With these identifications, the index takes the form

$$Z(q, t) = \text{Tr}_{\mathcal{H}[T_{5d}]} (-1)^F q^{S'_1} t^{-S'_2}, \quad (2.18)$$

where $S'_i = S_i - S_R$ for $i = 1, 2$, as claimed in [41]. Adapting to conventions from our earlier work [8, 9], we will henceforth switch to

$$q = q^{1/2}, \quad t = -(t/q)^{-1/2}. \quad (2.19)$$

² From these, one recovers $\tilde{Q} \sim \tilde{Q}_+ - \tilde{Q}_-$ being the singlet $\mathbf{1} \subset \mathbf{2} \otimes \mathbf{2}$. With the Omega-background, as opposed to more general $SU(2)$ holonomy, one may in addition preserve $\tilde{Q}' \sim \tilde{Q}_+ + \tilde{Q}_-$.

2.4.2 Open string sector

Let L be a special Lagrangian submanifold of the resolved conifold $X = \mathcal{O}(-1) \oplus \mathcal{O}(-1) \rightarrow \mathbb{CP}^1$. The low-energy dynamics of an M5-brane on $L \times S^1 \times \mathbb{R}^2$ is described by a 3d $\mathcal{N} = 2$ theory $T[L]$ on $S^1 \times \mathbb{R}^2$ [43, 44]. From this viewpoint, J_1 is a space–time rotation, however J_2 is now an R-symmetry. As stressed above, it only makes sense to turn on fugacities q, t in the index if the corresponding generators commute with the surviving supercharges. The presence of the M5-brane on \mathbb{R}^2 inside \mathbb{R}^4 breaks Lorentz invariance; therefore, we must re-investigate whether supercharges are preserved or not.

Recall our discussion of the 5d theory in a general background, which led to the existence of a single preserved supercharge \tilde{Q} . Since this transforms as a scalar in 4d, clearly it is also preserved by the presence of the M5 that breaks Lorentz invariance. However to define an index and its deformation by q, t , we need two supercharges. Without the brane this was made possible by the choice of a non-generic background, the Omega-background which breaks $SO(4)$ to $U(1)_1 \times U(1)_2$. As long as the defect lies in a plane \mathbb{R}^2 , that is either $\mathbb{R}_{\epsilon_1}^2$ or $\mathbb{R}_{\epsilon_2}^2$, it preserves the group of rotations of the Omega-background. To preserve two supercharges it was also crucial to perform a topological twist using a $U(1)_I$ subgroup of the $SU(2)_I$ R-symmetry. In general there is no reason to expect that neither $SU(2)_I$ nor $U(1)_I$ should be preserved by the presence of M5 on $L \times S^1 \times \mathbb{R}^2$. However, one may hope that there exist specific geometric configurations of L that allow to preserve at least the $U(1)_I$ subgroup required by the topological twist.

We will assume that $U(1)_I \subset SU(2)_I$ is preserved by the presence of M5 on L . This is a non-trivial and crucial assumption made in [41], whose geometric significance in our setting will be clarified in Sect. 3.3.2. With the topological twist, one may preserve the same two supercharges (2.16) discussed before introducing the M5. As already stressed, these coincide precisely with Q_r, \tilde{Q}_r from [41].

Finally, we come to the object of main interest for us: the partition function of 3d BPS states and its refinement. These consist of open M2-branes ending on the M5-brane, which give rise to BPS vortices of the 3d $\mathcal{N} = 2$ theory $T[L]$. The 3d index counting such BPS states is a Witten index, again deformed by fugacities coupled to symmetries of the theory that commute with \tilde{Q}_\pm and therefore with H :

$$Z(q, t) = \text{Tr}_{\mathcal{H}[T_{3d}]} (-1)^F q^{S'_1} t^{-S'_2} a^{Q_x} \mathcal{T}. \quad (2.20)$$

Here Q is the charge of a global $U(1)$ symmetry of $T[L]$ associated to rotations of the base \mathbb{CP}^1 of X [45], and \mathcal{T} is the charge of the topological $U(1)$ symmetry associated to the gauge $U(1)$ of $T[L]$ [46].³ Contributions to the index by states with $a^{2k} x^n$ correspond to M2-branes wrapping a relative homology cycle labeled by $(k, n) \in H_2(X, L)$. It is natural to switch to a different basis for q, t to distinguish between the spin of a BPS state (along $\mathbb{R}_{\epsilon_1}^2$) and its R-charge (along transverse

³ The fact that $T[L]$ is a $U(1)$ gauge theory follows from the fact that $b_1(L \approx S^1 \times \mathbb{R}^2) = 1$. The abelian 2-form on M5 reduced along the 1-cycle in L gives rise to an abelian gauge field in $T[L]$.

directions). Adopting (2.19) yields

$$Z(q, t) = \text{Tr}_{\mathcal{H}[T_{3d}]}(-1)^{2(J_1+J_2+J_I)} q^{2(J_1-J_2)} t^{2(J_2+J_I)} a^{\mathcal{Q}_x^T}, \quad (2.21)$$

where we lightened notation $J_I^3 \rightarrow J_I$. Spin J_I along the direction tangent to M_5 is detected only by q , not t . Conversely, the R-symmetry charge J_I is only detected by t , not q . When L is a knot conormal, this 3d index is expected to correspond to the refined HOMFLY-PT generating series of K (with symmetric colors) [2, 41].

3 Generalized quivers and HOMFLY-PT homology

In this section we analyze the relation between HOMFLY-PT homology and generalized quivers from various perspectives, which provides motivation and arguments for conjecture 1.2.

Remark 3.1 One of the implicit assumptions in the original formulation of the knots-quivers correspondence [10, 11] is that each node of the quiver has an associated change of variables where x_i is directly proportional to x . From a geometric perspective, this means that each one of the basic disks represented by nodes of Q has a boundary that wraps around the longitude of L_K exactly once. It was noticed in [8] that this assumption is not always satisfied (see Sect. 6 for concrete counterexamples), and an extension of the knots quivers correspondence was formulated [8, Conjecture 1.1]. This conjecture was erroneously stated on the level of the refined partition function—the problem is that it does not say what the refined contribution for higher level nodes would be. In this section we discuss such contributions.

In more physical terms, the basic disks corresponding to the nodes of Q are mutually linked and interact according to the quiver adjacency matrix. Together they generate the whole spectrum of BPS states corresponding to M2-branes wrapping embedded holomorphic curves [8, 9]. The quiver description expresses a BPS state winding d times around as a bound state of d copies of once-around basic disks, each corresponding to one of the nodes of Q . As mentioned above, for knots that do not admit such descriptions there are BPS states corresponding to curves whose boundary wraps d times around the longitude of L_K , which cannot be realized as bound states of once-around curves. In these cases the original formulation of the knots-quivers correspondence fails.

3.1 Geometry and combinatorics of multiply-wrapped basic disks

In this section we study the geometry of the basic holomorphic disks that are the nodes of our generalized quiver. We will first describe their geometry and then derive their multi-cover formulas. As mentioned above, quiver node curves appear for a $U(1)$ -symmetric configuration which arises as a degenerate limit when the knot conormal lies on top of the unknot conormal. This limit arises as follows, present the knot as a braid in a radius $r > 0$ tubular neighborhood of the unknot, as $r \rightarrow 0$ the knot collapses to a multiple of the unknot and accordingly the conormal of the knot collapses to a

multiple of the unknot conormal. Since the unknot conormal supports no basic higher genus curves, we expect all quiver nodes to correspond to disks. The simplest such curves are embedded disks and their multiple-cover formula is well-known.

Consider now an embedded holomorphic disk with connected boundary in class x^μ for $\mu > 1$. We apply so-called Symplectic Field Theory (SFT) stretching around L_K , see [47]. This is a degeneration of the complex structure under which holomorphic curves degenerate into several level holomorphic buildings, with parts near L_K (inside parts) and parts far from L_K (outside parts) joined at Reeb orbits in the unit cotangent bundle of L_K . In the case at hand, we pick a metric on $L_K \approx S^1 \times \mathbb{R}^2$ with only one simple closed geodesic, and correspondingly only two simple closed Reeb orbits which are the unit cotangent lifts of this geodesic with its two orientations. Then, since the unknot conormal has holomorphic curves that go in only one of the two directions, all inside parts of holomorphic buildings near L_K are multiples of the basic cylinder stretching from the simple Reeb orbit to the geodesic (with the positive orientation) in the zero section. In particular, our basic once-around disk becomes a two level building consisting of an outside sphere with puncture and an inside disk with puncture. The contribution to the partition function comes from multiple covers of this curve together with constant curves attached along it.

Since all curves near the Lagrangian, the inside parts in the stretched limit, are multiples of the basic punctured disk (stretching between the Reeb orbit and the unique geodesic in $S^1 \times \mathbb{R}^2$), we find that the inside part of the holomorphic building in the limit is a μ -fold cover of this basic punctured disk. The outside part of the curve, the upper level, is a once punctured curve asymptotic to the μ -fold cover of the basic Reeb orbit. The curve before the limit is assumed not to be a multiple cover. Assuming that it is somewhere injective also in the limit, this limit curve is generically embedded as well. The simplest such two-level building has a sphere with one puncture as its outside part and we define such buildings with inside part a μ -fold cover of the basic punctured disk and outside piece an embedded punctured sphere, as our new μ -times around basic curves. Note that for $\mu = 1$ we simply get stretched versions of our previous basic disks.

3.1.1 Generalized curves, the four-chain and deformations of M2–M5 configurations

We next consider how these two-level buildings and their multiple covers glue and how they contribute to the partition function counting generalized curves. Consider d -fold covers of the levels. The inside piece looks like a disk with an $U(1)$ -action with a fixed point of order μd at the Reeb orbit. The outside piece looks like a d -fold cover of a sphere with a single puncture. In Gromov–Witten counts of connected curves, a μd -fold cover of a disk with a single fixed point contributes

$$\frac{1}{\mu d} \left(\frac{1}{1 - q^{2\mu d}} \right). \quad (3.1)$$

To see this, we use a deformation argument. Consider first an embedded annulus stretching between two Lagrangians L and L' , and with standard normal bundle. Assume that the boundary of the annulus in L is homologically essential and lies

in homology class $\log x \neq 0 \in H_1(L)$, and that the boundary in L' is contractible. The d -fold cover of L then contributes

$$\frac{1}{d}x^d.$$

Assume now that the boundary in L' shrinks to a point. This leaves a disk with a d -fold branch point. As in the skein count [3], this disk is an instance of a 1-parameter family of disks that crosses L' . The intersection of this disk with the 4-chain of L' changes by $2d$ as they cross (d positive intersections become negative). If the disk contributes ξ , then invariance in the $U(1)$ -skein projected to homology and linking gives the equation

$$q^{2d}\xi - \xi = \frac{1}{d}x^d, \quad (3.2)$$

and we find

$$\xi = \frac{x^d}{d(1 - q^{2d})},$$

as claimed.

Consider now gluing on the outside piece. This outside piece breaks the symmetry; there are μ ways of gluing (here we glue first the underlying curve and then take multiple covers) giving instead the contribution

$$\mu \cdot \frac{1}{\mu d} \left(\frac{1}{1 - q^{2\mu d}} \right) = \frac{1}{d} \left(\frac{1}{1 - (q^{2\mu})^d} \right). \quad (3.3)$$

Therefore the contribution to the Gromov–Witten partition function from a single basic two-level configuration with boundary going μ times around the generator is

$$\exp \left(\sum_{d>0} \frac{1}{d} \frac{(x^\mu)^d}{1 - (q^\mu)^{2d}} \right) = (x^\mu, q^{2\mu})_\infty^{-1}. \quad (3.4)$$

Remark 3.2 Relation (3.2) has a suggestive interpretation from a physics viewpoint: the left-hand side represents contributions of M2-branes wrapping holomorphic curves belonging to the same family of deformations, and located on either side of an M5-brane on L' . On the right hand side, there is a contribution of an annulus with a boundary on L' . This is a kind of skein relation between M2 and M5-branes supported on higher-dimensional objects of total codimension one in the Calabi–Yau, see Fig. 2. (The objects are linking from the viewpoint of the A -model on X , where M2 is represented by a holomorphic curve and M5 by a Lagrangian. Lifting to M theory, the M2 couples to the three-form potential A_3 sourced by the M5 by $j_{M5} \sim dF_4$ where $F_4 = dA_3$ locally. Let $\tilde{F}_7 = \star F_4$ be the dual field in 11d; this is sourced by the M2 current j_{M2} with a boundary term correction $d\tilde{F}_7 = j_{M2} + H_3 \wedge j_{M5}$, where H_3 is the self-dual

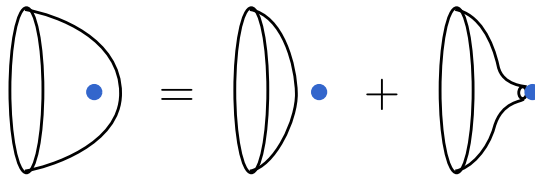


Fig. 2 Skein-like relation for an M2-brane wrapping an embedded holomorphic disk: when crossing an M5-brane, the M2 breaks up and leaves behind a new curve with a new boundary on the M5

field strength on the M5, which couples to the M2 boundary [48].) At the level of (plethystic-)exponentiated partition functions, this relation is expressed by the well-known property $(q^2x; q^2)_\infty = \frac{1}{1-x}(x; q^2)_\infty$. (This generalizes to μ -times around curves, see (3.18)) Tracking 4-chain intersections is key for establishing this relation via Gromov–Witten counting. Closing the puncture corresponding to the boundary on L , yields a similar relation between generating functions of M2-branes on spheres and disks $(q^2a^2; q^2; q^2)_\infty = (a^2; q^2)_\infty^{-1}(a^2; q^2; q^2)_\infty$, where a^2 is the flux of M5-branes on L linked by M2.

3.1.2 Orbifold models of multiply wrapped disks

As discussed above, two-level holomorphic buildings where the inside (the part near the Lagrangian) is a punctured un-branched cover of a punctured disk and where the outside (the part far from the Lagrangian) is an embedded punctured sphere are key objects in our generalized quivers. In order to understand the behavior of such holomorphic objects, we can view them from inside and move the embedded sphere part far away. This means shrinking the outside punctured sphere together with the Reeb orbit where it is attached to a point and that gives an orbifold disk. In this section we study topological strings on orbifolds.

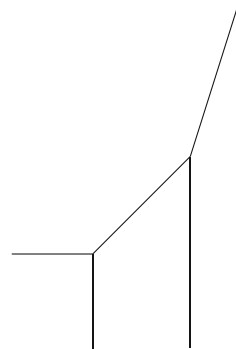
We start our discussion from the following identity, relating the partition function of a μ -times around basic disk to μ once-around basic disks, with specific B -field fluxes:

$$\begin{aligned} (x^\mu; q^{2\mu})_\infty^{-1} &= \prod_{n \geq 0} (1 - x^\mu q^{2\mu n})^{-1} = \prod_{k=0}^{\mu-1} \prod_{n \geq 0} (1 - \zeta^k x q^{2n})^{-1} \\ &= \prod_{k=0}^{\mu-1} (\zeta^k x; q^2)_\infty^{-1}, \end{aligned} \quad (3.5)$$

where ζ is a primitive μ -th root of unity. We will explain how such expressions appear from certain ‘fillings’ of cylindrical versions of punctured orbifold singularities. We start in the simplest non-trivial case, when $\mu = 2$. Here we simply have

$$(x^2; q^4)_\infty = (x; q^2)_\infty (-x; q^2)_\infty. \quad (3.6)$$

Fig. 3 Toric diagram of $\mathcal{O}(0) \oplus \mathcal{O}(-2) \rightarrow \mathbb{CP}^1$



This equation appears geometrically from the toric brane in $\mathcal{O}(0) \oplus \mathcal{O}(-2) \rightarrow \mathbb{CP}^1$ in a certain limit. Consider the toric diagram in Fig. 3. The mirror curve is

$$F(x, y) = 1 - y - (1 + Q)x + Qx^2, \quad (3.7)$$

with a single solution

$$y = (1 - x)(1 - Qx). \quad (3.8)$$

In the limit $Q \rightarrow e^{\pi i} = -1$ (the complexified Kähler modulus is purely B -field) this becomes

$$1 - y - x^2 = 0. \quad (3.9)$$

(Note that this is precisely the classical limit of (4.8).)

Switching from the classical to the quantum level, we consider a toric brane on the horizontal leg. Its partition function can be evaluated by topological vertex techniques⁴:

$$Z(x) = (x; q^2)_{\infty}^{-1} (Qx; q^2)_{\infty}^{-1}. \quad (3.10)$$

This is annihilated by the quantum curve

$$\hat{y} = (1 - \hat{x})(1 - Q\hat{x}), \quad (3.11)$$

whose classical limit recovers (3.8). Now an orbifold limit $Q \rightarrow -1$ turns the curve into

$$\hat{y} = (1 - \hat{x})(1 + \hat{x}) = 1 - \hat{x}^2 \quad (3.12)$$

⁴ Compared to topological vertex conventions, we absorb inessential powers of q in x and Q for cleaner expressions.

and the partition function collapses to

$$Z(x) \rightarrow (x; q^2)_\infty^{-1} (-x; q^2)_\infty^{-1} = (x^2; q^4)_\infty^{-1}. \quad (3.13)$$

This is precisely the proposal for the unrefined partition function of a twice-around basic disk. Indeed,

$$(x^2; q^4)_\infty^{-1} = \sum_{k \geq 0} \frac{x^{2k}}{(q^4; q^4)_k} \quad (3.14)$$

matches with the form proposed in (1.2) with $C_{11} = 0$, $\mu_1 = 2$ and $x_1 = x^2$.

In order to see the geometry underlying these calculations, consider the orbifold $\mathbb{C} \times (\mathbb{C}^2/(\mathbb{Z}/2\mathbb{Z}))$ and remove the codimension four fixed point locus $\mathbb{C} \times [0]$, where $[0]$ denotes the point in the orbifold quotient which is the image of $0 \in \mathbb{C}^2$. We view the resulting symplectic manifold as having a negative end (the negative half of the symplectization of standard contact \mathbb{RP}^3 times \mathbb{C}) near the removed locus and note that there are two fillings: the orbifold itself and $\mathcal{O}(-2) \oplus \mathcal{O}(0)$. In the latter filling we view the symplectic area of the sphere as zero since the filling is at negative infinity. We can now interpret the limit $Q \rightarrow -1$ as this negative end splitting off from $\mathcal{O}(-2) \oplus \mathcal{O}(0)$. When this happens, punctured versions of the curves remain in the punctured orbifold and these can be completed by curves in the actual orbifold filling. As the flux through the sphere at negative infinity is set to πi , the partition functions match. Geometrically, this can be interpreted as the fact that upper level connected curves with odd asymptotics cancel, whereas those with even asymptotics add. This means that all nonzero curves can be filled with the orbifold end or the πi flux $\mathcal{O}(-2) \oplus \mathcal{O}(0)$ and that the curve counts agree. Thus, from the viewpoint of curve counts in the two-level symplectic manifold, the two fillings give the same result. Moreover, as the filling $\mathcal{O}(-2) \oplus \mathcal{O}(0)$ moves toward negative infinity, the moduli space of curves in the upper level approaches the corresponding space for the orbifold. It is in this sense that taking the limit $Q \rightarrow -1$ should be understood.

Higher degree basic disks appear in more complicated orbifold quotients. The corresponding toric diagram is shown in Fig. 4 and gives the mirror curve

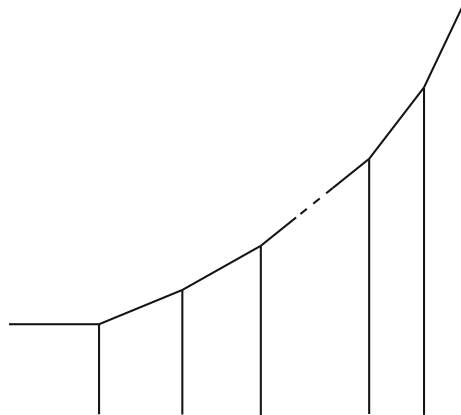
$$y = (1 - x)(1 - Q_1 x) \cdots (1 - Q_{\mu-1} x). \quad (3.15)$$

In analogy with the case $\mu = 2$ above, we take the limit $Q_k \rightarrow e^{\frac{2\pi i}{\mu} k}$ and get the mirror curve of the orbifold $\mathbb{C} \times (\mathbb{C}^2/(\mathbb{Z}/\mu\mathbb{Z}))$.

$$1 - y - x^\mu = 0. \quad (3.16)$$

On the quantum level this reproduces the identity (3.5). The geometric interpretation is as above: we count two level curves in the two level symplectic manifold. The upper level of this manifold is the orbifold with the central $\mathbb{C} \times [0]$ removed, viewed as a symplectic manifold with an end given by the negative half of the symplectization of the standard contact lens space $L(\mu, 1)$ times \mathbb{C} . The filling of the negative end is

Fig. 4 Toric diagram of the resolution of the orbifold $\mathbb{C} \times (\mathbb{C}^2/(\mathbb{Z}/\mu\mathbb{Z}))$



either the orbifold itself or the manifold given in Fig. 4 with zero-area spheres, since they live at negative infinity, and with B -field fluxes $\frac{2\pi i}{\mu}k$ so that curve counts are identical. The convergence of moduli spaces works in direct analogy with the $\mu = 2$ case.

3.1.3 Semi-classical consequences of basic disk denominators

It is worth noting that the difference between the standard denominators $(q^2; q^2)_{d_i}$ and $(q^{2\mu_i}; q^{2\mu_i})_{d_i}$ we propose in (1.2) can be seen already at the semi-classical level. Consider a single basic μ -times around disk with no self-linking. Then the partition function

$$P = \sum_{d \geq 0} \frac{x^{d\mu}}{(q^{2\mu}; q^{2\mu})_d} = (x^\mu; q^{2\mu})_\infty^{-1} \quad (3.17)$$

is annihilated by $1 - \hat{y} - \hat{x}^\mu$, since

$$\hat{y} \cdot (x^\mu; q^{2\mu})_\infty^{-1} = (q^{2\mu}x^\mu; q^{2\mu})_\infty^{-1} = (1 - x^\mu)(x^\mu; q^{2\mu})_\infty^{-1}. \quad (3.18)$$

The classical curve is therefore

$$1 - x^\mu - y = 0. \quad (3.19)$$

On the other hand, a partition function like

$$\tilde{P} = \sum_{d \geq 0} \frac{x^{d\mu}}{(q^2; q^2)_d} = (x^\mu; q^2)_\infty^{-1} \quad (3.20)$$

would behave as follows:

$$\hat{y} \cdot (x^\mu; q^2)_\infty^{-1} = (q^2x^\mu; q^2)_\infty^{-1} = (1 - x^\mu) \cdots (1 - x^\mu q^{2\mu-2})$$

$$(x^\mu; q^{2\mu})_\infty^{-1}. \quad (3.21)$$

The classical curve in this case is quite different:

$$(1 - x^\mu)^\mu - y = 0. \quad (3.22)$$

Therefore, in order to detect the difference between the two types of denominator, it is sufficient to compute the unrefined contributions from genus-zero basic curves to the augmentation polynomial. In Sect. 6 we will provide concrete examples where the distinguished form of the curve (3.19) appears.


3.2 Holomorphic curves viewed as BPS generators

The structure of HOMFLY-PT homology seems to indicate that it is more closely related to the expansion of the refined partition function of the theory $T[L_K]$ in terms of equivariant vortices than to the corresponding expansion in terms of basic holomorphic curves. This means that in order to extract homology information from basic holomorphic curves viewed as BPS generators, we must understand how to expand a configuration of such objects as a combination of vortices. In this section we discuss proposals for such an expansion and its origins. We study the expansions for single generators on the unrefined level, and then discuss how these might be refined. The discussion here is in a sense localized near the boundary of the curve and independent of other charges, which on the unrefined level comes from homology class, 4-chain intersections, self-linking, and—on the refined level—also on a certain framing density term that we discuss in Sect. 3.4.

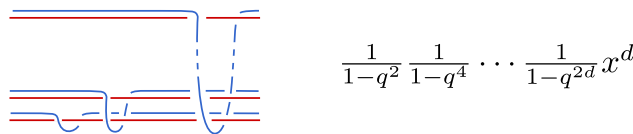
Consider a basic holomorphic curve. As explained in Sect. 3.1, such a curve consists of a punctured embedded sphere on the outside, asymptotic to a multiple of the unique Reeb orbit, and an unbranched multiple cover of the basic cylinder stretching from the simple Reeb orbit to the geodesic in the zero section on the inside.

In particular, our basic once-around disk becomes a two level building consisting of an outside sphere with puncture and an inside disk with puncture. The contribution to the partition function comes from multiple covers of this curve together with constant curves attached along it. Here we propose to push the contributions from the constants down to the boundary. In the limit we would find copies of the basic disk with branched covers of the constant disks attached to them at the boundary. We observe that at the level of generalized curves, these multiply covered constant disks give the same contributions as very thin holomorphic annuli with one boundary component linking the basic curve and the other one not linking it, that can intuitively be thought of as appearing when the boundaries of the basic disk joined by the constant disk are lifted apart. For a d -fold multiple cover of a basic disk, there is one such annulus on each level of magnification. The first annulus links all strands, the second all but one, etc., until the last annulus which links only one strand, see Fig. 5.

To support this picture, let us explain how it relates to the more familiar count of multiple covers of a single holomorphic disk with boundary on L_K . Recall that L_K

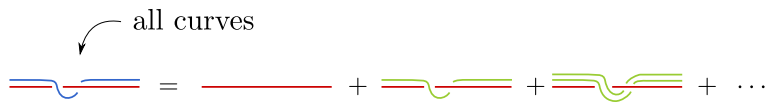


$$\frac{1}{1-q^2} x$$



$$\frac{1}{1-q^2} \frac{1}{1-q^4} \cdots \frac{1}{1-q^{2d}} x^d$$

all curves



$$\exp\left(-\sum_d \frac{y^d}{d}\right) = \frac{1}{1-y} = 1 + y + y^2 + \dots$$

Fig. 5 Contributions of pushed down constant annuli to generalized curve counts. Both boundaries of each annulus follow the longitude, one of the boundaries also wraps around a small meridian, linking with the boundary of the i -th strand. The overall holonomy is $y_i \cdot x \cdot x^{-1} = y_i$

carries a $U(1)$ local system, with meridian and longitudinal holonomies at the boundary denoted x , y . These holonomies provide (exponentiated) Darboux coordinates for the moduli space of abelian flat connections on $T^2 \simeq \partial L_K$. We denote their deformation quantization by \hat{x} , \hat{y} , obeying the relation $\hat{y}\hat{x} = q^2\hat{x}\hat{y}$. Any disks ending on L_K arise through the large N geometric transition, descending from a common holomorphic cylinder stretching between the zero-section in T^*S^3 and L_K . As the boundaries of this cylinder are the original knot $K \subset S^3$ and the longitude in L_K , its skein valued partition function will be given by (2.8), where $P_r(K; a, q)$ is the HOMFLY-PT polynomial of K in the r -th symmetric representation, and x^r is the $U(1)$ HOMFLY-PT skein element in L_K projected to homology and linking. For illustration, consider the unknot in reduced normalization, for which $P_r(0_1; a, q) = 1$. This gives the following partition function of a holomorphic disk

$$\psi(x) = P_{0_1}(x, a, q) = \sum_{r \geq 0} \frac{x^r}{(q^2; q^2)_r} = (x; q^2)_{\infty}^{-1} \quad (3.23)$$

From the viewpoint of $U(1)$ Chern–Simons on L_K , boundaries of worldsheet instantons wrapping the holomorphic disk give rise to infinite series of Wilson lines [49]. A Wilson line wrapping $r \geq 0$ times around L_K with k kinks on it contributes with $q^{2k}x^r$. The number of such Wilson lines is $c_{k,r}$, defined by the expansion

$$\psi(x) = \sum_{r \geq 0} \sum_{k \geq 0} c_{k,r} q^{2k} x^r. \quad (3.24)$$

The interpretation of $q^{2k}x^r$ as an r -times wrapped Wilson line with k kinks can be seen by noting that kinks are counted by powers of a as in Fig. 1, and by noting that in $U(1)$ Chern–Simons $a = q$. Incidentally, $c_{k,r}$ is also the dimension of the Hilbert space of BPS vortices of $T[L_K]$ with vorticity r and spin k [35].

Kinks on the boundary of a Wilson line can be traded with linking with a dual Wilson line using the $U(1)$ Chern–Simons skein algebra of variables \hat{x}, \hat{y} :

$$\frac{x^r}{(q^2; q^2)_r} =: \underbrace{\frac{1}{1-\hat{y}}\hat{x} \cdots \frac{1}{1-\hat{y}}\hat{x}}_r : \quad (3.25)$$

where $:$ is the normal ordering operation defined in [9]. Trading kinks with linking loops may be viewed as a ‘half’ of the $U(1)$ skein relation on L_K : the \hat{x} Wilson line with a small \hat{y} loop around it can be viewed as the over-crossing diagram in the first line of Fig. 1, while the kink corresponds to q times the smoothing also on the first line. Similarly the under-crossing can be traded with an anti-kink, which is q^{-1} times the smoothing. Consistency then implies that the over-crossing equals under-crossing times q^2 , in agreement with $\hat{y}\hat{x} = q^2\hat{x}\hat{y}$.

Once again, this specific ensemble of Wilson lines can be given a geometric interpretation in terms of curve counting. The factor $\frac{1}{1-\hat{y}}$ corresponds to an annulus with a boundary linking the boundary of the x -cylinder in L_K once, and with the other boundary linking zero times. Overall, the partition function resembles an x -annulus ending on L_K , with a linked \hat{y} -annulus on each strand of its multi-cover:

$$\psi(x) =: \sum_{r \geq 0} \left(\frac{1}{1-\hat{y}}\hat{x} \right)^r :=: \frac{1}{1-\frac{1}{1-\hat{y}}\hat{x}} : \quad (3.26)$$

The corresponding recursion relation is

$$\left(1 - \left(\frac{1}{1-\hat{y}}\hat{x} \right) \right) \psi = 1, \quad (3.27)$$

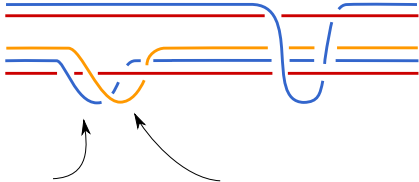
equivalent, upon left-multiplication by $1 - \hat{y}$, to the more familiar

$$(1 - \hat{y} - \hat{x})\psi = 0. \quad (3.28)$$

As remarked above, a single vortex would contribute $q^{2k}x^r$ corresponding to a Wilson line. On the geometric side, we repackage Wilson lines into linked holomorphic annuli. On the gauge theory side of $T[L_K]$, this repackaging corresponds to the definition of equivariant vortices.

Given this, we now propose to think about an equivariant vortex in the theory $T[L_K]$ simply as a configuration of the form above: on level d , there are d parallel copies of the central curve linked in the nested way by basic annuli, see Fig. 5.

We next consider the corresponding procedure applied to a μ times around generator. We propose that such generators become multiples of μ with constants and



$\exp\left(-\sum_d \frac{y^d}{d}\right) = \frac{1}{1-y}$
 $\exp\left(\sum_d \frac{(-ty)^d}{d}\right) = 1 + ty$

total contribution $: \frac{1+ty}{1-\hat{y}} \hat{x} \frac{1}{1-\hat{y}} \hat{x} :$

Fig. 6 A degree 2 generator with constants pushed down. The trivializations of the normal bundles to the annulus boundaries in the Lagrangian differs. This affects the signs in the count and correspond on the refined level to distinct t -powers

anti-constants attached on all intermediate covers. The constant and anti-constant push down to the boundary as almost identical annuli, where the second annulus has a twist in the trivialization on the boundary corresponding to t^κ with integer odd κ .

Let $\nu \in \mathbb{N}$ be a divisor of μ , and consider a contribution to the partition function of the form

$$\frac{x^\mu}{1 - q^{2\nu}}. \quad (3.29)$$

To refine this, we first write it in the form

$$: \hat{x}^{\mu-\nu} \frac{1}{1-\hat{y}} \hat{x}^\nu : \quad (3.30)$$

and then introduce a sequence of annuli and anti-annuli as follows

$$: \underbrace{\frac{1+t^{\text{odd}}\hat{y}}{1-\hat{y}}\hat{x} \cdots \frac{1+t^{\text{odd}}\hat{y}}{1-\hat{y}}\hat{x}}_{\mu-\nu} \frac{1}{1-\hat{y}}\hat{x} \underbrace{\frac{1+t^{\text{odd}}\hat{y}}{1-\hat{y}}\hat{x} \cdots \frac{1+t^{\text{odd}}\hat{y}}{1-\hat{y}}\hat{x}}_{\nu-1} : \quad (3.31)$$

The refinement does not just depend on μ , but also on a choice of divisor ν . This rule therefore leaves room for several possibilities, and we will discuss some of these in Sect. 6 and “Appendix B”.

For illustration consider the case $\mu = 2$, $\nu = 1$. Figure 6 shows the configuration for a twice-around generator with contribution

$$: \frac{1+t^{\pm 1}\hat{y}}{1-\hat{y}}\hat{x} \frac{1}{1-\hat{y}}\hat{x} : \quad (3.32)$$

$$\begin{aligned}
 & \text{Diagram 1} = q^4 \text{Diagram 2} = \text{Diagram 3} \\
 & \text{(Uses } \text{Diagram 4} = q \text{Diagram 5} \text{ , not true in } u(1) \text{ skein)} \\
 & \sum_{d_1, d_2 > 0} \text{Diagram 6} = \sum_{d_1, d_2 > 0} \text{Diagram 7} + \text{Diagram 8} + 1 \\
 & \frac{1}{(1-q^2)^2} = \frac{1+q^2}{(1-q^2)(1-q^4)}
 \end{aligned}$$

Fig. 7 Contributions on second level from two unlinked basic disks

Remark 3.3 The homology generators in (3.31) in general do not correspond to the basic disk generators, such as (3.17). For example the two generators in (3.32) do not correspond one-by-one to the two basic twice-around disks in Fig. 7. This indicates that there are collections of basic disks that are categorifed together, and then cannot be categorifed individually.

To illustrate the procedure, we next consider the second level of a system of two unlinked basic disks. We must express the configuration of two strands with an annulus linking each in terms of our standard basis, which leads to the counting of intersections presented in Fig. 7. In the first line we compute the powers of q arising from a singly-wrapped annulus linking with each disk boundary, resulting in q^{2+2} times the unlinked configuration (with annuli removed). As explained in the second line of the figure, this identity relies on the use of a projection from the $U(1)$ skein to the algebra of $U(1)$ Chern–Simons Wilson lines, which is characterized by the ‘half skein relation’ discussed earlier. In the last diagram on the first line we illustrate another use of this relation, whereby the same q^4 factor could arise from a single curve boundary linking now both disks. The third line illustrates the geometric interpretation of the identity reported at the bottom of the figure, where the two terms in the numerator correspond to each of the two summands, and the factors $(1-q^2)$ and $(1-q^4)$ in the denominator arise from linking with annuli linking, respectively, one of the disks, and both of them, recall Fig. 5.

We next look at this way of expanding states in terms of vortices and their Hilbert spaces. Consider an equivariant vortex. Its partition function is given by

$$\psi(x, q) = \sum_{d \geq 0} \frac{x^d}{(1-q^2) \cdots (1-q^{2d})}. \quad (3.33)$$

Expanding the denominators using geometric series, it is convenient to think of the Hilbert space at level d as follows. Consider the points in the simplex $x_1 \geq x_2 \geq \cdots x_d \geq 0$ with integer coordinates (n_1, \dots, n_d) . The dimension of the Hilbert

space of states with q -charge k is then the number of points in the intersection between the simplex and the plane $\sum_{j=1}^d x_j = k$.

The Hilbert space of mixed states of two vortices on level two as above looks like the integral points over the first quadrant and can be expressed as two copies of the simplex, one shifted by multiplication by q^2 . Similarly, one generator going μ times around corresponds to the points along the diagonal $x_1 = \dots = x_\mu$ and can be expressed as a sum of shifted simplices. This indicates that refinement applies to the Hilbert spaces associated to vortices individually.

We give one final perspective on vortices and homology. Viewing a vortex as an $U(1)$ -invariant fixed point in \mathbb{C} , we may compute its contribution to the partition function by Bott localization. Here we change coordinates and think of the d -fold vortex as a point in the configuration space of d points in \mathbb{C} thought of as the space of polynomials using the relation between roots and coefficients. The contribution

$$\frac{1}{(1 - q^2) \cdots (1 - q^{2d})} \quad (3.34)$$

now arises as the equivariant Chern character. For a μ times around generator, only the top degree coefficients of the polynomials are fixed, others are free to vary. This means we have a corresponding $\mathbb{C}^{\mu-1}$ family of fixed points with similar action on normal bundles. The contribution from the corresponding Bott manifold is

$$\frac{1}{(1 - q^{2d})} \cdot [(\mathbb{CP}^1)^{d-1}], \quad (3.35)$$

where we have replaced \mathbb{C} with \mathbb{CP}^1 and a fixed point also at infinity.

3.3 M2-branes wrapping holomorphic curves

In this section we discuss the physical and geometric interpretations of refinement, connecting the conjectures of [41] to our interpretation of the knot-quiver correspondence [8, 9]. The 3d $\mathcal{N} = 2$ index (2.20), proposed by [41], corresponds to the refined partition function of knot invariants. However, this index is well-defined if not just one, but *two* supercharges are preserved in the Omega-background and with an M5-brane inserted along $L \times S^1 \times \mathbb{R}^2$. We will now provide motivation for the existence of this additional supercharge, based on the presence of a certain geometric $U(1)$ symmetry, expanding on a suggestion of [41]. Eventually, this will lead us to a geometric interpretation of the R-charges of BPS states in terms of ‘self-linking densities’, consistent with our previous observations in [8]. Then, together with the study in Sect. 3.2, this gives our generalized quiver partition function.

The analysis of preserved supersymmetries that we develop here takes a different perspective from the one in Sect. 2.4. There we started with supercharges of the 5d theory engineered by X and examined which ones survive in presence of the Omega-background, and eventually also in presence of the M5-brane on $L \times S^1 \times \mathbb{R}^2$. Here we shall start with the worldvolume supersymmetry on the M5 and analyze how it is broken by introducing the Calabi–Yau background and by placing the brane on

L . An interesting novelty of this perspective is that it will clarify a little-appreciated consequence of the $U(1)$ symmetry postulated in [41]. As we will show, the existence of a $U(1)$ symmetry corresponds to a point in the moduli space of $T[L]$ with enhanced supersymmetry.

3.3.1 Conserved supercharges in the generic case

We study M-theory on the resolved conifold $X = \mathcal{O}(-1) \oplus \mathcal{O}(-1) \rightarrow \mathbb{CP}^1$ times $S^1 \times \mathbb{R}^4$, with an Omega-deformation turned on. This consists of rotations of the planes $\mathbb{R}^2 \times \mathbb{R}^2$ by independent phases $\epsilon_{1,2}$ when going around the S^1 [38, 39].⁵

The Calabi–Yau background preserves eight supercharges. This amount of supersymmetry is further reduced if we consider an M5-brane wrapped on a special Lagrangian submanifold $L \subset X$ times $S^1 \times \mathbb{R}_{\epsilon_1}^2$. Recall that a special Lagrangian is a Lagrangian calibrated by the holomorphic top form on X , which must have a constant phase along L , the phase determines which supercharges are preserved and which are broken by the M5-brane. Under a genericity assumption, such a configuration preserves four supercharges. Let us review how this works.

In a flat space the theory on an M5-brane would be the abelian 6d (2,0) SCFT, with 16 supercharges transforming as $(\mathbf{4}, \mathbf{4})$ spinors under $Spin(1, 5) \times Spin(5)$, with the second factor corresponding to the R-symmetry group. With the Calabi–Yau background, the latter is broken to $Spin(3) \times Spin(2)$, where $Spin(3)$ is a subgroup of the local rotations on X which leave L fixed, and $Spin(2) \simeq U(1)_2$ is the group of rotations of $\mathbb{R}_{\epsilon_2}^2$. The (2,0) 6d supercharges thus decompose as follows:

$$(\mathbf{4}, \mathbf{4}) \rightarrow (\mathbf{2}, \mathbf{2}; \mathbf{2})_{+1/2} \oplus (\mathbf{2}, \mathbf{2}; \mathbf{2})_{-1/2} \quad (3.36)$$

as representations of

$$\underbrace{Spin(3)_{TL} \times Spin(1, 2)_{S^1 \times \mathbb{R}_{\epsilon_1}^2}}_{\subset Spin(1, 5)} \times \underbrace{Spin(3)_{NL} \times Spin(2)_{\mathbb{R}_{\epsilon_2}^2}}_{\subset Spin(5)}. \quad (3.37)$$

The holonomy on X belongs to an $SU(3) \subset SU(4) \simeq Spin(6)$ subgroup. This induces non-trivial holonomies for both $Spin(3)_{TL}$ and $Spin(3)_{NL}$, further reducing the number of conserved supercharges. The special Lagrangian property of L implies that holonomies of the tangent and normal directions to L are related. This means that to any given loop $\gamma \in \pi_1(L)$ one may associate holonomies for both NL and TL , denoted, respectively, $g_{TL} \in Spin(3)_{TL}$ and $g_{NL} \in Spin(3)_{NL}$. Due to the fact that L is a special Lagrangian of X , these group elements are in fact related to each other, allowing one to perform a topological twist by considering the diagonal subgroup $Spin(3)_{dL} \subset Spin(3)_{TL} \times Spin(3)_{NL}$. Then, spinors in the $(\mathbf{2}, \mathbf{2})$ transform as $\mathbf{2} \otimes \mathbf{2} = \mathbf{1} \oplus \mathbf{3}$, implying that one out of four components is invariant under holonomy.

⁵ Recall that these rotations arise from the diagonal and anti-diagonal combination of Cartan generators of $U(1)_L \times U(1)_R \subset SU(2)_L \times SU(2)_R \simeq SO(4)$, via the identification $(g_L, g_R) = (e^{\epsilon_1 + \epsilon_2}, e^{\epsilon_1 - \epsilon_2})$.

This leaves four conserved supercharges, which transform as

$$(\mathbf{1}, \mathbf{2})_{+1/2} \oplus (\mathbf{1}, \mathbf{2})_{-1/2} \quad \text{under} \quad \text{Spin}(3)_{dL} \times \text{Spin}(1, 2)_{S^1 \times \mathbb{R}_{\epsilon_1}^2} \times \text{Spin}(2)_{\mathbb{R}_{\epsilon_2}^2}. \quad (3.38)$$

These are the four supercharges of $3d \mathcal{N} = 2$ theory $T[L]$ arising on the M5-brane worldvolume, along directions $S^1 \times \mathbb{R}_{\epsilon_1}^2$. This amount of supersymmetry can be preserved under generic conditions under our assumptions, namely for an M5-brane wrapping any special Lagrangian L in any Calabi–Yau threefold X .

3.3.2 Supersymmetry enhancement from a geometric $U(1)$ -symmetry

Following [41], the definition of a refined index requires an additional supercharge in addition to those in (3.38). In view of this we make the following assumption.

Assumption 3.4 The Lagrangian L is diffeomorphic to $S^1 \times \mathbb{R}^2$ and there exists a $U(1)$ -action on L which rotates the S^1 -factor. The corresponding vector field V defines a normal plane \mathbb{R}_V^2 at each point. Then $\partial \mathbb{R}_V^2$ is the contractible meridian on the torus ∂L .

The embedding $TL \subset TX$ defines a dual vector field JV normal to L (J is the complex structure on X). We view JV as the direction in which an M2-brane wrapping a holomorphic curve in X attaches to L . (If the M2 boundary lies along a flow line of V in TL , and the M2 wraps a holomorphic curve in X , its normal is tangent to a flow line of JV in $J \cdot TL \simeq NL$, using the local splitting $TX \simeq TL \oplus NL$.) Let \mathbb{R}_{NL}^2 be the family of planes normal to JV within NL . Now we come to the assumption: the existence of a $U(1)$ -action implies that the holonomy $g_{TL} \in \text{Spin}(3)_{TL}$ is actually *not generic*, but belongs to a subgroup $\text{Spin}(2)_V$ that rotates the planes \mathbb{R}_{TL}^2 tangent to \mathbb{R}_V^2 as one goes around S^1 corresponding to the boundary of a holomorphic curve. Since L is special Lagrangian, $g_{TL} = g_{NL}$ and therefore the holonomy induces a rotation of \mathbb{R}_{NL}^2 . The holonomy $g_V = g_{TL} = g_{NL} \in \text{Spin}(2)_{dL} \subset \text{Spin}(3)_{dL}$, so it rotates both summands in $\mathbb{R}_{TL}^2 \oplus \mathbb{R}_{NL}^2$ by the same amount, leaving fixed the ‘origin’ $S^1 \times \mathbb{R} \subset TL \times NL$, corresponding to the tangent and normal directions of a holomorphic curve wrapped by M2 attaching to L .

Our proposal is to identify $U(1)_I \equiv \text{Spin}(2)_{NL}$ as the R-symmetry of the 5d theory $T_{5d}[X]$ that is necessary to perform a topological twist to preserve additional supercharges leading to a refined index, recall the discussion from Sect. 2.4. We will elaborate on the details shortly.⁶

First, we wish to stress that $U(1)_I$ is an artifact of the string theory setup, and not a property of a garden-variety $3d \mathcal{N} = 2$ theory. On the one hand, while surviving $3d \mathcal{N} = 2$ spinors are invariant under $\text{Spin}(2)_{dL}$, they transform non-trivially under $U(1)_I$. On the other hand, $U(1)_I$ is *not* an automorphism of the $3d \mathcal{N} = 2$ super-Poincaré algebra, i.e., it is not an R-symmetry of the $3d$ theory. To establish these

⁶ This is a subgroup $U(1)_I \subset SU(2)_I$ of the R-symmetry group of the $4d \mathcal{N} = 2$ theory on \mathbb{R}^4 arising from reduction on the M-theory circle. It corresponds to the R-symmetry employed by [38, 39] in the topological twist to define refined partition functions of $4d \mathcal{N} = 2$ gauge theories.

claims, recall that surviving spinors arise from the branching rule $\mathbf{2} \otimes \mathbf{2} = \mathbf{1} \oplus \mathbf{3}$ for $\text{Spin}(3)_{dL} \subset \text{Spin}(3)_{TL} \times \text{Spin}(3)_{NL}$. Also recall that, following the above assumption, we identified a distinguished $\text{Spin}(2)_{TL} \times \text{Spin}(2)_{NL} \subset \text{Spin}(3)_{TL} \times \text{Spin}(3)_{NL}$, whose generators will be denoted J_{TL}^3, J_{NL}^3 . Working in a basis where J_{TL}^3, J_{NL}^3 are diagonal, we may reclassify the spinors in (3.36) as follows:

$$(\mathbf{4}; \mathbf{4}) \rightarrow (\pm 1/2, \mathbf{2}; \pm 1/2)_{+1/2} \oplus (\pm 1/2, \mathbf{2}; \pm 1/2)_{-1/2} \quad (3.39)$$

as representations of the following subgroup of (3.37)

$$\text{Spin}(2)_{TL} \times \text{Spin}(1, 2)_{S^1 \times \mathbb{R}_{\epsilon_1}^2} \times \text{Spin}(2)_{NL} \times \text{Spin}(2)_{\mathbb{R}_{\epsilon_2}^2}. \quad (3.40)$$

Topological twisting with reduced holonomy $\text{Spin}(2)_{TL} \times \text{Spin}(2)_{NL}$ implies retaining those supercharges that are invariant under the diagonal subgroup. In this case, these are the ones with opposite charges $j_V = -j_{JV}$ under $\text{Spin}(2)_{TL} \times \text{Spin}(2)_{NL}$:

$$(\pm 1/2, \mathbf{2}; \mp 1/2)_{+1/2} \oplus (\pm 1/2, \mathbf{2}; \mp 1/2)_{-1/2}. \quad (3.41)$$

This leaves a total of four plus four conserved supercharges, twice the generic amount in (3.38). To lighten notation, we will sometimes omit the representation labels under $\text{Spin}(1, 2)_{S^1 \times \mathbb{R}_{\epsilon_1}^2} \times \text{Spin}(2)_{\mathbb{R}_{\epsilon_2}^2}$, and simply use (j_V, j_{JV}) .

Among these, we can recognize the singlet $\mathbf{1}$ that survived in the general case (3.38). This must be a linear combination proportional to $(1/2, -1/2) - (-1/2, 1/2)$, since it arose as the second anti-symmetric power of $\mathbf{2}$ for the diagonal subgroup $\text{Spin}(3)_{dL}$. Overall, there are four supercharges in the singlet: a $\mathbf{2}$ of $\text{Spin}(1, 2)$ with $j_2 = +1/2$ and another with $j_2 = -1/2$. There is also a second combination of supercharges that is conserved, namely $(1/2, -1/2) + (-1/2, 1/2)$. While this is part of the triplet $\mathbf{3}$ and therefore not invariant under the generic $\text{Spin}(3)_{dL}$, it is nonetheless invariant under the reduced $\text{Spin}(2)_{dL}$. Again, this corresponds to four supercharges. Therefore, our assumptions on the geometry of L and the existence of a $U(1)$ -action imply doubling the supersymmetry from $3d \mathcal{N} = 2$ in the generic setting to $3d \mathcal{N} = 4$ in presence of $U(1)$.⁷

For Lagrangians $L = S^1 \times \mathbb{R}^2$ as above this has the following consequences. From the point of view of the theory $T[L]$ in the generic case, without the additional $U(1)$ -symmetry, the Hilbert space of states is generated by vortices and contains states of fixed vorticity x^r and fixed spin in the $\mathbb{R}_{\epsilon_1}^2$ -plane, q^{2s} . The partition function is a (super)trace which for fixed vorticity x^r gives a Laurent series in q^2 . As the state space is generated by vortices, the coefficients stabilize as the power of q^2 goes to infinity, and the coefficient of x^r can be expressed as $P_r(q^{\pm 2})(q^2; q^2)_r^{-1}$, where P_r is a polynomial with integer coefficients. With additional $U(1)$ -symmetry, there is an additional t -charge that refines this theory and its states. The Hilbert space is now

⁷ This fact was observed also in [41] albeit somewhat implicitly. From a physics viewpoint, this enhancement is also plausible from the viewpoint of the theory $T[L]$ of the unknot conormal. This is $N_f = 1$ SQED, which up to a (neutral) adjoint chiral can indeed be viewed as a $3d \mathcal{N} = 4$ theory in disguise. It is unclear if this enhancement is visible in the theory $T[L]$ for other knot conormals.

a sum of finite dimensional vector spaces of fixed charges $x^r q^{2s} t^l$. As before, after fixing the vorticity x^r the Poincaré polynomial of the vector spaces stabilizes and we can write it as $\mathcal{P}_r(q^{\pm 2}, t^{\pm 1})(q^2; q^2)_{r-1}^{-1}$, where \mathcal{P}_r is a polynomial with positive integer coefficients and such that $\mathcal{P}_r(q^{\pm 2}, -1) = P_r(q^{\pm 2})$.

3.3.3 Omega-background and 3d index

Now we come back to the definition of the refined 3d index (2.20). First we note that, while surviving supercharges are not neutral under $\text{Spin}(2)_{NL}$, neither do they transform in a representation of $\text{Spin}(2)_{NL}$. In this sense $U(1)_I$ is not a symmetry of the $3d \mathcal{N} = 2$ superalgebra. For this reason we consider linear combinations of the two conserved supercharges. In particular, one may view $(1/2, -1/2)$ and $(-1/2, 1/2)$ as being separately conserved. With this change of basis, supercharges transform as representations of $U(1)_I$: the first batch with charge $-1/2$, the second batch with charge $+1/2$. Overall, the surviving supercharges are $(\mathbf{2})_{j_V, j_2}$, where $j_V = -j_{JV}$ and $j_V, j_2 \in \{-1/2, +1/2\}$ are chosen independently. Note that $j_I \equiv j_{JV} = -j_V$ is the charge under $U(1)_I$.

The point of having supercharges with a well-defined charge under $U(1)_I$ is that one can turn on the Omega-background and use the $U(1)_I$ remnant of the 5d R-symmetry to perform a topological twist. The Omega-background means that as we go around the M-theory circle, we perform a rotation of $U(1)_1 \times U(1)_2 \times U(1)_I$. In particular, this breaks $\text{Spin}(1, 2)_{S^1 \times \mathbb{R}^2}$ to $U(1)_1$ and spinors $(\mathbf{2})_{j_V, j_2}$ get labeled by their $U(1)$ charges (j_1, j_2, j_I) . In this notation, the surviving supercharges are those with $j_1 = j_2 = -j_I$, as derived in (2.16). This can be shown to match precisely with the supercharges considered in [41].

3.4 R-charge, homological degree, and self-linking

In this section we provide a geometric analysis of the phenomena discussed in the previous section. The Lagrangian considered there is $S^1 \times \mathbb{R}^2$ and a neighborhood of it in the Calabi–Yau looks like its cotangent bundle $T^*(S^1 \times \mathbb{R}^2)$. We furthermore have a $U(1)$ -action that rotates the S^1 -direction, and which splits the normal bundle of the Lagrangian as $NL = \mathbb{R} \times \mathbb{R}_{NL}^2$. We can therefore write a neighborhood of the locus of the M5-brane as

$$(S^1 \times \mathbb{R}) \times \left(\mathbb{R}_{TL}^2 \times \mathbb{R}_{NL}^2 \right) \times \mathbb{R}_q^2 \times \mathbb{R}_{q^{-1}t}^2 \times S^1, \quad (3.42)$$

where normal directions lie in $\mathbb{R} \times \mathbb{R}_{NL}^2 \times \mathbb{R}_{q^{-1}t}^2$. Here \mathbb{R}_q^2 and $\mathbb{R}_{q^{-1}t}^2$ come from (2.21): they are the planes that are rotated by J_1 and J_2 , respectively. The topological twist reduces the structure group of this bundle to a diagonal $U(1)$ rotating both factors $\mathbb{R}_{NL}^2 \times \mathbb{R}_{q^{-1}t}^2$ in the same way.

3.4.1 Once-wrapped disks

We next read off the t -charge of an M2-brane wrapped on $(S^1 \times \mathbb{R}) \times S^1$. In the Calabi–Yau space this is a holomorphic curve along $S^1 \times \mathbb{R}$. By holomorphicity, its normal variation along the boundary is given by a vector field $(v, Jv) \in \mathbb{R}_{TL}^2 \times \mathbb{R}_{NL}^2$. This implies that, going around a loop in S^1 , the vector field v rotates in \mathbb{R}_{TL}^2 by an amount that equals that of Jv in \mathbb{R}_{NL}^2 . The former furthermore equals the self-linking C_{ii} in L . By the topological twist the rotation of Jv contributes to the t -degree and it follows that the corresponding t -charge of a d -fold cover is $q^{-C_{ii}d}(-t)^{C_{ii}d}$, in line with the conjectural identification of C_{ii} and the homological t -degree [10, 11].

We point out that the origin of the contribution $q^{C_{ii}d^2}$ to the partition function is different: it comes from counting q -power in the $U(1)$ -skein and then passing to homology and (self-)linking. In other words, the quadratic growth of powers of q corresponds to the contribution to the Gromov–Witten invariant from counting generalized holomorphic curves. In physics this corresponds to the open topological string partition function with an A -brane on L , where q arises through the M-theory interpretation of the string coupling constant [2]. There are C_{ii} crossings between d -fold covers of an underlying once-around curve which gives $q^{C_{ii}d^2}$. Overall we have contribution $q^{C_{ii}d^2 - C_{ii}d}(-t)^{C_{ii}d}$ for the d -fold cover of a once-around disk. We stress that this reasoning is based on a picture of M2-branes wrapping d times around, viewed as tightly packed copies of an underlying once-around disk.

Our prescription should recover the contribution to the unrefined partition function in the limit $t = -1$. On this level we should perturb multi-covers of the underlying curve and then count generalized curves. The geometry behind the count is the following. A contribution to C_{ii} can be thought of as an infinitesimal kink. After perturbation we find an actual kink with d^2 crossings; in order for this to be d times a curve in framing C_{ii} , we deform to make all innermost kinks very small and then pull them out, making them infinitesimal again and trading them for framing. This leaves $d(d-1)$ crossings, and summing contributions from all C_{ii} infinitesimal twists we eventually get $q^{C_{ii}d(d-1)}$. This agrees with the specialization to $t = -1$.

Remark 3.5 To round off our discussion on the geometric interpretation of the homological degree of BPS states, we offer yet another reason why such geometric information (the ‘wiggling’ of an M2-brane boundary) should play a role in the definition of the BPS partition function. M2-branes wrapping holomorphic curves produce Wilson lines for the $U(1)$ Chern–Simons theory on L . From the viewpoint of the full 6d $\mathcal{N} = (2, 0)$ theory describing the worldvolume dynamics of a single M5-brane, such Wilson lines correspond to reduction of Wilson surfaces. By supersymmetry, these involve integration along the boundary of the M2 of the abelian 2-form connection, as well as the five scalars. In particular, the latter transform as a vector under the $\text{Spin}(5)$ R-symmetry of the $(2, 0)$ theory. Recalling that R-symmetry corresponds to rotations transverse to the brane, the winding number of these scalars around the brane must correspond to their charge under R-symmetry. At the same time, the scalars parametrize embeddings of M5 in the transverse directions, and in particular they parametrize

the direction along which the M2 ends on M5. Yet again, this suggests that the wigglings of the M2 boundary is captured by the R-charge of a BPS state, which in the setup involving $L \subset X$ is eventually identified with the homological degree.

3.4.2 Multiply-wrapped disks

Our suggestion for refinement for multiply wrapped disks has two sources. The first arises when we express the contribution of the curve in terms of standard vortices, or geometrically in terms of a specific link as described in Sect. 3.2. Here, internal t -charge of the M2-brane is transferred to thin annuli and appears as a difference in framing along their two boundary components. The second comes from an external framing analogous to the framing of the standard basic disks discussed above.

To describe this external t -degree, we refer to Sect. 3.1.2 where multiply wrapped disks are related to disks in orbifolds and consider an M2-brane wrapped on a disk in a degree μ orbifold corresponding to (3.16). The t -charge arises from the $U(1)$ -action on L , and the M2-brane is invariant under this action (rotation along S^1) only if its boundary remains a tightly wrapped μ -fold cover of $S^1 \times \text{point}$. This means that its boundary gives a single Wilson line of charge μ rather than a μ -times around Wilson line of charge 1. As in Sect. 3.4.1, by holomorphicity and the topological twist that identifies rotations in \mathbb{R}_{NL} and $\mathbb{R}_{q^{-1}t}^2$, the t -degree is the framing of this charge- μ Wilson line, which in turn is determined by its self-linking. We define C_{ii} to be the framing density along the μ_i -fold boundary of the M2-brane, thus $C_{ii} \in \frac{1}{\mu_i}\mathbb{Z}$. This means that a single twist of the underlying simple curve corresponds to $C_{ii} = \frac{1}{\mu_i}$. The total twist in the normal bundle is then $C_{ii}\mu_i \in \mathbb{Z}$, which leads to the charge $x_i^d \sim q^{-C_{ii}\mu_i d}(-t)^{C_{ii}\mu_i d}$ for a d -fold cover of the μ -wrapped M2-brane. Next we consider the self-linking contribution to q -degree for generalized curves invariant under the covering transformation. We think of the framing $C_{ii}\mu_i$ of the underlying curve as a collection of infinitesimal kinks. These lift to $C_{ii}\mu_i^2$ kinks, giving the total contribution to the q -degree $q^{C_{ii}\mu_i^2 d^2}$ at the d -fold level of the brane. In summary we then have contributions proportional to $q^{C_{ii}\mu_i^2 d^2 - C_{ii}\mu_i d}(-t)^{C_{ii}\mu_i d}$ at the d -fold covering level.

Similarly to the once-around case, we consider the $t = -1$ specialization of this formula and the contribution to generalized curves after perturbation. As above we consider the lift to the d -fold cover. A μ_i -wrapped curve with $C_{ii}\mu_i^2$ infinitesimal kinks gives $C_{ii}\mu_i^2 d^2$ crossings at the d -fold covering level, after perturbation. In order to lift a curve d times around a curve with framing $C_{ii}\mu_i$, we trade the innermost kinks at $C_{ii}\mu_i$ of the crossings for framing, leaving a net $C_{ii}\mu_i^2 d^2 - C_{ii}\mu_i d$ crossings and hence an overall contribution of $q^{C_{ii}\mu_i d(\mu_i d - 1)}$.

We next consider a degree μ_i basic disk on a more general Lagrangian of topology $S^1 \times \mathbb{R}^2$. Here, as before, we get a $U(1)$ -symmetric boundary of the disk by SFT-stretching. In the limit where the embedded disk is split off, the lower piece close to the Lagrangian can be identified with the complement of the orbifold point in an orbifold disk. The addition of the orbifold point corresponds to adding the embedded disk ‘at infinity’. Again, the existence of a $U(1)$ -action on L implies that all boundaries of holomorphic curves should sit very close to each other, within an infinitesimal

neighborhood of the orbits $S^1 \times \text{point}$. The t -degree is then obtained from the framing of the once-around charge- μ boundary in the plane field normal to the orbits, and the contribution to the refined partition function at level d is $(-t)^{C_{ii}\mu_i d} q^{C_{ii}\mu_i^2 d^2 - C_{ii}\mu_i d}$, exactly as above.

3.5 HOMFLY-PT homology and geometric deformations

Sections 3.3.2 and 3.4 explain how holomorphic disks in a $U(1)$ -symmetric setting, via branched covers with constant ghost bubbles attached, generate symmetrically colored HOMFLY-PT homology. In this section we isolate the ingredients in this description and give a proposal for how they might give rise to a deformation invariant version: holomorphic curves for generic almost complex structures (constrained near the Lagrangian only) give a chain complex with a differential, the homology of which remains invariant and equals certain filtered quotients of HOMFLY-PT homology that recover all of the original HOMFLY-PT homology. Naturally, as a chain complex is not determined by its homology, the chain complexes we propose are not uniquely determined. The guiding principle for our definition is that it should reflect the underlying geometry and that it should model the initial $U(1)$ invariant situation as closely as possible.

3.5.1 Tracing the refined partition function under deformation

Recall the data that gave the generalized quiver partition function from a $U(1)$ -symmetric version of the knot conormal: a collection of numbered basic disks $i \in \{1, \dots, n\}$ together with linking densities C_{ij} measuring linking and self-linking between their boundaries. Here the holomorphic curves are in fact two-level holomorphic buildings in an SFT-stretched complex structure: the outside parts are embedded once punctured spheres, while the inside parts are unbranched covers of the trivial cylinder over the unique geodesic in $S^1 \times \mathbb{R}^2$. In this limit all curve boundaries are multiples of the unique geodesic, and the linking densities C_{ij} appear as the (normalized, relative) framing of these boundary components. We point out that the only curves near the Lagrangian that are invariant under the $U(1)$ -action are these unbranched covers of the punctured disk.

We next consider a class of deformations for which the picture above persists. To this end we express the data we have as follows: a collection of \mathcal{M}_i , moduli spaces of holomorphic punctured spheres asymptotic to Reeb orbits, and trivial cylinders near L_K with linking densities C_{ij} , where C_{ij} are integers if $\mu_i \neq \mu_j$ and $C_{ij} \in \frac{1}{\mu} \mathbb{Z}$ if $\mu_i = \mu_j = \mu$. We will now keep the trivial cylinders and linking densities C_{ij} , but allow for deformations of the outside curves. More precisely, we consider the moduli spaces \mathcal{M}_i for varying almost complex structure J_s on the outside part, while we keep J fixed and equal to the stretched structure near the negative end of the symplectic manifold (i.e., near the Lagrangian).

To organize this, we note that the homology data of each punctured sphere in \mathcal{M}_i is characterized by its Reeb multiplicity μ_i , its homology class a_i , and its 4-chain intersection q_i . We write $\mathcal{M}(\mu, \alpha, v; \chi = 1)$ for the moduli space of all embedded

punctured spheres i with $\mu_i = \mu$, $a_i = \alpha$, and $q_i = v$. Then

$$\mathcal{M}(\mu, \alpha, v; \chi = 1) = \bigcup_{\{i: \mu_i=\mu, a_i=\alpha, q_i=v\}} \mathcal{M}_i$$

is a space with a finite number of points, one for each disk i that has these quantum numbers. Furthermore, if their orientations are twisted by their orientation data at the boundary, all the points come with a positive sign.

We next study the moduli spaces $\mathcal{M}_s(\alpha, v, \mu; \chi = 1)$ corresponding to a 1-parameter family of almost complex structures J_s . We argue that a generic 1-parameter family gives a cobordism of moduli spaces with the following properties. At generic times s the actual spheres in the moduli space admit standard neighborhoods such that any other holomorphic curve inside such a neighborhood must be a branched cover of the basic sphere. This is analogous to what happens in the neighborhood of the central sphere in the resolved conifold: here any other holomorphic curve must lie completely over the central sphere. There are finitely many instances where there are Morse modifications in our 1-dimensional cobordism. Such instances correspond to birth/death of curves. Also for this phenomenon, there is a standard neighborhood of the sphere at the critical moment, that contains only the central curve and the two redundant curves for nearby times, while all other curves are multiple covers of these. We mention that also moduli spaces $\mathcal{M}(\alpha, \mu, v; \chi = \chi_0)$ of punctured embedded curves of Euler characteristic $\chi_0 < 1$ can be handled in the the same way and that our conjecture says that these moduli spaces are empty in the $U(1)$ -symmetric situation.

We next discuss how one might establish such a structural result, i.e., how to find cobordisms of basic $U(1)$ invariant curves with neighborhoods that contain all holomorphic curves and which objects the corresponding moduli spaces actually contain. One starts with the simplest punctured spheres with once-around boundary. Here the result on moduli spaces is straightforward: by minimality there can be no splitting and the moduli space gives a cobordism. We next consider embedded punctured spheres with boundaries that go twice around. The entire moduli space for these must also include certain two-level curves: two once-around spheres on the outside, with a branched covered trivial cylinder in the symplectization level. We do not perturb the cylinder, but equip it with both an obstruction bundle and with gluing data to the spheres above it, which then allows us to count. Once we check that these configurations contain all possible limits, we would get the required cobordism. The only configuration not accounted for in the SFT-compactification is then the one given by a branch-covered cylinder glued to two copies of the same once-around sphere. However, since the once-around sphere has a standard neighborhood, the whole curve would have to agree with this configuration at earlier times and then already from the first step, which contradicts our sphere starting out as embedded. After establishing the existence of neighborhoods for twice around disks, the argument proceeds to the next Reeb orbit covering level. It is clear how to continue: include all several level curves with branched covered cylinders at the negative end, the existence of the standard neighborhoods at earlier steps shows that the moduli space gives a 1-dimensional cobordism. Thus if we start from a finite number of moduli spaces, the cobordism class never changes as we deform J_s . The same argument works to show that the algebraic

count of embedded higher genus curves equals zero since there are no such curves at the starting $U(1)$ -symmetric configuration. We point out that an important property of the knot conormal used in this argument is that it can be placed so that all outside curves go positively around the basic geodesic. This is arranged by placing the conormal close to the toric Lagrangian on an external leg of the conifold toric diagram.

3.5.2 Partition functions with values in chain complexes

As explained in Sect. 3.5.1, we can find the symmetrically colored HOMFLY-PT homology from the moduli spaces of embedded curves $\mathcal{M}(\alpha, \nu, \mu; \chi = 1)$ for any generic almost complex structure with standard negative end near the Lagrangian, provided we know the linking information. For an actual deformation this is easy to trace, but it may also be useful to have a bifurcation analysis version of this. The behavior of the full chain complex is somewhat complicated, see Sect. 3.6, but certain filtered quotients, from which the full homology can be recovered, are simpler to trace. In this section we introduce these quotients and study them under homotopy.

We start by considering the filtration we will use for the $U(1)$ -symmetric configuration. Let K be a knot and Q its associated generalized quiver with set of nodes Q_0 . We subdivide the nodes according to their multiplicity and write $Q_0 = \bigcup_{\mu=1}^M Q_0(\mu)$, where $Q_0(\mu)$ is the set of nodes corresponding to disks of multiplicity μ . To each node j we associate a quiver variable x_j and basic charges

$$x_j = x^{\mu_j} q^{q_j} a^{a_j} q^{C_{jj}\mu_j} (-t)^{C_{jj}\mu_j}. \quad (3.43)$$

Then the refined partition function has the form

$$P_Q(x_1, \dots, x_m, q, t) = \sum_r h_r(a, q, t) \frac{x^r}{(q^2; q^2)_r}, \quad (3.44)$$

where h_r is a Laurent polynomial with positive integer coefficients that—we conjecture—equals the Poincaré polynomial of HOMFLY-PT homology in the r^{th} symmetric coloring. Here we will categorify this in a trivial way. We view the monomials in $h_r(a, q, t)$ together with the denominators as generators of a vector space of equivariant vortices of corresponding charges. Explicitly, to a summand $n \frac{a^k q^s t^v}{(q^2; q^2)_r}$, $n > 0$, we associate a vector space \mathbb{C}^n spanned by n equivariant vortices of charges $a^k q^s t^v x^r$. We further think of these vector spaces as a chain complex with the trivial differential. We write the chain complex $\mathcal{C}_0 = \bigoplus_r \mathcal{C}_{0,r}$ and its homology $\mathcal{H} = \bigoplus_r \mathcal{H}_r$, where the extra subscript 0 refers to the starting point of the deformation we will consider. As the differential δ_0 on \mathcal{C}_0 is trivial, we have $\mathcal{C}_0 = \mathcal{H}$.

We next consider a filtration on \mathcal{C}_0 . The vector space $\mathcal{C}_{0,r}$ is spanned by equivariant vortices. Each such vortex is a bound state of one or more basic disks x_j : it arises in the refined partition function as a coefficient of a unique combination of monomials of the form $x_{j_1}^{k_1} \cdots x_{j_l}^{k_l}$ and we define its filtration degree as the maximal multiplicity μ_{j_i} of the quiver variables x_{j_i} in this monomial. We then define $\mathcal{C}_{0,r}(k) \subset \mathcal{C}_{0,r}$ as

the subspace spanned by vortices of filtration degree $\leq k$, and $\mathcal{C}_0(k) = \bigoplus_r \mathcal{C}_{0,r}(k)$. Then

$$\mathcal{C}_0(1) \subseteq \mathcal{C}_0(2) \subseteq \cdots \subseteq \mathcal{C}_0(M) = \mathcal{C}_0. \quad (3.45)$$

Consider now the quotient $\mathcal{C}_0(k)/\mathcal{C}_0(k-1)$. It is rather complicated, spanned by all bound states of nodes of multiplicity $\leq k$ that contain at least one node of multiplicity k . However, if we restrict to the degree r part of the complex $\mathcal{C}_{0,r}(r)/\mathcal{C}_{0,r}(r-1)$, we find something simpler; here any monomial is a combination of multiplicity r generators and we can write the contribution to the generalized quiver partition function as a sum of collections of vortices of the following form:

$$h_j(q, t) \frac{x_j}{(q^2; q^2)_r}, \quad (3.46)$$

where $h_j(q, t)$ is a polynomial with positive coefficients.

We define a new chain complex of equivariant vortices generated only by the r times around nodes. We take $\mathcal{D}_0(r)$ to be the vector space of equivariant vortices corresponding to r times around disks. Recall that such vortices have partition functions

$$\frac{x^{rd}}{(q^{2r}; q^{2r})_d}. \quad (3.47)$$

We define $\mathcal{D}_0(r)$ to be the chain complex with trivial differential associated to the unrefined partition function, except for substituting the variables x_i by the above powers of x, a, q, t :

$$\check{P}_{Q(r)}(x, q, t) = P_{Q(r)}(\mathbf{x}; q^\mu), \quad (3.48)$$

where q^μ denotes the substitution of denominators $(q^2; q^2)_d$ by $(q^{2\mu}; q^{2\mu})_d$ in the quiver partition function (2.6) and where $Q_K(r)$ denotes the multiplicity r part of the quiver Q_K , i.e., all the degree r nodes and all weighted arrows connecting them (weighted according to (1.1)).

Let $\mathcal{G}(r)$ denote the homology of $\mathcal{D}_0(r)$ with the trivial differential. Geometrically, this is the vector space generated by the Bott equivariant vorticity r vortices as in (3.35). We will show below that for a generic path of complex structures J_s we can define a family of complexes \mathcal{D}_s with differentials δ_s such that the homology of δ_s is isomorphic to \mathcal{G} for each generic s .

Remark 3.6 We have $\mathcal{D}_0(1) = \mathcal{C}_0(1)$. Furthermore, since the quiver is finite, there is $R > 0$ such that $\mathcal{G}_s(r) = 0$ for $r > R$ and if we know $\mathcal{G}_{s,r}(r)$ for all $r \leq R$, then together with the framing density matrix C_{ij} , half-framing information, and the refinement information for all nodes of multiplicity ≥ 1 , we can recover \mathcal{H} .

We next consider redundant nodes. Consider a quiver node i of multiplicity $\mu_i = \mu$ with associated quiver variable x_i and linking density $C_{ii} = 0 \in \frac{1}{\mu}\mathbb{Z}$. Its μ -refined

partition function is given by

$$\check{P}_{(i)}(x, q, t) = \sum_{d_i} \frac{x_i^{d_i}}{(q^{2\mu}; q^{2\mu})_{d_i}}. \quad (3.49)$$

Consider also a quiver node i^* of multiplicity $\mu_{i^*} = \mu$ and with linking density $C_{i^*i^*} = \frac{1}{\mu}$. Then the μ -refined partition function of i^* in the quiver variable x_{i^*} reads

$$\check{P}_{(i^*)}(x, q, t) = \sum_{d_{i^*}} (-1)^{d_{i^*}} q^{\mu^2 d_{i^*}^2} \frac{x_{i^*}^{d_{i^*} \mu}}{(q^{2\mu}; q^{2\mu})_{d_{i^*}}}, \quad (3.50)$$

and setting $x_{i^*} = q^{-\mu}(-t)x_i$ we find that $P_{i,t=-1}(x_1) \cdot P_{i^*,t=-1}(x_{i^*}) = 1$. We call the pair (i, i^*) the degree μ *redundant pair* of linking density zero. We think of the redundant pair as a two node generalized quiver with nodes i and i^* with linking density matrix

$$\begin{pmatrix} 0 & 0 \\ 0 & \frac{1}{\mu} \end{pmatrix}. \quad (3.51)$$

We define the degree μ redundant pair of linking density $f \in \frac{1}{\mu}\mathbb{Z}$ by a fractional framing change on the linking density zero pair. Thus its linking density matrix is instead

$$\begin{pmatrix} f & f \\ f & f + \frac{1}{\mu} \end{pmatrix}. \quad (3.52)$$

Since framing change alters the partition function of a quiver according to the substitution $x_i \mapsto q^{\mu_i^2 f}(-t)^{f\mu_i} x_i$, the unrefined partition function of a redundant pair is still 1.

The degree 1 redundant pair is a ‘standard’ redundant pair noticed first in [11] and explained in terms of multi-cover skein relations in [9].

Remark 3.7 We comment on the geometry of redundant pairs. Think of the node 1_0 as an orbifold disk. Its corresponding canceling disk should have underlying framing different by one twist. We can imagine undoing the twist and picking up μ_1 4-chain intersection, the shift in quiver variable $q^{-\mu_1}$ can be thought of as 4-chain intersections canceling these and returning the original disk.

The fractional framing change of the redundant pair corresponds to framing in the μ_1 -fold cover where the lift lives and indicates that a framed redundant pair cannot be equivariantly separated.

We next define a set of chain complexes $\mathcal{D}_0(r)$ for integers $r > 0$. This complex is generated by the punctured spheres in the moduli spaces $\mathcal{M}(\mu, \alpha, \nu)$ where $\mu = r$. Let the linking matrix be C_{ij} . Consider the 1-parameter family J_s of almost complex structure and the corresponding moduli spaces $\mathcal{M}_s(\mu, \alpha, \nu)$. When J_s moves away from

the $U(1)$ -symmetric configuration, the moduli spaces undergo Morse modifications at birth/death instances and is otherwise unchanged. We will describe corresponding changes in the chain complex. At a birth moment s_0 , the chain complex at times slightly before s_0 , $\mathcal{D}_{s_0-\epsilon}(r)$, changes by addition of a redundant pair to a new chain complex $\mathcal{D}_{s_0+\epsilon}(r)$ with differential $\delta_{s_0+\epsilon}$ such that the homology of $\delta_{s_0+\epsilon}$ is equal to that of $\delta_{s_0-\epsilon}$ (and hence still equal to $\mathcal{G}(r)$). Below we show that such a differential exists. At death moments the chain complex changes by removal of a redundant pair, and similarly the homology is unchanged.

3.5.3 The differential on \mathcal{D}_ϵ

We show that the required differential exists. Let Q be a generalized quiver with m nodes of vorticity μ . The birth of a redundant pair of nodes involves modifying Q by adding a pair of nodes which link with all previous m nodes in the same way, resulting in a new quiver Q' . The signs of the two spheres in the redundant pairs are opposite. This means that their framings differ by one unit when the orientation data are pushed to the boundary, and the disks must form a redundant pair as the partition function stays unchanged at the unrefined level.

Therefore $P_{Q'} = P_Q \cdot 1$ where the identity is represented as follows

$$1 = \sum_{r \geq 0} \sum_{d=0}^r (-1)^{(\rho+1)r+d} q^{\mu \rho r^2 + \mu(r-d)^2 + 2\mu r(\alpha_1 d_1 + \dots + \alpha_m d_m)} \frac{x_{m+1}^d x_{m+2}^{r-d}}{(q^{2\mu}; q^{2\mu})_d (q^{2\mu}; q^{2\mu})_{r-d}}. \quad (3.53)$$

Here μ is the multiplicity of the redundant pair of disks $x_{m+1} \sim x_{m+2} \sim x^\mu$, while $\rho = \mu C_{m+1,m+1} = \mu C_{m+2,m+2} - 1 = \mu C_{m+1,m+2}$ is the integer self- and mutual linking of the pair of new nodes, and $\alpha_i = C_{i,m+1}\mu_i = C_{i,m+2}\mu_i$ is the linking between the pair and the i^{th} pre-existing node. The identity is true provided that $x_{m+2} = q^{-\mu} x_{m+1}$, and reduces to [9, Eq. (4.19)] when $\mu = 1$.

Recall that we allow $C_{m+1,m+2}$ to be valued in $\frac{1}{\mu}\mathbb{Z}$ since $\mu_{m+1} = \mu_{m+2} = \mu$. In connection with this, note that at a redundant pair of disks the $U(1)$ -symmetry has necessarily been broken, disk boundaries are no longer tightly packed, and single strands of a μ -times around disk can link with strands of other disks individually. For perturbations not too far from the $U(1)$ -symmetric setting, we need to relax integrality of mutual linking C_{ij} only for pairs of disks with the same homology data (the same μ - and a -degree). More general perturbations may however require further relaxing integrality of the linking matrix. Understanding this would require a further study of the geometry of perturbations, which we leave to future work.

At the refined level (3.53) ceases to hold. By our general rules on the assignment of homological degree, we refine the partition function by setting $x_{m+2} = -tq^{-\mu} x_{m+1}$, which reflects the fact that $\mu C_{m+2,m+2} = \mu C_{m+1,m+1} + 1$. This deforms (3.53) as

follows:

$$\begin{aligned}
 & \sum_{r \geq 0} x_{m+1}^r \sum_{d=0}^r (-1)^{(\rho+1)r+d} q^{\mu \rho r^2 + \mu(r-d)^2 + 2\mu r(\alpha_1 d_1 + \dots + \alpha_m d_m)} \\
 & \quad \frac{(-t q^{-\mu})^{r-d}}{(q^{2\mu}; q^{2\mu})_d (q^{2\mu}; q^{2\mu})_{r-d}} \\
 & = \sum_{r \geq 0} x_{m+1}^r (-1)^{\rho r} q^{\mu(\rho+1)r^2 - \mu r + 2\mu r(\alpha_1 d_1 + \dots + \alpha_m d_m)} \\
 & \quad \frac{(1 + t q^{2\mu(r-1)}) \dots (1 + q^{2\mu} t)(1 + t)}{(q^{2\mu}; q^{2\mu})_r}.
 \end{aligned} \tag{3.54}$$

While this is not equal to 1 anymore, it is an expression of the form

$$1 + (1 + t) \sum_{r \geq 1} \frac{x^{\mu r}}{(q^{2\mu}; q^{2\mu})_r} \cdot f_r(a, q, t), \tag{3.55}$$

where the Laurent polynomial $f_r(a, q, t)$ is a sum of integer multiples of monomials.⁸ We require the differential to map a vortex corresponding to a monomial $q^s a^r t^k$ in $1 \cdot f_r(a, q, t)$ to $q^s a^r t^{k+1}$ in $t \cdot f_r(a, q, t)$ and to be 0 on all other vortices. This gives a differential of degree $(a, q, t) = (0, 0, 1)$ with desired properties.

Remark 3.8 It is crucial to keep the denominators $(q^{2\mu}; q^{2\mu})_r$ of Bott-equivariant vortices here. Switching to the usual denominator $(q^2; q^2)_{\mu r}$ of standard equivariant vortices spoils the positivity of coefficient in the numerator. The positivity of the coefficients is what allows us to define the required differential, which then allows us to interpret the partition function as the Poincaré polynomial of the complex \mathcal{D} of Bott-vortices defined above. In order to carry out the same program for a chain complex generated by standard vortices, one would have to introduce other types of generators, see Sect. 3.6 for an analogous discussion.

Remark 3.9 The differential δ_s defined in this way depends on the path of almost complex structures J_s as well as choices of near which basic disks the redundant pair should be located. It would be interesting to consider the construction of chain homotopies of different differentials on \mathcal{D}_s that came from different paths. (Note that any two such paths are homotopic since the space of almost complex structures is contractible.)

Remark 3.10 In the same way as combinations of basic disks give the HOMFLY-PT homology in (3.31), one can get the HOMFLY-PT homology from the homology of the complex \mathcal{D} .

⁸ The overall sign is fixed by $(-1)^{\rho r}$ and there are no cancellations inside this expression.

3.6 Unlinking and multiple disks

When defining the differentials δ_s in the complexes \mathcal{D}_s in Sect. 3.5.2, we worked with a stretched almost complex structure that allowed us to keep holomorphic disk boundaries fixed. This was essential when demonstrating the existence of chain complexes still generated by equivariant vortices and with invariant homology, along paths of almost complex structures. Similar constructions not keeping all symmetry require additional generators of new types. To illustrate this, we consider the basic unlinking operation in the presence of nodes with multiplicity > 1 .

Recall that in the case of embedded disks there are, besides the birth/death of redundant pairs of nodes, also other operations on quivers that do not affect the partition function [9]. The most basic such move is unlinking, where two linked nodes are replaced by two nodes with mutual linking decreased by one unit, together with a new node obtained by gluing the other two. We discuss the counterpart of this for multiply wrapped disks, and show that such an identity involving multiply wrapped disks cannot exist, unless we introduce certain additional holomorphic objects. This then indicates that $U(1)$ -invariant configurations are essential for defining HOMFLY-PT homology, and that a much more involved description is required if one allows to break that symmetry near the boundary.

To see how unlinking works for multiply covered disks, we consider crossing a simple disk in class x_1 with a μ -times around disk in class x_2 . The contribution to the partition function from a μ -times around disk can be written as a product

$$\Psi_{q^\mu}(x_2) = \Psi_q(\zeta)\Psi_q(e^{\frac{2\pi i}{\mu}}\zeta) \cdots \Psi_q(e^{\frac{2\pi i(\mu-1)}{\mu}}\zeta), \quad (3.56)$$

see Eq. (4.2), where here ζ is a root of $\zeta^\mu = x_2$, and Ψ_q is defined in. We next assume that there is a disk x_1 that links once equivariantly with x_2 . To see the partition function after unlinking, we average over all possible unlinkings, and get

$$\Psi_q(x_1)\Psi_q(x_2) \cdot \left(\frac{1}{\mu} \sum_{k=0}^{\mu-1} \Psi_q^{-1}(qe^{\frac{2\pi ik}{\mu}}\zeta x_1) \right) = \Psi_q(x_1)\Psi_q(x_2)\phi(x_2x_1^\mu), \quad (3.57)$$

where

$$\phi(x_2x_1^\mu) = \sum_{d=0}^{\infty} (-q)^{\mu^2 d^2} \frac{(qx_2x_1^\mu)^d}{(q^2; q^2)_{\mu d}}. \quad (3.58)$$

This latter function is a new contribution from a μ -times around disk with a simple disk attached. For unlinking of more complicated disks we would similarly get new objects, and more of them when we unlink further. To categorify these changes, we would need to find contributions on the refined level as well as necessary differentials.

4 Recursion relations for generalized quiver partition functions

A fundamental property of partition functions of knot invariants is the fact that they obey certain types of recursion relations. In [8, 9] we showed that quiver partition functions share this property, in fact leading to a decomposition of (quantum) A-polynomials (and generalizations thereof) into universal building blocks. In this section we review these properties, and extend them to include generalized partition functions with multiply wrapped disk nodes.

4.1 Non-commutative variables

In [9] it was shown that the partition function of a quiver Q can be conveniently expressed by introducing non-commutative variables

$$\mathbb{P}_Q = \Psi_q(X_m) \cdot \Psi_q(X_{m-1}) \cdots \Psi_q(X_1), \quad (4.1)$$

where

$$\Psi_q(\xi) = \sum_{k \geq 0} \frac{q^k}{(q^2; q^2)_k} \xi^k, \quad X_i = (-1)^{C_{ii}} q^{C_{ii}-1} \hat{x}_i \hat{y}_i^{C_{ii}} \prod_{j < i} \hat{y}_j^{C_{ij}}. \quad (4.2)$$

The non-commuting variables obey quantum torus relations $X_i X_j = q^{2A_{ij}} X_j X_i$, where A is an antisymmetrization of the quiver matrix determined by a choice of ordering of nodes. This is based on the convention that $\hat{y}_i \hat{x}_j = q^{2\delta_{ij}} \hat{x}_j \hat{y}_i$. The quiver partition function is obtained from \mathbb{P}_Q by normal ordering, defined as taking all the \hat{y}_i variables to the right, where they become trivial and the action of \hat{x}_i is just multiplication by x_i :

$$P_Q = : \mathbb{P}_Q :. \quad (4.3)$$

We can apply this idea to generalized partition function and write (1.2) in operator form, as a generalization of (4.1). We single out a node, whose variable we denote x_0 , and rewrite the partition function as follows:

$$\begin{aligned} P_Q &= \sum_{d_0, d} \left[(-1)^{C_{00}\mu_0 d_0 + \sum_i C_{ii}\mu_i d_i} q^{C_{00}\mu_0^2 d_0^2 + 2 \sum_i C_{0i}\mu_0 \mu_i d_0 d_i + \sum_{i,j} C_{ij}(\mu_i d_i)(\mu_j d_j)} \right. \\ &\quad \times \left(\frac{x_0^{d_0}}{(q^{2\mu_0}; q^{2\mu_0})_{d_0}} \right) \left(\prod_{i>0} \frac{x_i^{d_i}}{(q^{2\mu_i}; q^{2\mu_i})_{d_i}} \right) \Big] \\ &=: \left[\sum_{d_0} (-1)^{C_{00}\mu_0 d_0} q^{C_{00}\mu_0^2 d_0^2} \left(\frac{\hat{x}_0^{d_0}}{(q^{2\mu_0}; q^{2\mu_0})_{d_0}} \right) \left(\prod_{i>0} \hat{y}_i^{\mu_i C_{0i}} \right)^{\mu_0 d_0} \right] \\ &\quad \times \left[\sum_d (-1)^{\sum_i C_{ii}\mu_i d_i} q^{\sum_{i,j} C_{ij}(\mu_i d_i)(\mu_j d_j)} \left(\prod_{i>0} \frac{\hat{x}_i^{d_i}}{(q^{2\mu_i}; q^{2\mu_i})_{d_i}} \right) \right] : \quad (4.4) \end{aligned}$$

where we employed quantum torus variables with the usual q -commutator $\hat{y}_i \hat{x}_j = q^{2\delta_{ij}} \hat{x}_j \hat{y}_i$. Next, we rewrite the first sum as an operator using $(\hat{x}_0 \hat{y}_0^k)^n = \hat{x}_0^n \hat{y}_0^{kn} q^{(n^2-n)k}$, with $n = d_0$ and $k = C_{00}\mu_0^2$. This gives

$$\begin{aligned}
 P_Q &=: \left[\sum_{d_0} (-1)^{C_{00}\mu_0 d_0} q^{C_{00}\mu_0^2 d_0} \left(\frac{(\hat{x}_0 \hat{y}_0^{C_{00}\mu_0^2})^{d_0}}{(q^{2\mu_0}; q^{2\mu_0})_{d_0}} \right) \left(\prod_{i>0} \hat{y}_i^{\mu_i C_{0i}} \right)^{\mu_0 d_0} \right] \\
 &\quad \times \left[\sum_d (-1)^{\sum_i C_{ii}\mu_i d_i} q^{\sum_{i,j} C_{ij}(\mu_i d_i)(\mu_j d_j)} \left(\prod_{i>0} \frac{\hat{x}_i^{d_i}}{(q^{2\mu_i}; q^{2\mu_i})_{d_i}} \right) \right] : \\
 &=: \left[\sum_{d_0} \frac{((-1)^{C_{00}\mu_0} q^{C_{00}\mu_0^2} \hat{x}_0 \hat{y}_0^{C_{00}\mu_0^2})^{d_0}}{(q^{2\mu_0}; q^{2\mu_0})_{d_0}} \left(\prod_{i>0} \hat{y}_i^{\mu_i C_{0i}} \right)^{\mu_0 d_0} \right] \\
 &\quad \times \left[\sum_d (-1)^{\sum_i C_{ii}\mu_i d_i} q^{\sum_{i,j} C_{ij}(\mu_i d_i)(\mu_j d_j)} \left(\prod_{i>0} \frac{\hat{x}_i^{d_i}}{(q^{2\mu_i}; q^{2\mu_i})_{d_i}} \right) \right] : \\
 &=: \Psi_{q^{\mu_0}} \left((-1)^{C_{00}\mu_0} q^{C_{00}\mu_0^2 - \mu_0} \hat{x}_0 \hat{y}_0^{C_{00}\mu_0^2} \prod_{i>0} \hat{y}_i^{\mu_0 \mu_i C_{0i}} \right) \\
 &\quad \times \left[\sum_d (-1)^{\sum_i C_{ii}\mu_i d_i} q^{\sum_{i,j} C_{ij}(\mu_i d_i)(\mu_j d_j)} \left(\prod_{i>0} \frac{\hat{x}_i^{d_i}}{(q^{2\mu_i}; q^{2\mu_i})_{d_i}} \right) \right] : \quad (4.5)
 \end{aligned}$$

Iterating on all remaining nodes, we eventually rewrite the generalized partition function as $P_Q =: \mathbb{P}_Q$, the normal ordering of a suitable operator

$$\mathbb{P}_Q = \Psi_{q^{\mu_m}}(X_m) \cdot \Psi_{q^{\mu_{m-1}}}(X_{m-1}) \cdots \Psi_{q^{\mu_1}}(X_1), \quad (4.6)$$

with Ψ defined in (4.2), and with variables defined as follows:

$$X_i = (-1)^{C_{ii}\mu_i} q^{C_{ii}\mu_i^2 - \mu_i} \hat{x}_i \hat{y}_i^{C_{ii}\mu_i^2} \prod_{j<i} \hat{y}_j^{\mu_i \mu_j C_{ij}}. \quad (4.7)$$

4.2 A-polynomials for generalized partition function

Let us next turn to recursion relations obeyed by generalized quiver partition functions. The advantage of the operator form of the partition function is that we can easily read off the recursion relation. Notice that

$$(1 - \hat{y} - \hat{x}^\mu) \Psi_{q^\mu}(\hat{x}^\mu) = 0. \quad (4.8)$$

This may also be recast as $(1 - \hat{y}_i^\mu - \hat{x}_i) \Psi_{q^\mu}(\hat{x}_i) = 0$ in the language of single-node variables where $\hat{x}_i \sim \hat{x}^\mu$, $\hat{y} \sim \hat{y}_i^\mu$.

Next, let us introduce a symmetrized version of variables X_i (4.7) akin to (4.15):

$$X'_i = (-1)^{C_{ii}\mu_i} q^{C_{ii}\mu_i^2 - \mu_i} \hat{x}_i \hat{y}_i^{C_{ii}\mu_i^2} \prod_{j=i}^m \hat{y}_j^{\mu_i \mu_j C_{ij}}. \quad (4.9)$$

These are commuting variables $X'_i X'_j = X'_j X'_i$. Moreover, the partition function (4.6) may as well be replaced by an analogous expression \mathbb{P}'_Q obtained from \mathbb{P}_Q by replacing $X_i \rightarrow X'_i$. The two have the same normal ordering: $\mathbb{P}'_Q := \mathbb{P}_Q := P_Q$ since the substitution of X'_i corresponds to right-multiplication by suitable powers of \hat{y}_i , as previously discussed in Sect. 4.1.

Then, the partition function (4.6), or more precisely its surrogate \mathbb{P}'_Q , must be annihilated by operators \hat{A}_i :

$$\hat{A}_i \mathbb{P}'_Q = 0 \quad \forall i = 1, \dots, m, \quad (4.10)$$

defined as

$$\hat{A}_i = (1 - \hat{y}_i^{\mu_i} - X'_i). \quad (4.11)$$

This statement is obvious for $i = m$ since it corresponds to the first factor in (4.6). But now recall that the choice of ordering of nodes in \mathbb{P}'_Q , the surrogate of (4.6) upon replacing X_i by X'_i , is arbitrary since variables X'_i commute with each other. Therefore, if \hat{A}_m annihilates the partition function, so must \hat{A}_i for any $i = 1, \dots, m$.

4.2.1 Example: a twice-around basic disk

If the above derivation may appear a bit formal, we can easily rederive this result for the special case of a single μ -times around basic disk with partition function (1.2). Taking for simplicity $\mu = 2$ and x_i equal to x^μ , we have

$$P_Q(x, q) = \sum_{d \geq 0} \frac{x^{2d}}{(q^4; q^4)_d} \quad (4.12)$$

Now notice that

$$\begin{aligned} : \hat{x}^2 P_Q(\hat{x}, q) &:= \sum_{d \geq 0} \frac{x^{2(d+1)}}{(q^4; q^4)_d} = \sum_{d \geq 1} \frac{x^{2d}}{(q^4; q^4)_{d-1}} = \sum_{d \geq 1} \frac{x^{2d}}{(q^4; q^4)_d} (1 - q^{2d}) \\ &= (1 - \hat{y}) \sum_{d \geq 0} \frac{x^{2d}}{(q^4; q^4)_d} = : (1 - \hat{y}) P_Q(\hat{x}, q) :, \end{aligned} \quad (4.13)$$

so

$$\hat{A}(\hat{x}, \hat{y}, q) = 1 - \hat{y} - \hat{x}^2, \quad (4.14)$$

in agreement with the specialization of (4.11) to $\mu_i = 2$.

4.3 The toric brane property

We now discuss a new connection between quiver descriptions of generic knot conormals, and the toric brane corresponding to the unknot conormal. This property is best explained in the formalism of quantum variables introduced in our previous work [9], suitably modified.

4.3.1 A distinguished basis of quantum variables

The presentation of the quiver partition function as the normal-ordered expression of \mathbb{P}_Q is clearly not unique. It is ambiguous by right-multiplication by any function of the quantum torus variables \hat{y}_i that evaluates to 1 when all $y_i \rightarrow 1$. We will use this freedom to switch to a new set of non-commuting variables that reveals new structures of the knot homology encoded by the quiver. From now we assume that all quiver nodes correspond to basic disks wrapping once-around, i.e., such that $\mu_i = 1$ for all i ; the general case will be discussed later.

As a first intermediate step, we introduce the variables

$$X'_i = (-q)^{C_{ii}} \hat{x}_i \prod_{j=1}^m \hat{y}_j^{C_{ij}}, \quad (4.15)$$

which appear in the quantum quiver A -polynomials, see [9]. Note that these variables are mutually commutative: $X'_i X'_j = X'_j X'_i$.

For the purpose of studying structures in knot homologies, we consider a slightly different set of variables defined as

$$Z_i = X'_i \prod_{j < i} \hat{y}_j. \quad (4.16)$$

These obey quantum torus relations:

$$Z_j Z_i = q^{2 \operatorname{sgn}(j-i)} Z_i Z_j. \quad (4.17)$$

We will denote the Z_i the *toric brane variables*.

Remark 4.1 Thinking geometrically of the boundaries of the disks as curves very close to the central S^1 in $S^1 \times \mathbb{R}^2$, the variables X'_i correspond to an unlinked collection of parallel circles, whereas the collection Z_i correspond to a collection of curves obtained from this by introducing linking so that strands i and j link with linking number $i - j$.

Note that the definition of Z_i and their algebra depend on a choice of ordering of nodes of the quiver. Later we will discuss a certain preferred choice. With any choice

of ordering for quiver nodes, we claim that the operator $\tilde{\mathbb{P}}_Q = \sum_{r \geq 0} \frac{1}{(q^2; q^2)_r} \tilde{\mathbb{P}}_r$ with

$$\tilde{\mathbb{P}}_r = \sum_{|d|=r} \begin{bmatrix} r \\ d \end{bmatrix}_{q^2} Z_1^{d_1} \cdots Z_m^{d_m} \quad (4.18)$$

has the property that its normal ordering recovers the quiver partition function P_Q :

$$: \tilde{\mathbb{P}}_Q : = P_Q(\mathbf{x}; q). \quad (4.19)$$

This is because monomials of $\tilde{\mathbb{P}}_Q$ are related to those of \mathbb{P}_Q by right multiplication by \hat{y}_i -variables, which is invisible to normal ordering.

Recalling the definition of the q -multinomial,

$$\begin{bmatrix} r \\ d \end{bmatrix}_{q^2} = \frac{(q^2; q^2)_r}{(q^2; q^2)_{d_1} \cdots (q^2; q^2)_{d_m}}, \quad (4.20)$$

and the algebraic property (4.17), we find that $\tilde{\mathbb{P}}_r$ takes a very simple form:

$$\tilde{\mathbb{P}}_r = (Z_1 + \cdots + Z_m)^r. \quad (4.21)$$

A proof of this formula is given in Appendix A. In the limit $q \rightarrow 1$, this statement reduces to the multinomial theorem.

4.3.2 The toric brane recursion relation

Expression (4.21) shows that there is a universal recursion relation among knot homologies (at least for those knots which admit a quiver description with once-around generators):

$$\tilde{\mathbb{P}}_r = (Z_1 + \cdots + Z_n) \tilde{\mathbb{P}}_{r-1}. \quad (4.22)$$

The recursion relation (4.22) exhibits an exponential growth property that reflects analogous growth behavior of colored link homologies. On the other hand, and more important for the present discussion, is the fact that (4.22) coincides precisely with the recursion relation that characterizes the partition function of a toric brane in \mathbb{C}^3 (which corresponds to the unknot conormal partition function, in reduced normalization). In fact the quiver partition function written in terms of Z_i takes the same exact form:

$$\tilde{\mathbb{P}}_Q = \sum_{r \geq 0} \frac{1}{(q^2; q^2)_r} (Z_1 + \cdots + Z_r)^r = \prod_{n \geq 0} (1 - q^{2n} Z)^{-1} = (Z; q^2)_\infty^{-1} \quad (4.23)$$

in terms of the variable

$$Z = Z_1 + \cdots + Z_m. \quad (4.24)$$

In other words, the quiver partition function takes the form of a toric brane partition function in this coordinate, after normal ordering

$$P_Q(\mathbf{x}; q) =: (Z; q^2)_\infty^{-1} : \quad (4.25)$$

This is the remarkable *toric brane property* of quivers (so far we have assumed that all basic nodes wrap exactly once-around the conormal, but soon we will extend this to generalized quivers).

Recalling that $\hat{y} = \prod_i \hat{y}_i$ is the quantum meridian holonomy on ∂L_K , it follows that Z satisfies

$$\hat{y} Z = q^2 Z \hat{y}. \quad (4.26)$$

Using this relation, it is easy to see that

$$(1 - \hat{y} - Z) P_Q(\mathbf{x}; q) = 0. \quad (4.27)$$

This is exactly the quantum curve of a toric brane in \mathbb{C}^3 . The change of variables $x_i \rightarrow Z_i$ then shows that the HOMFLY-PT partition function of *any* knot (admitting a quiver description with once-around generators) obeys a new relation, which takes the form of an unknot quantum curve (the partition function of a toric brane in \mathbb{C}^3 corresponds to the unknot conormal in the conifold in reduced normalization). This has consequences for the structure of knot homologies, which we will analyze in Sect. 5.

Finally we relax the assumption that all quiver nodes are basic disks with $\mu_i = 1$, and consider the more general case where $\mu_i > 1$ for some nodes. If longitudes of basic disks are given by $x_i \sim x^{\mu_i}$, then meridians contribute in proportional amounts to the overall meridian at ∂L_K , namely $\hat{y} = \hat{y}_1^{\mu_1} \hat{y}_2^{\mu_2} \cdots \hat{y}_m^{\mu_m}$. Ordering nodes so that $\mu_1 \geq \mu_2 \geq \cdots \geq \mu_m$, we introduce $Z^{(n)} = \sum_{i \in I_n} Z_i$, where I_n is a set of indices for which $\mu_i \geq n$. $I_0 = I_1$ contains all indices and $Z^{(0)} = Z^{(1)} = Z$. I_2 contains indices for which $\mu_i \geq 2$ (for all thin knots it is empty), and so on. Then the generalization of the toric brane property is encoded by the following quantum curve:

$$\begin{aligned} \hat{y} P_Q(\mathbf{x}; q) &= \hat{y}_1^{\mu_1} \hat{y}_2^{\mu_2} \cdots \hat{y}_m^{\mu_m} \text{Exp} \left(\frac{Z_1 + Z_2 + \cdots + Z_m}{1 - q^2} \right) \\ &= \text{Exp} \left(\frac{(q^2 - 1) q^{2n_{\max}} Z^{(n_{\max})} + \cdots + (q^2 - 1) q^2 Z^{(2)} + (q^2 - 1) Z^{(1)} + Z^{(0)}}{1 - q^2} \right) \\ &= (1 - q^{2n_{\max}} Z^{(n_{\max})}) \cdots (1 - q^2 Z^{(2)}) (1 - Z^{(1)}) P_Q(\mathbf{x}; q). \end{aligned} \quad (4.28)$$

Remark 4.2 The definition (4.24) of the toric brane variables shares tantalizing similarities with partition functions of framed BPS states. In [50] it was observed that the expectation values of a ‘UV’ line operator of a rank- N theory, engineered by a stack of M5-branes wrapping a complex curve C , admits a decomposition as a linear combination of expectation values of ‘IR’ line operators of a low-energy $U(1)$ theory,

arising from a single M5 wrapping a covering $\Sigma \rightarrow C$. Both UV and IR line operators are engineered by M2-branes attached to the M5-system. In our setup the Z_i correspond to expectation values of $U(1)$ Wilson lines on the Lagrangian L wrapped by a single M5-brane. The expansion of Z as a sum with integer coefficient in the Z_i then suggests an interpretation of Z as the expectation value of a line operator in a ‘UV’ theory, obtained by wrapping a stack of M5 on another three-manifold L' . The quantum curve (4.27) identifies a natural candidate: L' should be the toric brane, or unknot conormal, on which a stack of M5 is wrapped. The line operator on L' is described by (4.27), and arises from an M2-brane ending on L' along a curve. In the infrared the multiple M5-branes on L' merge and branch, resolving into a single brane wrapping a covering of L' , corresponding to L . The M2-curve gets lifted to the various basic disks on L , linking as described by the quiver. This interpretation of Z as a line operator in the toric brane is therefore consistent with viewing L as a covering of L' , in line with the general assumption, underlying the geometric origin of quivers, that boundaries of basic holomorphic curves in L all lie very close to the zero-section $S^1 \times \text{point}$.

5 Homology structure encoded in the quiver

The possibility of describing knot invariants using quivers enables translating quiver properties to HOMFLY-PT homology. In this section we will study how redundant pairs and toric brane variables are reflected in structures of HOMFLY-PT homology. For simplicity, we will assume that all nodes of the quiver have multiplicity $\mu_i = 1$.

5.1 Redundant pairs and \mathfrak{sl}_1 pairs

In Sect. 3.5.2 we described the degree μ redundant pair of nodes. Now we want to study its relationship with the d_N differential of [7]. We consider the simplest possible case in which we have a quiver consisting of a single degree 1 redundant pair of nodes without any other vertices and arrows. This means that the quiver adjacency matrix is given by

$$C = \begin{pmatrix} 0 & 0 \\ 0 & 1 \end{pmatrix} \quad (5.1)$$

and we demand $x_1 = qx_2$.

Now we consider the t -deformation of the degree 1 redundant pair of nodes, following the rule $t_i = C_{ii}$. This means that

$$x_2 = x_1 q^{-1}(-t). \quad (5.2)$$

Note that after t -deformation nodes 1 and 2 are no longer redundant and the quiver partition function is given by

$$P_Q(x_1, x_2; q) = 1 + \frac{x_1 + (-q)x_2}{1 - q^2} + \cdots = 1 + \frac{1+t}{1-q^2}x_1 + \cdots. \quad (5.3)$$

(As a cross-check, we can see that $t = -1$ leads to $P_Q = 1$.)

We observe that relation (5.2) is reminiscent of the shift in (a, q, t) -degrees involved in the definition of d_N differentials in [7]. Indeed, deforming (5.2) into

$$x_2 = x_1 a^2 q^{-2N-1}(-t) \quad (5.4)$$

corresponds to the statement that homology generators corresponding to nodes 1 and 2 are connected by a d_N differential which shifts (a, q, t) -degrees by $(-2, 2N, -1)$, respectively, which matches [7] for $N > 0$ (after adapting conventions). Note that when $a = q^N$, (5.4) reduces back to (5.2).

Keeping a generic and taking $N = 1$ leads to the most important building block of the uncolored homology: the canceling differential d_1 . Since (\mathcal{H}_r, d_1) is isomorphic to one-dimensional $\mathcal{H}_1^{\mathfrak{sl}_1}$, all quiver nodes but one are grouped into pairs of the form

$$(x_i, x_j = x_i a^2 q^{-3}(-t)). \quad (5.5)$$

We call such (x_i, x_j) \mathfrak{sl}_1 pairs. Note that elements of \mathfrak{sl}_1 pairs cancel each other at any level (any representation S^r) in the d_1 -cohomology. This is in line with the expectation that \mathfrak{sl}_1 knot homology is the same for all knots, with only one generator surviving for each symmetric coloring (the one corresponding to the unknot). In particular, the unique surviving generator in the first homology $\mathcal{H}_1^{\mathfrak{sl}_1}$ must correspond to a node of the quiver, which we call the *spectator* node.

5.1.1 Relation to prequivers

Nodes in \mathfrak{sl}_1 pairs are closely related to a particular prequiver introduced in [51]. The basic idea is that all nodes of the quiver come in pairs, except for the spectator node. Furthermore, within each pair the two variables are related as in (5.5), suggesting that node x_j can be viewed as a bound state of node x_i with an additional x -independent node with variable $x_* = a^2 q^{-3}(-t)$. Indeed, it was observed in [9] that introducing such an extra node with a single unit of linking to x_i would result in a bound state like the node x_j , via a procedure of unlinking. In [51] this idea was developed in greater detail, suggesting the following:

Conjecture 5.1 *For each knot K with refined partition function that has a quiver description as in the original knots-quivers correspondence (i.e., with $x_i \sim x$) there exists a unique quiver Q corresponding to K with adjacency matrix of the form*

$$C = \begin{pmatrix} 0 & F_1 & F_2 & \cdots & F_k \\ F_1^T & D_1 & U_{12} & \cdots & U_{1k} \\ F_2^T & U_{12}^T & D_2 & \cdots & U_{2k} \\ \vdots & \vdots & \vdots & \ddots & \vdots \\ F_k^T & U_{1k}^T & U_{2k}^T & \cdots & D_k \end{pmatrix}, \quad (5.6)$$

where

$$F_i = [\check{C}_{0i} \check{C}_{0i}], \quad D_i = \begin{bmatrix} \check{C}_{ii} & \check{C}_{ii} \\ \check{C}_{ii} & \check{C}_{ii} + 1 \end{bmatrix}, \quad U_{ij} = \begin{bmatrix} \check{C}_{ij} & \check{C}_{ij} \\ \check{C}_{ij} + 1 & \check{C}_{ij} + 1 \end{bmatrix},$$

$$\check{C}_{mn} \in \mathbb{Z}. \quad (5.7)$$

Here the diagonal block D_i corresponds to the self-interaction of the i -th \mathfrak{sl}_1 pair (note that D_i is a framed version of (5.1)), the block U_{ij} corresponds to the interaction between i -th and j -th \mathfrak{sl}_1 pairs, the zero in the top-left corner of C to the spectator node, and F_i corresponds to the interaction between the spectator and i -th \mathfrak{sl}_1 pair.

Using Eqs. (5.6), (5.7), we can define a *prequiver* \check{Q} [51] with an adjacency matrix given by

$$\check{C} = \begin{pmatrix} 0 & \check{C}_{01} & \check{C}_{02} & \cdots & \check{C}_{0k} \\ \check{C}_{01}^T & \check{C}_{11} & \check{C}_{12} & \cdots & \check{C}_{1k} \\ \check{C}_{02}^T & \check{C}_{12}^T & \check{C}_{22} & \cdots & \check{C}_{2k} \\ \vdots & \vdots & \vdots & \ddots & \vdots \\ \check{C}_{0k}^T & \check{C}_{1k}^T & \check{C}_{2k}^T & \cdots & \check{C}_{kk} \end{pmatrix}. \quad (5.8)$$

Nodes of the prequiver correspond to the spectator node and \mathfrak{sl}_1 pairs, while arrows correspond to interactions among them. Note that using Eqs. (5.6)–(5.8) one can easily reconstruct C from \check{C} . Moreover, since the change of variables for the \mathfrak{sl}_1 pair (x_i, x_j) satisfies (5.5), the changes of variables for Q and \check{Q} read

$$\mathbf{x} = \begin{pmatrix} \check{x}_0 \\ \check{x}_1 \\ \check{x}_1 a^2 q^{-3}(-t) \\ \check{x}_2 \\ \check{x}_2 a^2 q^{-3}(-t) \\ \vdots \\ \check{x}_k \\ \check{x}_k a^2 q^{-3}(-t) \end{pmatrix}, \quad \check{\mathbf{x}} = \begin{pmatrix} \check{x}_0 \\ \check{x}_1 \\ \check{x}_2 \\ \vdots \\ \check{x}_k \end{pmatrix}, \quad (5.9)$$

and we have

$$\sum_{\check{d}} (-q)^{\check{d} \cdot C \cdot \check{d}} \frac{\mathbf{x}^{\check{d}}}{(q^2; q^2)_{\check{d}}} = \sum_{\check{d}} (-a^2 q^{-2} t; q^2)_{\check{d}_1 + \cdots + \check{d}_k} (-q)^{\check{d} \cdot \check{C} \cdot \check{d}} \frac{\check{\mathbf{x}}^{\check{d}}}{(q^2; q^2)_{\check{d}}}. \quad (5.10)$$

Let us see how it works on the example of the trefoil. In that case the quiver and the change of variables are given by [10, 11]

$$C = \begin{pmatrix} 0 & F_1 \\ F_1^T & D_1 \end{pmatrix} = \begin{pmatrix} 0 & 1 & 1 \\ 1 & 2 & 2 \\ 1 & 2 & 3 \end{pmatrix}, \quad \mathbf{x} = \begin{pmatrix} xa^2q^{-2} \\ xa^2(-t)^2 \\ xa^4q^{-3}(-t)^3 \end{pmatrix}, \quad (5.11)$$

whereas the prequiver and corresponding change of variables read [51]

$$\check{C} = \begin{pmatrix} 0 & 1 \\ 1 & 2 \end{pmatrix}, \quad \check{\mathbf{x}} = \begin{pmatrix} xa^2q^{-2} \\ xa^2(-t)^2 \end{pmatrix}. \quad (5.12)$$

One can also check that Eq. (5.10) is satisfied.

As we mentioned earlier, the transition between (5.12) and (5.11), called splitting in [51], can be interpreted in terms of the unlinking procedure described in [9]. We can consider a quiver node corresponding to a curve that does not wind around L_K and links node number 2:

$$C = \begin{pmatrix} 0 & 1 & 1 & 0 \\ 1 & 2 & 1 & 1 \\ 0 & 1 & 1 & 0 \end{pmatrix}, \quad \mathbf{x} = \begin{pmatrix} xa^2q^{-2} \\ xa^2(-t)^2 \\ a^2q^{-3}(-t) \end{pmatrix}. \quad (5.13)$$

Then unlinking node number 2 and the new node leads to

$$C = \begin{pmatrix} 0 & 1 & 1 & 0 \\ 1 & 2 & 2 & 0 \\ 1 & 2 & 3 & 0 \\ 0 & 0 & 0 & 0 \end{pmatrix}, \quad \mathbf{x} = \begin{pmatrix} xa^2q^{-2} \\ xa^2(-t)^2 \\ xa^4q^{-3}(-t)^3 \\ a^2q^{-3}(-t) \end{pmatrix}. \quad (5.14)$$

After unlinking, the last (x -independent) node is completely detached from the rest of the quiver. Its contribution to the partition function is an overall multiplicative factor $(a^2q^{-3}(-t); q^2)^{-1}$. We view it as part of the closed sector and when discarding this node, we recover the trefoil quiver and its partition function (5.11).

We conjecture that the refined partition function of every knot corresponding to a quiver with $x_i \sim x$ can be recovered (up to a x -independent prefactor) from a prequiver linked to an extra node which does not wind around L_K . This is true for all examples analyzed in [51]. Basing on the results of this paper, we also know that one could mirror the reasoning presented in this section starting from the differential d_{-1} [15]. This would lead the other choice of spectator node and different form of the blocks in the matrix C , but all structural properties would be analogous.

We expect Conjecture 5.1 to have a natural extension to include multiply-wrapped basic disks, where some of the multiply-wrapped disks can be viewed as products of unlinking between a ‘primitive’ multiply-wrapped disk, and a distinguished disk which does not wrap around the longitude of L_K and that links one of the μ_i strands. It is not clear from currently available calculations how such pairs are organized.

Direct computations for colored HOMFLY-PT polynomials for knots that require multiply-wrapped generators would help understanding this.

5.2 Knot homologies in toric brane variables: a new grading

In this section and the next one we use the toric brane variables to illustrate a property of colored knot homologies. We start here by defining a certain grading that will later be used to describe the structure of a spectral sequence involving knot homologies with different colorings.

Recall the ambiguity in the definition of toric brane variables due to a choice of ordering of the nodes of the quiver Q . Recall that each node corresponds to a basic disk, with interactions among basic disks determined by their mutual linking in L_K corresponding to quiver arrows, and the spectrum of bound states is encoded in P_Q [8].

While everything that follows holds independently of the specific choice made (*mutatis mutandis*), it will be convenient to fix this choice at least partially. For this purpose, we recall that for any knot its homology in the fundamental representation and *reduced* normalization must have an odd number of generators. There is a distinguished spectator disk, while the remaining disks arrange in \mathfrak{sl}_1 pairs, as discussed in Sect. 5.1.

We adopt an ordering where the spectator node comes first and \mathfrak{sl}_1 pairs are labeled by $2i, 2i + 1$ for $i \geq 1$. Let us recall that, in the language of quivers, an \mathfrak{sl}_1 pair of disks is characterized by

$$C_{2i+1,2i+1} = C_{2i,2i} + 1, \quad x_{2i+1} = x_{2i} a^2 q^{-3} (-t). \quad (5.15)$$

We do not specify how \mathfrak{sl}_1 pairs should be ordered among themselves, but simply assign Z_1 to the distinguished spectator node and Z_{2i}, Z_{2i+1} to the pairs. Note that

$$Z_{2i+1} = Z_{2i} a^2 q^{-2} t \hat{y}_{2i} \prod_j \hat{y}_j^{C_{2i+1,j} - C_{2i,j}}. \quad (5.16)$$

In particular, this means that in (4.22), when Z_{2i}, Z_{2i+1} act on the *same* term $\sim \hat{\mathbf{x}}^{\mathbf{d}} \subset \tilde{\mathbb{P}}_{r-1}$ with $|\mathbf{d}| = r - 1$, they produce two terms in $\tilde{\mathbb{P}}_r$ with well-defined shift of degrees:

$$: Z_{2i+1} \hat{\mathbf{x}}^{\mathbf{d}} : = a^2 t q^{-2+2d_{2i}+2} \sum_{j=1}^m d_j (C_{2i+1,j} - C_{2i,j}) : Z_{2i} \hat{\mathbf{x}}^{\mathbf{d}} :. \quad (5.17)$$

This relation will be instrumental for defining a new differential on the S^r homology.

If a knot K has a corresponding quiver Q , one may consider a grading on the S^r -colored HOMFLY-PT homology \mathcal{H}_r induced by the dimension vector \mathbf{d} . The \mathbf{d} -grading subsumes t -grading and a -grading, but not the q -grading—this is clear from the form of the quiver partition function with $x_i = x a^{a_i} q^{l_i} (-t)^{C_{ii}}$ (we have $l_i = q_i - C_{ii}$ and assume that $\mu_i = 1$ for all quiver nodes):

$$P_Q = \sum_{\mathbf{d}} (-q)^{\sum_{i,j=1}^m C_{ij} d_i d_j} \prod_{i=1}^m \frac{(x a^{a_i} q^{l_i} (-t)^{C_{ii}})^{d_i}}{(q^2; q^2)_{d_i}}$$

$$\begin{aligned}
&= \sum_r \frac{1}{(q^2; q^2)_r} \sum_{|\mathbf{d}|=r} \begin{bmatrix} r \\ \mathbf{d} \end{bmatrix}_{q^2} (-q)^{\sum_{i,j=1}^m C_{ij} d_i d_j} \\
&\quad \prod_{i=1}^m (x a^{a_i} q^{l_i} (-t)^{C_{ii}})^{d_i},
\end{aligned} \tag{5.18}$$

In general, the grading by (\mathbf{d}, q) is more refined than (or at least as refined as) the triple grading (2.3). As the latter can always be recovered, we will henceforth focus on (\mathbf{d}, q) gradings.

Recall that we are working under the assumption that $x_i \sim x$ for all quiver nodes. Then the partition function of the quiver can be organized by x -degree, corresponding to S^r -coloring of the HOMFLY-PT polynomial, as in the second line of (5.18). The S^r -colored superpolynomial is then a sum of terms with distinct \mathbf{d} -degrees such that $|\mathbf{d}| = r$. In particular, terms of degree \mathbf{d} take the form of the q -binomial $\begin{bmatrix} r \\ \mathbf{d} \end{bmatrix}_{q^2}$ times a monomial. Let $\kappa_n(\mathbf{d})$ be the coefficients of $\begin{bmatrix} r \\ \mathbf{d} \end{bmatrix}_{q^2} = \sum_{n \geq 0} \kappa_n(\mathbf{d}) q^{2n}$, which are positive integers.⁹ The partition function may be then expressed as

$$\begin{aligned}
P_Q &= \sum_r \frac{1}{(q^2; q^2)_r} \sum_{|\mathbf{d}|=r} \sum_{n \geq 0} \kappa_n(\mathbf{d}) q^{2n} (-q)^{\sum_{i,j=1}^m C_{ij} d_i d_j} \\
&\quad \prod_{i=1}^m (x a^{a_i} q^{l_i} (-t)^{C_{ii}})^{d_i}.
\end{aligned} \tag{5.19}$$

Using the \mathbf{d} -degree we may introduce a nonlinear shift of the q -grading, to just retain the ‘ n -grading’ induced by the q -multinomial

$$n_{\text{degree}} = \frac{1}{2} \left(q_{\text{degree}} - \sum_{i,j=1}^m C_{ij} d_i d_j - \sum_i l_i d_i \right). \tag{5.20}$$

This way of grading states in \mathcal{H}_r is precisely what is accomplished by switching to variables Z_i . For example, at level $r = 2$ in (4.18) and (4.21) one has terms such as

$$\begin{aligned}
\begin{bmatrix} 2 \\ \mathbf{d} = (1, 1, 0, \dots) \end{bmatrix}_{q^2} Z_1 Z_2 &= \left(\underbrace{1}_{n=0} + \underbrace{q^2}_{n=1} \right) \cdot Z_1 Z_2 = Z_1 Z_2 + Z_2 Z_1 \\
&\subset (Z_1 + Z_2 + \dots)^2.
\end{aligned} \tag{5.21}$$

These two terms both have $\mathbf{d} = (1, 1, 0, \dots)$ but are distinguished by $n = 0$ and $n = 1$.

⁹ To see positivity, one may note that it holds for coefficients of the q -binomial [52, Theorem 6.1] Then one may recursively express the q -multinomial in terms of nested q -binomials, as we did in Appendix A.

Adopting the (n, \mathbf{d}) -grading of \mathcal{H}_r , we deduce its universal structure from (4.21):

$$\mathcal{H}_r = \bigoplus_{|d|=r, n \geq 0} \mathbb{C}^{\kappa_n(\mathbf{d})} \otimes \mathcal{H}_{\mathbf{d}, n}, \quad (5.22)$$

where $\mathcal{H}_{\mathbf{d}, n} \simeq \mathbb{C}$ is one-dimensional.¹⁰

5.3 Traces of a spectral sequence of symmetrically colored knot homologies

Having introduced the necessary notions of quiver grading on knot homologies together with the toric brane property, we are now in a position to lay out some of their most interesting consequences. We present a simple structure that appears on the knot homologies, which is reminiscent of a spectral sequence.

Pages of the spectral sequence correspond to HOMFLY-PT homologies with different colorings by symmetric representations. The non-trivial data that we will provide corresponds to a definition for the differentials of the spectral sequence. (These should *not* be confused with the differentials that define the colored HOMFLY-PT homologies. The structure we are about to discuss is more similar to, although not quite the same as, the one conjectured in [53].) We should stress that our considerations are motivated by structures observed at the level of partition functions, and we will provide only partial information about differentials in the spectral sequence.

We introduce linear maps

$$\mathbf{d}_r : \mathcal{H}_r \rightarrow \mathcal{H}_r, \quad (5.23)$$

which map vectors (more properly, one-dimensional subspaces) with degrees

$$\begin{aligned} & \left\{ \begin{array}{l} \mathbf{d} = (d_1, \dots, d_{2i}, d_{2i+1}, \dots) \\ n \end{array} \right. \\ & \mapsto \left\{ \begin{array}{l} \mathbf{d}' = (d_1, \dots, d_{2i} + 1, d_{2i+1} - 1, \dots) \\ n - 2d_{2i}, \end{array} \right. \end{aligned} \quad (5.24)$$

for one choice of $i = 1, \dots, \frac{1}{2}(m^r - 1)$, which depends on the specific subspace in question. Of course, this does not fully specify the map, for two reasons. On the one hand, different subspaces of $\mathcal{H}_{\mathbf{d}, n}$ may be mapped to different $\mathcal{H}_{\mathbf{d}', n'}$ depending on the possible ways (labeled by i) of trading a unit of d_{2i+1} for a unit of d_{2i} . On the other hand, from (5.22) the overall subspace of degree (\mathbf{d}, n) has dimension $\kappa_n(\mathbf{d}, n)$, so there are $\kappa_n(\mathbf{d}, n) \times \kappa_n(\mathbf{d}', n')$ possible choices. A more concrete realization of this map will be provided shortly.

Nevertheless, we claim that the map exists, as a consequence of formula (4.22). It follows from the same formula that the map can be defined in such a way that it is

¹⁰ The choice of ordering of basic disks does not influence this structure. Different choices are related by elements of $\text{End } \mathbb{C}^{\kappa_n(\mathbf{d})}$.

nilpotent:

$$\mathbf{d}_r^2 = 0. \quad (5.25)$$

One way to describe the maps \mathbf{d}_r in some detail is to consider the free group F_m generated by $S = \{a_1, \dots, a_m\}$, where m is the number of nodes in \mathcal{Q} . We then consider an element of the group ring $\mathbb{Z}[F_m]$ defined by

$$g_r = (a_1 + \dots + a_m)^r = \sum_{(i_1, \dots, i_r)} \sum_{\sigma \in S_r} a_{\sigma(i_1)} \cdots a_{\sigma(i_r)}, \quad (5.26)$$

where the first sum runs over all distinct partially ordered sets (i_1, \dots, i_r) with $i_1 \leq i_2 \leq \dots \leq i_r$ with $1 \leq i_k \leq m$. By construction, all monomials are distinct and there are $m^r = \dim \mathcal{H}_r$ of them. In particular, monomials of g_r are in 1–1 correspondence with generators of \mathcal{H}_r in a suitable basis:

$$\mathcal{H}_r \simeq \sum_{(i_1, \dots, i_r)} \sum_{\sigma \in S_r} a_{\sigma(i_1)} \cdots a_{\sigma(i_r)} \cdot \mathbb{C}. \quad (5.27)$$

We do not specify the details of this map. The only constraint is that the choice of map must be compatible with the one obtained by replacing $a_i \rightarrow Z_i$, and with a subsequent identification of the normally ordered expression with the polynomial of degree x^r in $P_{\mathcal{Q}}$.¹¹

The linear map \mathbf{d}_r can now be described as follows: its action depends only on the first letter a_j in a given monomial $a_j \cdots \subset g_r$, labeling the corresponding one-dimensional subspace of \mathcal{H}_r :

$$\mathbf{d}_r : \begin{cases} (a_1 \cdots) \cdot \mathbb{C} \mapsto 0 \\ (a_{2i} \cdots) \cdot \mathbb{C} \mapsto 0 \\ (a_{2i+1} \cdots) \cdot \mathbb{C} \mapsto (a_{2i} \cdots) \cdot \mathbb{C}. \end{cases} \quad (5.28)$$

Ellipses denote any word of $r - 1$ letters, which is furthermore understood to be identical on the *lhs* and *rhs* of the last line. Up to normalization of the basis, this defines \mathbf{d}_r explicitly. Nilpotency follows directly.

An interesting property of the maps \mathbf{d}_r is that they endow the S^r -colored HOMFLY-PT homologies of a knot with the structure of a spectral sequence, in the sense that

$$H^*(\mathcal{H}_r, \mathbf{d}_r) \simeq \mathcal{H}_{r-1}, \quad (5.29)$$

where \simeq involves a regrading, which will be detailed shortly. The \mathcal{H}_r are pages of a spectral sequence, where the r -ordering is decreasing.

¹¹ Each monomial of g_r maps to a certain (\mathbf{d}, n) degree. There are $\kappa_n(\mathbf{d})$ mapping to a given (\mathbf{d}, n) . On the other hand the multiplicity of $\mathcal{H}_{\mathbf{d}, n}$ in (5.22) is $\kappa_n(\mathbf{d})$ -dimensional. So there are $\kappa_n(\mathbf{d})!$ ways to map, any choice is admissible.

The claim (5.29) can be established easily with the aid of $\tilde{\mathbb{P}}_r$ written in terms of variables Z_i , as in (4.22). In fact, the specific form of \mathbf{d}_r given in (5.28) corresponds to pairing up all terms of the type $(Z_{2i} + Z_{2i+1}) \prod_{k=1}^{r-1} q^{(\cdots)} Z_{i_1} \cdots Z_{i_k}$, where $\prod_{k=1}^{r-1} q^{(\cdots)} Z_{i_1} \cdots Z_{i_k}$ is any monomial in $\tilde{\mathbb{P}}_{r-1}$. What remains after pairwise cancellations of these terms is precisely a regraded copy of $\tilde{\mathbb{P}}_{r-1}$:

$$\tilde{\mathbb{P}}_r \supset Z_1 \cdot \tilde{\mathbb{P}}_{r-1} = \left[x a^\Sigma q^{-\Sigma} (-q)^{C_{11}} \prod_j \hat{y}_j^{C_{1j}} \right] \cdot \tilde{\mathbb{P}}_{r-1}, \quad (5.30)$$

where the shift of various degrees can be summarized as follows:

$$\begin{aligned} x^{r-1} &\rightarrow x^r, & a^\# &\rightarrow a^{\#+\Sigma}, \\ t^\# &\rightarrow t^\#, & q^\# &\rightarrow q^{\#-\Sigma+C_{11}+2\sum_{j=1}^m d_j C_{1j}}. \end{aligned} \quad (5.31)$$

5.3.1 Example: trefoil

For the trefoil knot in reduced normalization, the generators of \mathcal{H}_1 and \mathcal{H}_2 have, respectively, the following degrees:

		\mathcal{H}_2	a	q	t	
		Z_1^2	4	-4	0	
		Z_2^2	4	8	4	
		Z_3^2	8	6	6	
\mathcal{H}_1	a	q	t			
Z_1	2	-2	0	$Z_1 Z_2$	4	2
Z_2	2	2	2	$Z_2 Z_1$	4	4
Z_3	4	0	3	$Z_2 Z_3$	6	6
		$Z_3 Z_2$	6	8	5	
		$Z_1 Z_3$	6	0	3	
		$Z_3 Z_1$	6	2	3	

(5.32)

Here the spectator node is Z_1 , while the \mathfrak{sl}_1 pair is (Z_2, Z_3) . Therefore, in \mathcal{H}_2 the differential \mathbf{d}_r pairs up terms of types $(Z_2 Z_i, Z_3 Z_i)$ for $i = 1, 2, 3$ (cf. (5.17)):

$$\begin{aligned} Z_2 Z_1 : (4, 4, 2) &\text{ with } Z_3 Z_1 : (6, 2, 3), \\ Z_2 Z_2 : (4, 8, 4) &\text{ with } Z_3 Z_2 : (6, 8, 5), \\ Z_2 Z_3 : (6, 6, 5) &\text{ with } Z_3 Z_3 : (8, 6, 6), \end{aligned} \quad (5.33)$$

leaving three terms corresponding to a regrading of \mathbb{P}_1'' (cf. (5.31)):

$$Z_1^2 : (4, -4, 0) \quad Z_1 Z_2 : (4, 2, 2) \quad Z_1 Z_3 : (6, 0, 3). \quad (5.34)$$

5.3.2 Sketch of the differential from \mathcal{H}_r to \mathcal{H}_{r-l}

Once we have a differential relating \mathcal{H}_r to \mathcal{H}_{r-1} , it is natural to wonder if there is a generalization that decreases color by multiple steps $S^r \rightarrow S^{r-l}$ for any $l \leq r$. Let us begin by rewriting

$$P_r = : (Z_1 + Z_{\mathfrak{s}l_1})^r : \quad (5.35)$$

where $Z_{\mathfrak{s}l_1} = Z - Z_1$ contains all $\mathfrak{s}l_1$ pairs (and excludes the spectator):

$$Z_{\mathfrak{s}l_1} = \sum_{i=1}^k Z_{2i} + Z_{2i+1}. \quad (5.36)$$

In the simplest case when $l = 1$, we have

$$P_r = : (Z_1 + Z_{\mathfrak{s}l_1}) P_{r-1} : \quad (5.37)$$

and we can see that $Z_1 P_{r-1}$ is just a regrading of P_{r-1} . We can cancel $Z_{\mathfrak{s}l_1} P_{r-1}$ by defining a differential:

$$\begin{aligned} Z_1 P_{r-1} &\xrightarrow{\mathbf{d}_1} 0, \\ Z_{2i} P_{r-1} &\xrightarrow{\mathbf{d}_1} 0, \\ Z_{2i+1} P_{r-1} &\xrightarrow{\mathbf{d}_1} Z_{2i} P_{r-1}, \end{aligned} \quad (5.38)$$

whose homology corresponds (by construction) to $Z_1 P_{r-1}$, a regrading of \mathcal{H}_{r-1} . This is the usual differential discussed so far $\mathbf{d}_1 \equiv \mathbf{d}$, in agreement with (5.28).

For $l = 2$ we have

$$P_r = : (Z_1^2 + Z_1 Z_{\mathfrak{s}l_1} + Z_{\mathfrak{s}l_1} Z_1 + Z_{\mathfrak{s}l_1}^2) P_{r-2} : . \quad (5.39)$$

Then we define

$$\begin{aligned} Z_1^2 P_{r-2} &\xrightarrow{\mathbf{d}_2} 0, \\ Z_1 Z_{2i+1} P_{r-2} &\xrightarrow{\mathbf{d}_2} Z_1 Z_{2i} P_{r-2}, \\ Z_1 Z_{2i} P_{r-2} &\xrightarrow{\mathbf{d}_2} 0, \\ Z_{2i+1} Z_j P_{r-2} &\xrightarrow{\mathbf{d}_2} Z_{2i} Z_j P_{r-2}, \\ Z_{2i} Z_j P_{r-2} &\xrightarrow{\mathbf{d}_2} 0, \end{aligned} \quad (5.40)$$

whose homology corresponds, by construction, to $Z_1^2 P_{r-2}$, a regrading of \mathcal{H}_{r-2} .

For general l we write

$$\begin{aligned}
 Z_1^l P_{r-l} &\xrightarrow{d_l} 0, \\
 Z_1^{l-1} Z_{2i+1} P_{r-l} &\xrightarrow{d_l} Z_1^{l-1} Z_{2i} P_{r-l}, \\
 Z_1^{l-1} Z_{2i} P_{r-l} &\xrightarrow{d_l} 0, \\
 &\vdots \\
 Z_1^{l-n} Z_{2i+1} Z_{j_1} Z_{j_2} \cdots Z_{j_{m-1}} P_{r-l} &\xrightarrow{d_l} Z_1^{l-n} Z_{2i} Z_{j_1} Z_{j_2} \cdots Z_{j_{m-1}} P_{r-l}, \\
 Z_1^{l-n} Z_{2i} Z_{j_1} Z_{j_2} \cdots Z_{j_{m-1}} P_{r-l} &\xrightarrow{d_l} 0,
 \end{aligned} \tag{5.41}$$

whose homology corresponds (by construction) to $Z_1^l P_{r-l}$, a suitable regrading of \mathcal{H}_{r-l} .

6 Examples with multiply-wrapped basic disks

In this section we discuss concrete examples of geometries where multiply-wrapped basic disks appear naturally, and cross-check proposals discussed in previous sections. We point out that the available data to which we compare is limited and sometimes conjectural.

6.1 The line in real projective 3-space

In this section we study the example of the conormal of the real projective line in real projective space, where a multiply wrapped disk appears in a smooth, non-orbifold geometry.

Consider the curve

$$1 - y + a^2 x^2 y - x^2 + \gamma = 0. \tag{6.1}$$

This curve was derived in [14] as the zero set of the augmentation polynomial of the knot contact homology of the projective line \mathbb{RP}^1 in \mathbb{RP}^3 . Viewing the latter as a $(\mathbb{Z}/2\mathbb{Z})$ -orbifold of S^3 , in the large N limit this is also the moduli space of a toric brane sitting at the orbifold point in a $(\mathbb{Z}/2\mathbb{Z})$ -orbifold of the resolved conifold. To see this directly, we observe that this is a genus-one curve with six asymptotic regions. There are horizontal asymptotic legs at $x \rightarrow 0$ with $y \rightarrow \gamma$, and at $x \rightarrow \infty$ with $y \rightarrow 1/a^2$. There are also pairs of vertical asymptotic legs, located at $x \rightarrow \pm a^{-2}$ with $y \rightarrow \infty$, and at $x \rightarrow \pm \sqrt{1+\gamma}$ with $y \rightarrow 0$.

Let us focus on the limit $\gamma = 0$, in which the curve is doubly covered by the unknot mirror curve $1 - y - x + a^2 xy = 0$ through the change of variable $x \rightarrow \pm x^{1/2}$. The vertical external legs of the conifold geometry now sit at $x = \pm a^{-1}$ and $x = \pm 1$. In particular, each pair of legs is separated by $\log(-1) = i\pi$, precisely as the external legs

of Fig. 3 in the limit $Q \rightarrow -1$. Indeed, taking also $a \rightarrow 0$ and switching orientation $y \rightarrow y^{-1}$ turns (6.1) into (3.12). This confirms that (3.12) describes a toric brane in the $(\mathbb{Z}/2\mathbb{Z})$ orbifold of \mathbb{C}^3 , namely the half-geometry of the $(\mathbb{Z}/2\mathbb{Z})$ orbifold of the resolved conifold obtained by sending $a^2 \rightarrow 0$.

Since the brane described by (6.1) at $\gamma = 0$ sits at the orbifold point, the upshot of this analysis is that any holomorphic curve ending on it must have boundary that wraps around the longitude *twice*. This is so because otherwise such a curve in the brane would not bound any holomorphic curve away from the orbifold point. This is the large N dual of the statement that such a brane was engineered as the conormal of the line in \mathbb{RP}^3 , which is likewise non-bounding: only its double cover can bound curves in $T^*\mathbb{RP}^3$. This observation provides an independent confirmation from knot contact homology (a rigorous check, in fact), that curve counting in our orbifold toy model (3.8) really features a basic twice-around curves, as claimed in (3.13). In particular, this dispels any potential ambiguities concerning reinterpretations of (3.13) as two once-around disks in the vein of (3.6), since the boundaries in class x cannot bound any curves in the orbifold, where the brane is stuck at the orbifold locus.

A similar analysis of the conormal of the shortest closed geodesic in lens space $L(\mu, 1)$ shows how degree μ basic disk generators appears.

6.2 The knot 9_{42}

Our next example of multiply-wrapped basic holomorphic curves is the knot conormal of the knot 9_{42} . The superpolynomial in the fundamental representation is [15]

$$P_1(a, q, t) = a^{-2} \left(\frac{1}{q^2 t^2} + q^2 \right) + \left(q^4 t^3 + \frac{1}{q^4 t} + 2t + 1 \right) + a^2 \left(q^2 t^4 + \frac{t^2}{q^2} \right). \quad (6.2)$$

In a standard quiver picture, each generator of the first homology \mathcal{H}_1 would correspond to a node whose change of variables (2.10) would involve the following (a, q, t) degrees:

a_i	$q_i - C_{ii}$	$t_i = C_{ii}$
2	-2	4
2	-4	2
0	1	3
0	-1	1
0	-1	1
0	0	0
0	-3	-1
-2	2	0
-2	0	-2

(6.3)

Now let us temporarily assume that all higher BPS states arise from bound states of the basic once-around curves corresponding to the generators (6.3), as in the original formulation of the knots-quivers correspondence of [10, 11]. Then the quiver partition function would predict the following contributions at level x^2 :

$$\begin{aligned}
 P_Q|_{x^2} = & a^{-2} \left((q^2 + 1) t^3 q^{2C_{3,8}+6} + \frac{(q^2 + 1) q^{2C_{6,9}-2}}{t^2} + \frac{(q^2 + 1) q^{2C_{7,9}-6}}{t^3} \right. \\
 & + (q^2 + 1) t q^{2C_{3,9}+2} + (q^2 + 1) t q^{2C_{4,8}+2} + \frac{(q^2 + 1) q^{2C_{4,9}-2}}{t} \\
 & + (q^2 + 1) t q^{2C_{5,8}+2} + \frac{(q^2 + 1) q^{2C_{5,9}-2}}{t} + \frac{(q^2 + 1) q^{2C_{7,8}-2}}{t} \\
 & + (q^2 + 1) q^{2C_{6,8}+2} \Big) \\
 & + a^2 \left((q^2 + 1) t^7 q^{2C_{1,3}+6} + (q^2 + 1) t^5 q^{2C_{1,4}+2} + (q^2 + 1) t^5 q^{2C_{1,5}+2} \right. \\
 & + (q^2 + 1) t^4 q^{2C_{1,6}+2} + (q^2 + 1) t^3 q^{2C_{1,7}-2} + (q^2 + 1) t^5 q^{2C_{2,3}+2} \\
 & + (q^2 + 1) t^3 q^{2C_{2,4}-2} + (q^2 + 1) t^3 q^{2C_{2,5}-2} + (q^2 + 1) t^2 q^{2C_{2,6}-2} \\
 & \left. + (q^2 + 1) t q^{2C_{2,7}-6} \right) \\
 & + a^4 \left((q^2 + 1) t^6 q^{2C_{1,2}} + q^{12} t^8 + t^4 \right) + a^{-4} \left(\frac{(q^2 + 1) q^{2C_{8,9}}}{t^2} + \frac{1}{q^8 t^4} + q^4 \right) \\
 & + (q^2 + 1) t^4 q^{2C_{1,8}+4} + (q^2 + 1) t^2 q^{2C_{1,9}} + (q^2 + 1) t^2 q^{2C_{2,8}} \\
 & + (q^2 + 1) t^4 q^{2C_{3,4}+4} \\
 & + (q^2 + 1) t^4 q^{2C_{3,5}+4} + (q^2 + 1) t^3 q^{2C_{3,6}+4} + (q^2 + 1) t^2 q^{2C_{3,7}} \\
 & + (q^2 + 1) t^2 q^{2C_{4,5}} \\
 & + (q^2 + 1) t q^{2C_{4,6}} + (q^2 + 1) t q^{2C_{5,6}} + \frac{(q^2 + 1) q^{2C_{6,7}-4}}{t} + (q^2 + 1) q^{2C_{2,9}-4} \\
 & + (q^2 + 1) q^{2C_{4,7}-4} + (q^2 + 1) q^{2C_{5,7}-4} + q^{14} t^6 + 2q^2 t^2 + \frac{1}{q^{10} t^2} + 1 \quad (6.4)
 \end{aligned}$$

in terms of unknown linking numbers C_{ij} .

This prediction should be compared to the superpolynomial for the second symmetric representation P_2 . While at present no direct computation of this is available, a conjectural expression was communicated to us by Marko Stošić [54].¹² A key feature of P_2 is the presence of terms of order a^{-6} , from which one can readily deduce that the two expressions cannot quite agree

$$P_2 \neq P_Q|_{x^2}. \quad (6.5)$$

¹² This conjecture was communicated to us as an improvement of the earlier result from [7], which is discussed in Appendix B.

Moreover, the number of generators of degree $a^{-6}x^2$ is 6, and they appear to come in pairs of the following type

$$\frac{1 + q^4 t^{\pm 1}}{(1 - q^2)(1 - q^4)}. \quad (6.6)$$

As far as we are aware, 9_{42} is the simplest knot where multiply-wrapped basic disks appear. The known expressions for the first and second colored superpolynomials provide evidence for deviations from the standard form of the knots-quivers correspondence.

Acknowledgements We thank Marko Stošić and Paul Wedrich for insightful discussions and for sharing results. TE is supported by the Knut and Alice Wallenberg Foundation as a Wallenberg scholar KAW2020.0307 and by the Swedish Research Council VR2020-04535. In different stages of this work PK was supported by the Polish Ministry of Education and Science through its programs Mobility Plus (1667/MOB/V/2017/0) and the Polish National Science Centre through Sonata grant (2022/47/D/ST2/02058). PL is supported by NCCR SwissMAP, funded by the Swiss National Science Foundation.

Data Availability The datasets generated and analyzed during the current study are available from the corresponding author on reasonable request.

Declarations

Conflict of interest On behalf of all authors, the corresponding author states that there is no conflict of interest.

Open Access This article is licensed under a Creative Commons Attribution 4.0 International License, which permits use, sharing, adaptation, distribution and reproduction in any medium or format, as long as you give appropriate credit to the original author(s) and the source, provide a link to the Creative Commons licence, and indicate if changes were made. The images or other third party material in this article are included in the article's Creative Commons licence, unless indicated otherwise in a credit line to the material. If material is not included in the article's Creative Commons licence and your intended use is not permitted by statutory regulation or exceeds the permitted use, you will need to obtain permission directly from the copyright holder. To view a copy of this licence, visit <http://creativecommons.org/licenses/by/4.0/>.

A Inductive derivation of the q -multinomial identity

We would like to prove that

$$\sum_{|d|=r} \begin{bmatrix} r \\ d \end{bmatrix}_{q^2} Z_1^{d_1} \cdots Z_m^{d_m} = (Z_1 + \cdots + Z_m)^r \quad (\text{A.1})$$

with Z_i obeying the algebra (4.17) and with the q -multinomial coefficient a finite polynomial in q with positive integer coefficients, defined as in (4.20).

For $m = 1$, the identity is trivial. Now suppose it holds for a given m , and consider adding one variable

$$\sum_{|\mathbf{d}|=r} \begin{bmatrix} r \\ \mathbf{d} \end{bmatrix}_{q^2} Z_1^{d_1} \cdots Z_m^{d_m} Z_{m+1}^{d_{m+1}} = (Z_1 + \cdots + Z_m + Z_{m+1})^r. \quad (\text{A.2})$$

The *lhs* can be recast as follows:

$$\sum_{k=0}^r \left(\sum_{|\mathbf{d}'|=k} \begin{bmatrix} r-k \\ \mathbf{d}' \end{bmatrix}_{q^2} Z_1^{d'_1} \cdots Z_m^{d'_m} \right) \begin{bmatrix} r \\ k \end{bmatrix}_{q^2} Z_{m+1}^k, \quad (\text{A.3})$$

where $k = d_{m+1}$, \mathbf{d}' is a dimension vector consisting of the first m entries in $\mathbf{d} = (\mathbf{d}', k)$, and we used

$$\begin{bmatrix} r \\ \mathbf{d} \end{bmatrix}_{q^2} = \begin{bmatrix} r-k \\ \mathbf{d}' \end{bmatrix}_{q^2} \begin{bmatrix} r \\ k \end{bmatrix}_{q^2}, \quad (\text{A.4})$$

which follows from the definition of the q -multinomial. Using the identity on m variables, the *lhs* can be further simplified:

$$\sum_{k=0}^r \begin{bmatrix} r \\ k \end{bmatrix}_{q^2} Z^{r-k} Z_{m+1}^k, \quad (\text{A.5})$$

where $Z = Z_1 + \cdots + Z_m$. Notice that $Z_{m+1} \cdot Z = q^2 Z \cdot Z_{m+1}$. Therefore, we only need to prove the following binomial identity with non-commutative variables:

$$\sum_{k=0}^r \begin{bmatrix} r \\ k \end{bmatrix}_{q^2} Z^{r-k} Z_{m+1}^k = (Z + Z_{m+1})^r. \quad (\text{A.6})$$

In fact, this equation is a consequence of Gauss' q -binomial theorem, see [52, Theorem 5.1].

B A stronger conjecture on refinement

Here we collect an alternative, and stronger, conjecture on the refinement of partition function (1.2)

$$P_Q(\mathbf{x}; q, t) = \sum_{\mathbf{d}} (-1)^{\sum_i C_{ii} \mu_i d_i} q^{\sum_{i,j} C_{ij} (\mu_i d_i) (\mu_j d_j)} \prod_{i=1}^m \frac{x_i^{d_i}}{(q^2; q^2)_{\mu_i d_i}} \frac{(-q^2 t^{\sigma_i}; q^2)_{d_i \mu_i}}{(-q^2 \mu_i t^{\sigma_i}; q^2 \mu_i)_{d_i}}. \quad (\text{B.1})$$

The motivation for this conjecture comes from results for the second-symmetric HOMFLY-PT homology of the knots 9_{42} and 10_{132} . We now provide supporting evidence based on these.

B.1 The knot 9_{42}

We consider again the knot 9_{42} , with superpolynomial in the fundamental representation (6.2), and with corresponding quiver prediction for the second-level generators as in (6.4).

This prediction can be compared to the superpolynomial for the second symmetric representation conjectured in [7]:

$$\begin{aligned}
 P_2(a, q, t) = & 1 + (q^2 + 1) \left(\frac{1}{a^2 q^4 t^3} + 1 \right) \left(\frac{q^2}{a^2 t} + 1 \right) \left(a^2 q^2 t^4 + \frac{a^2 t^2}{q^2} \right) \\
 & + (q^2 + 1) \left(\frac{1}{a^2 q^6 t^3} + 1 \right) \left(\frac{1}{a^2 q^4 t^3} + 1 \right) \left(\frac{q^2}{a^2 t} + 1 \right) \\
 & \times (a^2 q^6 t^6 + a^2 q^6 t^5 + a^4 q^4 t^6 + 2a^2 q^2 t^5 + a^2 t^4 + q^2 t^4 + t^3) \\
 & + (q^2 + 1) \left(\frac{1}{t} + 1 \right) \left(\frac{1}{a^2 q^6 t^3} + 1 \right) \left(\frac{1}{a^2 q^4 t^3} + 1 \right) \left(\frac{q^2}{a^2 t} + 1 \right) \\
 & \times (a^4 q^8 t^8 + a^2 q^8 t^7 + a^2 q^4 t^5 + a^4 q^2 t^6 + a^2 t^4 + q^6 t^5 + t^3) \\
 & + \left(\frac{1}{a^2 t} + 1 \right) \left(\frac{1}{a^2 q^6 t^3} + 1 \right) \left(\frac{1}{a^2 q^4 t^3} + 1 \right) \\
 & \left(\frac{q^2}{a^2 t} + 1 \right) (a^4 q^{12} t^8 + a^4 t^4). \tag{B.2}
 \end{aligned}$$

In fact, one can readily deduce that the two expressions cannot quite agree

$$P_2 \neq P_Q|_{x^2}, \tag{B.3}$$

because of the terms of degree a^{-6} present in P_2 .

Although knowing the first and second colored superpolynomials is not quite enough to fix all the linking numbers C_{ij} , it is nevertheless instructive to make an ansatz for the latter so as to reproduce at least part of the second-degree superpolynomial. Upon making such a (non-unique) ansatz for the linking numbers C_{ij} (this affects only terms of a -degree ≥ -4), we may then compute the difference between the two, which turns out to be

$$P_2 - P_Q|_{x^2} = a^{-6} \tilde{p}_{-6} + a^{-4} \tilde{p}_{-4} + a^{-2} \tilde{p}_{-2} + a^0 \tilde{p}_0 + a^2 \tilde{p}_2 + a^4 \tilde{p}_4, \tag{B.4}$$

where

$$\tilde{p}_{-6} = \left(\frac{1}{q^6 t^4} + \frac{1}{q^8 t^4} + \frac{1}{q^8 t^5} + \frac{1}{q^2 t^3} \right) (q^2 t + 1) + \left(\frac{1}{q^8 t^4} + \frac{1}{q^2 t^2} \right) \left(\frac{q^2}{t} + 1 \right),$$

$$\begin{aligned}
\tilde{p}_{-4} &= \left(\frac{1}{q^2 t^2} + \frac{2}{q^4 t^2} + \frac{1}{q^4 t^3} + \frac{1}{q^6 t^3} + \frac{2}{q^8 t^3} + \frac{1}{q^{10} t^4} + \frac{2}{q^2 t} \right. \\
&\quad \left. + q^4 + q^2 + \frac{2}{t} \right) (q^2 t + 1) \\
&\quad + \left(\frac{q^2}{t} + 1 \right) \left(\frac{1}{q^4 t^2} + \frac{1}{q^8 t^2} + \frac{1}{q^8 t^3} + \frac{2}{q^{10} t^3} + q^4 t + q^2 t \right. \\
&\quad \left. + \frac{2}{q^2 t} + \frac{3}{q^4 t} + \frac{1}{q^2} + 1 \right), \\
\tilde{p}_{-2} &= (q^2 t + 1) \left(q^8 t^3 + q^8 t^2 + q^6 t^2 + 2q^4 t^2 + \frac{2}{q^6 t^2} + \frac{1}{q^8 t^2} \right. \\
&\quad \left. + \frac{1}{q^{10} t^2} + \frac{1}{q^{10} t^3} + 3q^2 t + \frac{3}{q^4 t} + \frac{2}{q^6 t} + \frac{1}{q^8 t} + \frac{4}{q^2} + \frac{2}{q^4} + 2t + 3 \right) \\
&\quad + \left(\frac{q^2}{t} + 1 \right) \left(q^8 t^4 + 2q^4 t^3 + q^4 t^2 + 3q^2 t^2 \right. \\
&\quad \left. + \frac{1}{q^{10} t^2} + \frac{3t}{q^2} + \frac{t}{q^4} + \frac{2}{q^6 t} + \frac{3}{q^4} + \frac{1}{q^6} + t^2 + 3t \right), \\
\tilde{p}_0 &= (q^2 t + 1) \left(q^{10} t^5 + q^8 t^4 + 4q^6 t^3 + 5q^4 t^3 + q^4 t^2 \right. \\
&\quad \left. + 3q^2 t^3 + 2q^2 t^2 + q^2 t + \frac{4t}{q^2} + \frac{2t}{q^4} + \frac{1}{q^8 t} + \frac{2}{q^6} + 2t^2 \right) \\
&\quad + \left(\frac{q^2}{t} + 1 \right) \left(q^{10} t^6 + 2q^8 t^5 + q^6 t^5 + 2q^6 t^4 + q^2 t^3 \right. \\
&\quad \left. + \frac{5t^2}{q^2} + \frac{2t^2}{q^4} + \frac{2t}{q^6} + \frac{1}{q^8} + 2t^3 \right), \\
\tilde{p}_2 &= (q^2 t + 1) \left(q^{12} t^6 + q^{10} t^6 + q^8 t^6 + q^6 t^5 + 2q^6 t^4 + 2q^4 t^4 + 2q^2 t^4 + \frac{t^2}{q^2} \right. \\
&\quad \left. + \frac{t^2}{q^4} + t^4 + t^3 + t^2 \right) \\
&\quad + \left(\frac{q^2}{t} + 1 \right) \left(q^8 t^7 + q^6 t^6 + q^4 t^5 + 2q^2 t^5 + \frac{t^3}{q^4} + t^4 \right), \\
\tilde{p}_4 &= (q^2 t + 1) (q^8 t^7 + q^2 t^5) + \left(\frac{q^2}{t} + 1 \right) (q^8 t^8 + q^2 t^6).
\end{aligned}$$

The number of generators at each level is

	a^{-6}	a^{-4}	a^{-2}	a^0	a^2	a^4
P_2	12	60	124	129	64	12
$P_Q _{x^2}$	0	4	20	33	20	4

(B.5)

The difference, divided by two to account for the correction to the denominator $1 - q^4$ of (1.2) vs $(1 - q^2)(1 - q^4)$ of knot homology, gives the number of new disks wrapping around L_K twice.

The difference (B.4), corresponding precisely to the contributions of the new twice-wrapped basic disks, organizes into sums of terms with overall factors of the form $(1 + t^{\pm 1}q^2)$, level by level in powers of a . This fact is non-trivial evidence supporting our proposal for the refined version of the generalized partition function (B.1), noting that setting $d_i = 1$, $\mu_i = 2$ gives

$$\begin{aligned} \frac{1}{(q^2; q^2)_{\mu_i d_i}} \frac{(-q^2 t^{\pm 1}; q^2)_{d_i \mu_i}}{(-q^{2\mu_i} t^{\pm 1}; q^{2\mu_i})_{d_i}} &= \frac{1}{(q^2; q^2)_2} \frac{(-q^2 t^{\pm 1}; q^2)_2}{(-q^4 t^{\pm 1}; q^4)_1} \\ &= \frac{1 + q^2 t^{\pm 1}}{(1 - q^2)(1 - q^4)}. \end{aligned} \quad (\text{B.6})$$

The denominator matches with the one accompanying the superpolynomial for \mathcal{H}_2 , while the numerator is exactly the type of binomial that organizes (B.4). It should be noted that the expression (B.2) is in fact conjectural. In this regard, the evidence supporting our proposal for the refined generalized partition function (B.1) is not conclusive.

B.2 The knot 10_{132}

Another example is provided by the knot conormal of the knot 10_{132} , and we discuss it following the steps from the analysis of 9_{42} .

The superpolynomial in the fundamental representation is given by [15]

$$\begin{aligned} P_1(a, q, t) &= a^2 \left(q^2 (t^3 + t^2) + \frac{t+1}{q^2} \right) + a^4 \left(q^4 t^6 + \frac{t^2}{q^4} + (2t^4 + t^3) \right) \\ &\quad + a^6 \left(q^2 t^7 + \frac{t^5}{q^2} \right) \end{aligned}$$

This corresponds to quiver generators with (a, q, t) degrees

a_i	$q_i - C_{ii}$	$t_i = C_{ii}$
6	-5	7
6	-7	5
4	-2	6
4	-4	4
4	-4	4
4	-3	3
4	-6	2
2	-1	3
2	0	2
2	-3	1
2	-2	0

(B.7)

Now let us again temporarily assume that all higher BPS states arise from bound states of the basic once-around curves corresponding to the generators (B.7), as in the original formulation of the knots-quivers correspondence of [10, 11]. Then, we would have the following contribution to the partition function for the coefficient of x^2 :

$$\begin{aligned}
 P_Q|_{x^2} = & \left((q^2 + 1)t^{12}q^{2c_{1,2}} + t^{14}q^{18} + t^{10}q^6 \right) a^{12} \\
 & + \left((q^2 + 1)t^{13}q^{2c_{1,3}+6} + (q^2 + 1)t^{11}q^{2c_{1,4}+2} + (q^2 + 1)t^{11}q^{2c_{1,5}+2} \right. \\
 & + (q^2 + 1)t^{10}q^{2c_{1,6}+2} + (q^2 + 1)t^9q^{2c_{1,7}-2} + (q^2 + 1)t^{11}q^{2c_{2,3}+2} \\
 & + (q^2 + 1)t^9q^{2c_{2,4}-2} + (q^2 + 1)t^9q^{2c_{2,5}-2} + (q^2 + 1)t^8q^{2c_{2,6}-2} \\
 & \left. + (q^2 + 1)t^7q^{2c_{2,7}-6} \right) a^{10} \\
 & + \left((q^2 + 1)t^{10}q^{2c_{1,8}+4} + (q^2 + 1)t^9q^{2c_{1,9}+4} + (q^2 + 1)t^8q^{2c_{1,10}} \right. \\
 & + (q^2 + 1)t^7q^{2c_{1,11}} \\
 & + (q^2 + 1)t^8q^{2c_{2,8}} + (q^2 + 1)t^7q^{2c_{2,9}} + (q^2 + 1)t^6q^{2c_{2,10}-4} \\
 & + (q^2 + 1)t^5q^{2c_{2,11}-4} \\
 & + (q^2 + 1)t^{10}q^{2c_{3,4}+4} + (q^2 + 1)t^{10}q^{2c_{3,5}+4} \\
 & + (q^2 + 1)t^9q^{2c_{3,6}+4} + (q^2 + 1)t^8q^{2c_{3,7}} \\
 & + (q^2 + 1)t^8q^{2c_{4,5}} + (q^2 + 1)t^7q^{2c_{4,6}} \\
 & + (q^2 + 1)t^6q^{2c_{4,7}-4} + (q^2 + 1)t^7q^{2c_{5,6}} \\
 & + (q^2 + 1)t^6q^{2c_{5,7}-4} + (q^2 + 1)t^5q^{2c_{6,7}-4} + t^{12}q^{20} \\
 & \left. + 2t^8q^8 + t^6q^6 + t^4q^{-4} \right) a^8 \\
 & + \left((q^2 + 1)t^9q^{2c_{3,8}+6} + (q^2 + 1)t^8q^{2c_{3,9}+6} + (q^2 + 1)t^7q^{2c_{3,10}+2} \right. \\
 & + (q^2 + 1)t^6q^{2c_{3,11}+2} + (q^2 + 1)t^7q^{2c_{4,8}+2} + (q^2 + 1)t^6q^{2c_{4,9}+2} \\
 & + (q^2 + 1)t^5q^{2c_{4,10}-2} + (q^2 + 1)t^4q^{2c_{4,11}-2} + (q^2 + 1)t^7q^{2c_{5,8}+2} \\
 & + (q^2 + 1)t^6q^{2c_{5,9}+2} + (q^2 + 1)t^5q^{2c_{5,10}-2} + (q^2 + 1)t^4q^{2c_{5,11}-2} \\
 & + (q^2 + 1)t^6q^{2c_{6,8}+2} + (q^2 + 1)t^5q^{2c_{6,9}+2} + (q^2 + 1)t^4q^{2c_{6,10}-2} \\
 & + (q^2 + 1)t^3q^{2c_{6,11}-2} + (q^2 + 1)t^5q^{2c_{7,8}-2} + (q^2 + 1)t^4q^{2c_{7,9}-2} \\
 & \left. + (q^2 + 1)t^3q^{2c_{7,10}-6} + (q^2 + 1)t^2q^{2c_{7,11}-6} \right) a^6
 \end{aligned}$$

$$\begin{aligned}
& + \left((q^2 + 1) t^5 q^{2c_{8,9}+4} + (q^2 + 1) t^4 q^{2c_{8,10}} + (q^2 + 1) t^3 q^{2c_{8,11}} \right. \\
& + (q^2 + 1) t^3 q^{2c_{9,10}} + (q^2 + 1) t^2 q^{2c_{9,11}} \\
& \left. + (q^2 + 1) t q^{2c_{10,11}-4} + t^6 q^{10} + t^4 q^8 + t^2 q^{-2} + q^{-4} \right) a^4, \quad (\text{B.8})
\end{aligned}$$

in terms of unknown linking numbers C_{ij} . This prediction can be compared to the superpolynomial for the second symmetric representation [54]

$$P_2(a, q, t) = a^0 p_0 + a^2 p_2 + a^4 p_4 + a^6 p_6 + a^8 p_8 + a^{10} p_{10} + a^{12} p_{12}, \quad (\text{B.9})$$

where

$$\begin{aligned}
p_0 = & \frac{t^{2n_1-8}}{q^6} + \frac{t^{2n_1-8}}{q^8} + \frac{t^{2n_2-7}}{q^4} + \frac{t^{2n_2-7}}{q^6} + \frac{t^{2n_3-8}}{q^2} + t^{2n_3-8} + q^2 t^{2n_4-7} + t^{2n_4-7} \\
& + \frac{t^{2n_5-8}}{q^2} + \frac{t^{2n_5-8}}{q^4} + \frac{t^{2n_6-7}}{q^2} + \frac{t^{2n_6-7}}{q^4} \\
& + q^6 t^3 + q^4 t^3 + q^6 t^2 + q^4 t^2 + q^2 t^2 + t^2 + \frac{3t}{q^2} + 3t \\
& + \frac{2}{q^2} + \frac{1}{q^4} + \frac{1}{q^6} + \frac{2}{q^6 t} + \frac{2}{q^8 t} + \frac{1}{q^6 t^2} + \frac{1}{q^8 t^2} + 2, \\
p_2 = & \frac{t^{2n_1-7}}{q^6} + \frac{2t^{2n_1-7}}{q^8} + \frac{t^{2n_1-7}}{q^{10}} + \frac{2t^{2n_1-5}}{q^2} + \frac{t^{2n_1-5}}{q^4} + t^{2n_1-5} + \frac{t^{2n_2-6}}{q^4} \\
& + \frac{2t^{2n_2-6}}{q^6} + \frac{t^{2n_2-6}}{q^8} + q^2 t^{2n_2-4} + \frac{t^{2n_2-4}}{q^2} + 2t^{2n_2-4} + \frac{2t^{2n_3-7}}{q^2} \\
& + \frac{t^{2n_3-7}}{q^4} + t^{2n_3-7} + q^6 t^{2n_3-5} + 2q^4 t^{2n_3-5} + q^2 t^{2n_3-5} + q^2 t^{2n_4-6} + \frac{t^{2n_4-6}}{q^2} \\
& + 2t^{2n_4-6} + q^8 t^{2n_4-4} + 2q^6 t^{2n_4-4} + q^4 t^{2n_4-4} + \frac{t^{2n_5-7}}{q^2} + \frac{2t^{2n_5-7}}{q^4} + \frac{t^{2n_5-7}}{q^6} \\
& + q^4 t^{2n_5-5} + 2q^2 t^{2n_5-5} + t^{2n_5-5} + \frac{t^{2n_6-6}}{q^2} + \frac{2t^{2n_6-6}}{q^4} + \frac{t^{2n_6-6}}{q^6} \\
& + q^4 t^{2n_6-4} + 2q^2 t^{2n_6-4} + t^{2n_6-4} + q^{12} t^6 + 2q^{10} t^6 + q^8 t^6 \\
& + q^{12} t^5 + 2q^{10} t^5 + 3q^8 t^5 + 3q^6 t^5 \\
& + q^4 t^5 + q^8 t^4 + 6q^6 t^4 + 9q^4 t^4 + 4q^2 t^4 + 4q^6 t^3 + 7q^4 t^3 + 8q^2 t^3 \\
& + \frac{2t^3}{q^2} + 7t^3 + q^4 t^2 + 2q^2 t^2 \\
& + \frac{12t^2}{q^2} + \frac{5t^2}{q^4} + 8t^2 + \frac{7t}{q^2} + \frac{5t}{q^4} + \frac{3t}{q^6} + \frac{t}{q^8} + 4t + \frac{1}{q^2} + \frac{1}{q^4}
\end{aligned}$$

$$\begin{aligned}
& + \frac{2}{q^6} + \frac{4}{q^8} + \frac{2}{q^{10}} + \frac{1}{q^6 t} + \frac{2}{q^8 t} + \frac{1}{q^{10} t}, \\
p_4 = & \frac{t^{2n_1-6}}{q^8} + \frac{t^{2n_1-6}}{q^{10}} + \frac{3t^{2n_1-4}}{q^2} + \frac{3t^{2n_1-4}}{q^4} + \frac{t^{2n_1-4}}{q^6} \\
& + t^{2n_1-4} + q^4 t^{2n_1-2} + q^2 t^{2n_1-2} + \frac{t^{2n_2-5}}{q^6} + \frac{t^{2n_2-5}}{q^8} + q^2 t^{2n_2-3} + \frac{3t^{2n_2-3}}{q^2} \\
& + \frac{t^{2n_2-3}}{q^4} + 3t^{2n_2-3} + q^6 t^{2n_2-1} + q^4 t^{2n_2-1} + \frac{t^{2n_3-6}}{q^2} + \frac{t^{2n_3-6}}{q^4} + q^6 t^{2n_3-4} \\
& + 3q^4 t^{2n_3-4} + 3q^2 t^{2n_3-4} + t^{2n_3-4} + q^{10} t^{2n_3-2} + q^8 t^{2n_3-2} \\
& + \frac{t^{2n_4-5}}{q^2} + t^{2n_4-5} + q^8 t^{2n_4-3} + 3q^6 t^{2n_4-3} + 3q^4 t^{2n_4-3} + q^2 t^{2n_4-3} \\
& + q^{12} t^{2n_4-1} + q^{10} t^{2n_4-1} + \frac{t^{2n_5-6}}{q^4} + \frac{t^{2n_5-6}}{q^6} + q^4 t^{2n_5-4} + 3q^2 t^{2n_5-4} \\
& + \frac{t^{2n_5-4}}{q^2} + 3t^{2n_5-4} + q^8 t^{2n_5-2} + q^6 t^{2n_5-2} + \frac{t^{2n_6-5}}{q^4} + \frac{t^{2n_6-5}}{q^6} + q^4 t^{2n_6-3} \\
& + 3q^2 t^{2n_6-3} + \frac{t^{2n_6-3}}{q^2} + 3t^{2n_6-3} + q^8 t^{2n_6-1} + q^6 t^{2n_6-1} \\
& + q^{16} t^9 + q^{14} t^9 + q^{16} t^8 + 2q^{14} t^8 + 3q^{12} t^8 + 2q^{10} t^8 \\
& + q^{14} t^7 + 4q^{12} t^7 + 9q^{10} t^7 + 7q^8 t^7 \\
& + q^6 t^7 + 2q^{12} t^6 + 8q^{10} t^6 + 12q^8 t^6 + 14q^6 t^6 + 8q^4 t^6 \\
& + q^2 t^6 + q^{10} t^5 + 6q^8 t^5 + 13q^6 t^5 \\
& + 20q^4 t^5 + 15q^2 t^5 + 3t^5 + q^8 t^4 + 4q^6 t^4 + 13q^4 t^4 + 17q^2 t^4 \\
& + \frac{8t^4}{q^2} + \frac{t^4}{q^4} + 15t^4 + 3q^4 t^3 \\
& + 8q^2 t^3 + \frac{14t^3}{q^2} + \frac{11t^3}{q^4} + \frac{2t^3}{q^6} + 10t^3 + q^4 t^2 + q^2 t^2 \\
& + \frac{8t^2}{q^2} + \frac{7t^2}{q^4} + \frac{4t^2}{q^6} + \frac{2t^2}{q^8} + 2t^2 \\
& + \frac{t}{q^2} + \frac{3t}{q^4} + \frac{2t}{q^6} + \frac{2t}{q^8} + \frac{2t}{q^{10}} + \frac{1}{q^4} + \frac{1}{q^8} + \frac{1}{q^{10}}, \\
p_6 = & \frac{t^{2n_1-3}}{q^2} + \frac{2t^{2n_1-3}}{q^4} + \frac{t^{2n_1-3}}{q^6} + q^4 t^{2n_1-1} + 2q^2 t^{2n_1-1} \\
& + t^{2n_1-1} + q^6 t^{2n_2} + 2q^4 t^{2n_2} + q^2 t^{2n_2} + \frac{2t^{2n_2-2}}{q^2} + \frac{t^{2n_2-2}}{q^4} + t^{2n_2-2} \\
& + q^4 t^{2n_3-3} + 2q^2 t^{2n_3-3} + t^{2n_3-3} + q^{10} t^{2n_3-1} + 2q^8 t^{2n_3-1} + q^6 t^{2n_3-1}
\end{aligned}$$

$$\begin{aligned}
& + q^{12}t^{2n_4} + 2q^{10}t^{2n_4} + q^8t^{2n_4} + q^6t^{2n_4-2} + 2q^4t^{2n_4-2} + q^2t^{2n_4-2} \\
& + q^2t^{2n_5-3} + \frac{t^{2n_5-3}}{q^2} + 2t^{2n_5-3} + q^8t^{2n_5-1} + 2q^6t^{2n_5-1} + q^4t^{2n_5-1} \\
& + q^8t^{2n_6} + 2q^6t^{2n_6} + q^4t^{2n_6} + q^2t^{2n_6-2} \\
& + \frac{t^{2n_6-2}}{q^2} + 2t^{2n_6-2} + q^{18}t^{11} + q^{16}t^{11} + q^{18}t^{10} + 3q^{16}t^{10} \\
& + 3q^{14}t^{10} + q^{12}t^{10} + 3q^{16}t^9 \\
& + 6q^{14}t^9 + 10q^{12}t^9 + 9q^{10}t^9 + 2q^8t^9 + 3q^{14}t^8 + 9q^{12}t^8 \\
& + 15q^{10}t^8 + 14q^8t^8 + 5q^6t^8 + q^{12}t^7 \\
& + 9q^{10}t^7 + 18q^8t^7 + 22q^6t^7 + 17q^4t^7 + 5q^2t^7 + q^{10}t^6 + 9q^8t^6 \\
& + 18q^6t^6 + 21q^4t^6 + 18q^2t^6 \\
& + 7t^6 + q^8t^5 + 2q^6t^5 + 9q^4t^5 + 15q^2t^5 + \frac{9t^5}{q^2} + \frac{2t^5}{q^4} + 14t^5 \\
& + q^4t^4 + 7q^2t^4 + \frac{9t^4}{q^2} + \frac{6t^4}{q^4} \\
& + \frac{2t^4}{q^6} + 11t^4 + q^2t^3 + \frac{3t^3}{q^2} + \frac{4t^3}{q^4} + \frac{2t^3}{q^6} + \frac{t^3}{q^8} + t^3 + \frac{t^2}{q^4} + \frac{2t^2}{q^6} + \frac{t^2}{q^8}, \\
p_8 = & q^2t^{2n_1} + t^{2n_1} + q^4t^{2n_2+1} + q^2t^{2n_2+1} + q^8t^{2n_3} + q^6t^{2n_3} + q^{10}t^{2n_4+1} \\
& + q^8t^{2n_4+1} + q^6t^{2n_5} + q^4t^{2n_5} + q^6t^{2n_6+1} + q^4t^{2n_6+1} \\
& + q^{20}t^{12} + 2q^{18}t^{12} + 3q^{16}t^{12} \\
& + q^{14}t^{12} + 2q^{18}t^{11} + 4q^{16}t^{11} + 4q^{14}t^{11} + 2q^{12}t^{11} \\
& + 2q^{16}t^{10} + 7q^{14}t^{10} + 12q^{12}t^{10} \\
& + 13q^{10}t^{10} + 6q^8t^{10} + 2q^{14}t^9 + 9q^{12}t^9 + 14q^{10}t^9 \\
& + 13q^8t^9 + 6q^6t^9 + 3q^{10}t^8 + 12q^8t^8 \\
& + 15q^6t^8 + 14q^4t^8 + 6q^2t^8 + 3q^8t^7 + 12q^6t^7 + 14q^4t^7 \\
& + 9q^2t^7 + 4t^7 + q^6t^6 + 2q^4t^6 \\
& + 6q^2t^6 + \frac{3t^6}{q^2} + \frac{t^6}{q^4} + 6t^6 + q^2t^5 + \frac{4t^5}{q^2} + \frac{t^5}{q^4} + 4t^5 + \frac{t^4}{q^4}, \\
p_{10} = & t^{13}q^{20} + 2t^{13}q^{18} + t^{12}q^{18} + 3t^{13}q^{16} + 3t^{12}q^{16} + 2t^{13}q^{14} \\
& + 3t^{12}q^{14} + 3t^{11}q^{14} + t^{12}q^{12} \\
& + 6t^{11}q^{12} + 3t^{10}q^{12} + 8t^{11}q^{10} + 7t^{10}q^{10} + 5t^{11}q^8 + 6t^{10}q^8 \\
& + 3t^9q^8 + 2t^{10}q^6 + 5t^9q^6 \\
& + 2t^8q^6 + 4t^9q^4 + 4t^8q^4 + 2t^9q^2 + 2t^8q^2 + t^7q^2 + t^7, \\
p_{12} = & t^{14}q^{18} + t^{14}q^{16} + t^{13}q^{16} + t^{14}q^{14} + t^{13}q^{14}
\end{aligned}$$

$$+ t^{12}q^{12} + 2t^{12}q^{10} + t^{11}q^{10} + t^{12}q^8 + t^{11}q^8 + t^{10}q^6,$$

and n_1, \dots, n_6 are some (unknown) integer numbers.

As for 9_{42} , the main point is that the two expressions cannot agree:

$$P_2 \neq P_Q|_{x^2}, \quad (\text{B.10})$$

this time because of the terms of degree a^0 and a^2 present in P_2 .

In fact, we may compute the difference, upon making a (non-unique) ansatz for the linking numbers C_{ij} (this affects only terms of degree $\geq a^4$)

$$P_2 - P_Q|_{x^2} = a^0 \tilde{p}_0 + a^2 \tilde{p}_2 + a^4 \tilde{p}_4 + a^6 \tilde{p}_6 + a^8 \tilde{p}_8 + a^{10} \tilde{p}_{10} + a^{12} \tilde{p}_{12}, \quad (\text{B.11})$$

where

$$\begin{aligned} \tilde{p}_0 &= (q^2t + 1) \left(q^4t^2 + \frac{1}{q^8t^2} + \frac{1}{q^2t^8} + \frac{1}{q^4t^8} + \frac{1}{q^6t^8} + \frac{1}{q^8t^8} \right. \\ &\quad \left. + \frac{t}{q^2} + \frac{1}{q^6t} + \frac{1}{q^8t} + \frac{2}{q^2} + \frac{1}{t^8} + t \right) \\ &\quad + \left(\frac{q^2}{t} + 1 \right) \left(q^4t^3 + \frac{1}{q^4t^7} + \frac{2t}{q^2} + \frac{1}{q^8t} \right), \\ \tilde{p}_2 &= (q^2t + 1) \left(q^{10}t^5 + q^8t^5 + 2q^6t^4 + \frac{q^6}{t^5} + 2q^4t^4 + 3q^4t^3 \right. \\ &\quad \left. + \frac{2q^4}{t^5} + 3q^2t^3 + \frac{2q^2}{t^5} \right. \\ &\quad \left. + \frac{5t^2}{q^2} + \frac{2}{q^2t^5} + \frac{1}{q^4t^5} + \frac{2}{q^2t^7} + \frac{2}{q^4t^7} + \frac{2}{q^6t^7} + \frac{2}{q^8t^7} + \frac{1}{q^{10}t^7} \right. \\ &\quad \left. + \frac{2t}{q^2} + \frac{3t}{q^4} + \frac{t}{q^6} + \frac{1}{q^{10}t} + \frac{1}{q^4} + \frac{1}{q^6} + \frac{2}{q^8} + 4t^2 + \frac{2}{t^5} + \frac{1}{t^7} \right) \\ &\quad + \left(\frac{q^2}{t} + 1 \right) \left(q^{10}t^6 + q^8t^6 + q^6t^5 + q^4t^5 + 4q^4t^4 \right. \\ &\quad \left. + 4q^2t^4 + q^2t^3 + \frac{q^2}{t^4} + \frac{2t^3}{q^2} \right. \\ &\quad \left. + \frac{4t^2}{q^2} + \frac{4t^2}{q^4} + \frac{1}{q^4t^6} + \frac{1}{q^6t^6} + \frac{t}{q^4} + \frac{t}{q^8} + \frac{1}{q^8} + \frac{2}{q^{10}} + 2t^3 + \frac{1}{t^4} \right), \\ \tilde{p}_4 &= (q^2t + 1) \left(q^{14}t^8 + q^{12}t^7 + 2q^{10}t^7 + 2q^{10}t^6 + \frac{q^{10}}{t^2} \right. \\ &\quad \left. + q^8t^7 + 5q^8t^6 + 3q^8t^5 + \frac{q^8}{t^2} \right. \\ &\quad \left. + 4q^6t^6 + 5q^6t^5 + q^6t^4 + \frac{q^6}{t^2} + \frac{q^6}{t^4} + 8q^4t^5 + q^4t^3 + \frac{q^4}{t^2} + \frac{3q^4}{t^4} + q^2t^5 \right. \end{aligned}$$

$$\begin{aligned}
& + 9q^2t^4 + \frac{q^2}{t^2} + \frac{4q^2}{t^4} + \frac{8t^3}{q^2} + \frac{6t^3}{q^4} + \frac{3t^2}{q^2} + \frac{4t^2}{q^4} + \frac{2t^2}{q^6} \\
& + \frac{t^2}{q^8} + \frac{4}{q^2t^4} + \frac{3}{q^4t^4} + \frac{1}{q^6t^4} + \frac{1}{q^2t^6} + \frac{1}{q^4t^6} + \frac{1}{q^6t^6} + \frac{1}{q^8t^6} \\
& + \frac{1}{q^{10}t^6} + \frac{t}{q^4} + \frac{2t}{q^6} + \frac{t}{q^8} + \frac{t}{q^{10}} + \frac{1}{q^{10}} + t^5 + t^4 + 3t^3 + \frac{4}{t^4} \Big) \\
& + \left(\frac{q^2}{t} + 1 \right) \left(q^{14}t^9 + q^{12}t^8 + q^{10}t^8 + 2q^{10}t^7 + 2q^8t^7 \right. \\
& + q^8t^6 + q^6t^7 + 2q^6t^6 + 7q^4t^6 \\
& + 2q^4t^5 + 13q^2t^5 + 2q^2t^4 + q^2t^3 + \frac{q^2}{t^3} + \frac{2t^4}{q^2} + \frac{t^4}{q^4} + \frac{t^3}{q^2} + \frac{3t^3}{q^4} \\
& + \frac{t^3}{q^6} + \frac{t^2}{q^6} + \frac{1}{q^2t^3} + \frac{1}{q^6t^5} + \frac{q^6}{t} + \frac{t}{q^{10}} + 2t^5 + 5t^4 + \frac{2}{t^3} \Big),
\end{aligned}$$

$$\begin{aligned}
\tilde{p}_6 = & \left(q^2t + 1 \right) \left(q^{16}t^{10} + q^{16}t^9 + q^{14}t^{10} + 2q^{14}t^9 + q^{14}t^8 + q^{12}t^9 \right. \\
& + 3q^{12}t^8 + q^{12}t^7 + 7q^{10}t^8 + 4q^{10}t^7 + 6q^8t^8 + 6q^8t^7 + 4q^8t^6 + q^6t^8 \\
& + 6q^6t^7 + 8q^6t^6 + 2q^6t^5 + q^4t^7 \\
& + 11q^4t^6 + 4q^4t^5 + \frac{q^4}{t^3} + 10q^2t^6 + 5q^2t^5 + 3q^2t^4 + \frac{2q^2}{t^3} \\
& + \frac{3t^4}{q^2} + \frac{5t^4}{q^4} + \frac{t^3}{q^2} + \frac{t^2}{q^8} + \frac{2}{q^2t^3} \\
& + \frac{2}{q^4t^3} + \frac{1}{q^6t^3} + \frac{q^{10}}{t} + \frac{2q^8}{t} + \frac{2q^6}{t} + \frac{2q^4}{t} + \frac{2q^2}{t} \\
& + 3t^6 + 5t^5 + 4t^4 + t^3 + \frac{2}{t^3} + \frac{1}{t} \Big) \\
& + \left(\frac{q^2}{t} + 1 \right) \left(q^{14}t^{10} + q^{12}t^{10} + q^{12}t^9 + 2q^{10}t^9 \right. \\
& + q^8t^9 + q^8t^8 + q^8t^7 + 3q^6t^8 + 2q^6t^7 \\
& + q^6t^6 + 3q^4t^7 + 2q^2t^7 + q^2t^6 + q^2t^5 + \frac{t^5}{q^2} + \frac{2t^5}{q^4} + \frac{t^4}{q^4} + \frac{2t^4}{q^6} + \frac{t^3}{q^8} \\
& + \frac{1}{q^2t^2} + q^6 + q^4 + 4t^6 + 3t^5 + t^4 + \frac{1}{t^2} \Big), \\
\tilde{p}_8 = & \left(q^2t + 1 \right) \left(2q^{16}t^{11} + q^{14}t^{11} + q^{14}t^{10} + q^{12}t^{10} + 4q^{12}t^9 \right. \\
& + 9q^{10}t^9 + 5q^8t^9 + 2q^8t^8 \\
& + 3q^6t^8 + 4q^6t^7 + 9q^4t^7 + 2q^2t^7 + 3q^2t^6 + \frac{2t^5}{q^2} + q^8
\end{aligned}$$

$$\begin{aligned}
& + q^6 + q^4 + q^2 + t^6 + 3t^5 + 1) \\
& + \left(\frac{q^2}{t} + 1\right) (2q^{16}t^{12} + q^{14}t^{12} + 2q^{14}t^{11} + 2q^{12}t^{11} + 2q^{12}t^{10} \\
& + 5q^{10}t^{10} + 3q^8t^{10} + 3q^8t^9 + 4q^6t^9 + 3q^6t^8 \\
& + 8q^4t^8 + 2q^2t^8 + 2q^2t^7 + q^4t + t^6), \\
\tilde{p}_{10} = & (q^2t + 1) (q^{18}t^{12} + 2q^{16}t^{12} + 2q^{14}t^{12} + q^{12}t^{11} + 2q^{12}t^{10} \\
& + 5q^{10}t^{10} + 4q^8t^{10} + q^6t^9 + 2q^6t^8 + 3q^4t^8 + q^2t^8) \\
& + \left(\frac{q^2}{t} + 1\right) (q^{14}t^{13} + q^{12}t^{12} + q^{10}t^{11} + 2q^8t^{11} + q^6t^{10}), \\
\tilde{p}_{12} = & (q^2t + 1) (q^{14}t^{13} + q^{10}t^{11} + q^8t^{11}) + \left(\frac{q^2}{t} + 1\right) q^{14}t^{14}.
\end{aligned}$$

The difference turns out to have the general form

$$P_2 - P_Q|_{x^2} = (q^2t + 1) [\dots] + \left(\frac{q^2}{t} + 1\right) [\dots]. \quad (\text{B.12})$$

and the number of generators at each level is

$$\begin{array}{c|cccccccc}
& a^0 & a^2 & a^4 & a^6 & a^8 & a^{10} & a^{12} & \\
\hline
P_2 & 36 & 172 & 352 & 384 & 237 & 80 & 12 & \\
P_Q|_{x^2} & 0 & 0 & 16 & 40 & 41 & 20 & 4 &
\end{array} . \quad (\text{B.13})$$

The difference, divided by two to account for the correction to the denominator $1 - q^4$ of (1.2) vs $(1 - q^2)(1 - q^4)$ of knot homology, gives the number of new disks wrapping around L_K twice.

The known expressions for the first and second colored superpolynomials provide further robust evidence for deviations from the standard form of the knots-quivers correspondence, adding to the case of 9_{42} . In addition, we observe how the difference (B.12), corresponding precisely to the contributions of the new twice-wrapped basic disks, organizes into sums of terms with overall factors of the form $(1 + t^{\pm 1}q^2)$, level by level in powers of a .

As for 9_{42} , it should be noted that the expression (B.9) for the second symmetrically colored HOMFLY-PT is conjectural. In this regard, the evidence supporting our proposal for the refined generalized partition function (B.1) is not conclusive.

C Comparing $T[L_K]$ and $T[Q]$ in view of knot homology

We collect here some comments on how the theory $T[L_K]$ is more closely related to knot homology than its dual description $T[Q]$.

At level x^2 , the quiver partition function has terms proportional to $x_i x_j / [(q^2; q^2)_1]^2$. The partition function of $T[L_K]$ is obtained by substitution of quiver variables $x_i = x_i(x, a, q)$. Such terms appear as $(1 + q^2)x_i x_j / (q^2; q^2)_2$, i.e., with a different denominator:

$$\frac{1}{(1 - q^2)^2} \rightarrow \frac{1 + q^2}{(1 - q^2)(1 - q^4)}. \quad (\text{C.1})$$

This is somewhat unnatural from the viewpoint of $T[Q]$ since it ‘doubles’ the contribution of certain generators of the Hilbert space of BPS vortices. On the other hand, from the viewpoint of $T[L_K]$, this change of denominator, and similar changes at higher orders in x , arise naturally and therefore the Hilbert space of level r BPS vortices in $T[L_K]$ is more closely related to HOMFLY-PT homologies of knots. Physically, the difference between the denominator $(q^2; q^2)_2$ in $T[L_K]$ and $((q^2; q^2)_1)^2$ in $T[Q]$ comes from viewing a vortex with vorticity 2 as a bound state of two *distinguishable* vortices (each with vorticity 1) in $T[Q]$ versus viewing it as a bound state of two *indistinguishable* vortices with vorticity 1 in $T[L_K]$.

Let us discuss another point concerning denominators in the partition function. Consider a d -times around node which is *not* a bound state of once-around disks. It will contribute to the partition function $P_K(x, a, q)$ by a term of the form

$$\frac{a^\alpha q^\beta x^2}{1 - q^{2d}}. \quad (\text{C.2})$$

The contribution of this term to the HOMFLY-PT polynomial with S^d -coloring will then be obtained by correcting the denominator by multiplication and division by $(1 - q^2) \cdots (1 - q^{2(d-1)})$:

$$\frac{(1 - q^2) \cdots (1 - q^{2(d-1)}) a^\alpha q^\beta}{(q^2; q^2)_d}. \quad (\text{C.3})$$

From the viewpoint of a quiver-like description it is somewhat unnatural to compensate the denominator by this extra factor: it multiplies the contribution of a single fundamental curve (a d times around basic disk) by 2^{d-1} and it produces terms with opposite signs in the numerator. See Definition 1.1 for a framework where the corrected denominator appears naturally and where there is a refinement that retains positivity.

References

1. Witten, E.: Quantum field theory and the Jones polynomial. Commun. Math. Phys. **121**(3), 351–399 (1989)

2. Ooguri, H., Vafa, C.: Knot invariants and topological strings. *Nucl. Phys. B* **577**, 419–438 (2000). [arXiv:hep-th/9912123](#)
3. Ekholm, T., Shende, V.: Skeins on branes. [arXiv:1901.08027](#)
4. Ekholm, T., Shende, V.: Colored HOMFLYPT counts holomorphic curves. [arXiv:2101.00619](#)
5. Khovanov, M.: A categorification of the Jones polynomial. *Duke Math. J.* **101**, 359–426 (2000). [arXiv:math/9908171](#)
6. Gukov, S., Schwarz, A., Vafa, C.: Khovanov–Rozansky homology and topological strings. *Lett. Math. Phys.* **74**, 53–74 (2005). [arXiv:hep-th/0412243](#)
7. Gukov, S., Stosic, M.: Homological algebra of knots and BPS states. *Geom. Topol. Monogr.* **18**, 309–367 (2012). [arXiv:1112.0030](#)
8. Ekholm, T., Kucharski, P., Longhi, P.: Physics and geometry of knots-quivers correspondence. *Commun. Math. Phys.* **379**(2), 361–415 (2020). [arXiv:1811.03110](#)
9. Ekholm, T., Kucharski, P., Longhi, P.: Multi-cover skeins, quivers, and 3d $\mathcal{N} = 2$ dualities. *JHEP* **02**, 018 (2020). [arXiv:1910.06193](#)
10. Kucharski, P., Reineke, M., Stosic, M., Sulkowski, P.: BPS states, knots and quivers. *Phys. Rev. D* **96**(12), 121902 (2017). [arXiv:1707.02991](#)
11. Kucharski, P., Reineke, M., Stosic, M., Sulkowski, P.: Knots-quivers correspondence. *Adv. Theor. Math. Phys.* **23**(7), 1849–1902 (2019). [arXiv:1707.04017](#)
12. Kontsevich, M., Soibelman, Y.: Stability structures, motivic Donaldson–Thomas invariants and cluster transformations. [arXiv:0811.2435](#)
13. Efimov, A.: Cohomological Hall algebra of a symmetric quiver. *Compos. Math.* **148**(4), 1133–1146 (2012). [arXiv:1103.2736](#)
14. Ekholm, T., Ng, L.: Higher genus knot contact homology and recursion for colored HOMFLY-PT polynomials. *Adv. Theor. Math. Phys.* **24**(8), 2067–2145 (2020). [arXiv:1803.04011](#)
15. Dunfield, N.M., Gukov, S., Rasmussen, J.: The superpolynomial for knot homologies. *Exp. Math.* **15**(2), 129–159 (2006). [arXiv:math/0505662](#)
16. Freyd, P., Yetter, D., Hoste, J., Lickorish, W.B.R., Millett, K., Ocneanu, A.: A new polynomial invariant of knots and links. *Bull. Am. Math. Soc. (N.S.)* **12**(2), 239–246 (1985)
17. Przytycki, J., Traczyk, P.: Invariants of links of Conway type. *Kobe J. Math.* **4**, 115–139 (1987)
18. Jones, V.: A polynomial invariant for knots via von Neumann algebras. *Bull. Am. Math. Soc.* **12**, 103–111 (1985)
19. Reshetikhin, N., Turaev, V.G.: Ribbon graphs and their invariants derived from quantum groups. *Commun. Math. Phys.* **127**(1), 1–26 (1990)
20. Khovanov, M., Rozansky, L.: Matrix factorizations and link homology. *Fund. Math.* **199**, 1–91 (2008). [arXiv:math/0401268](#)
21. Khovanov, M., Rozansky, L.: Matrix factorizations and link homology II. *Geom. Topol.* **12**, 1387–1425 (2008). [arXiv:math/0505056](#)
22. Cautis, S.: Remarks on coloured triply graded link invariants. *Algebraic Geom. Topol.* **17**(6), 3811–3836 (2017). [arXiv:1611.09924](#)
23. Robert, L.-H., Wagner, E.: A closed formula for the evaluation of \mathfrak{sl}_n -foams. *Quantum Topol.* **11**(3), 411–487 (2020). [arXiv:1702.04140](#)
24. Ehrig, M., Tubbenhauer, D., Wedrich, P.: Functoriality of colored link homologies. *Proc. Lond. Math. Soc.* **117**(5), 996–1040 (2018). [arXiv:1703.06691](#)
25. Queffelec, H., Rose, D. E. V., Sartori, A.: Annular evaluation and link homology. [arXiv:1802.04131](#)
26. Gorsky, E., Wedrich, P.: Evaluations of annular Khovanov–Rozansky homology. [arXiv:1904.04481](#)
27. Oblomkov, A., Rozansky, L.: Soergel bimodules and matrix factorizations. [arXiv:2010.14546](#)
28. Gorsky, E., Hogancamp, M., Mellit, A.: Tautological classes and symmetry in Khovanov–Rozansky homology. [arXiv:2103.01212](#)
29. Kirillov, A.: Quiver representations and quiver varieties. In: *Graduate Studies in Mathematics*. American Mathematical Society (2016)
30. Kontsevich, M., Soibelman, Y.: Cohomological Hall algebra, exponential Hodge structures and motivic Donaldson–Thomas invariants. *Commun. Num. Theor. Phys.* **5**, 231–352 (2011). [arXiv:1006.2706](#)
31. Meinhardt, S., Reineke, M.: Donaldson–Thomas invariants versus intersection cohomology of quiver moduli. [arXiv:1411.4062](#)
32. Franzen, H., Reineke, M.: Semi-stable Chow–Hall algebras of quivers and quantized Donaldson–Thomas invariants. [arXiv:1512.03748](#)
33. Stosic, M., Wedrich, P.: Rational links and DT invariants of quivers. [arXiv:1711.03333](#)

34. Stosic, M., Wedrich, P.: Tangle addition and the knots-quivers correspondence. *J. Lond. Math. Soc.* (2021). <https://doi.org/10.1112/jlms.12433>. [arXiv:2004.10837](https://arxiv.org/abs/2004.10837)
35. Dimofte, T., Gukov, S., Hollands, L.: Vortex counting and Lagrangian 3-manifolds. *Lett. Math. Phys.* **98**, 225–287 (2011). [arXiv:1006.0977](https://arxiv.org/abs/1006.0977)
36. Gopakumar, R., Vafa, C.: M-theory and topological strings—I. [arXiv:hep-th/9809187](https://arxiv.org/abs/hep-th/9809187)
37. Gopakumar, R., Vafa, C.: M-theory and topological strings—II. [arXiv:hep-th/9812127](https://arxiv.org/abs/hep-th/9812127)
38. Nekrasov, N.A.: Seiberg–Witten prepotential from instanton counting. *Adv. Theor. Math. Phys.* **7**(5), 831–864 (2003). [arXiv:hep-th/0206161](https://arxiv.org/abs/hep-th/0206161)
39. Nekrasov, N., Okounkov, A.: Seiberg–Witten theory and random partitions. In: *The Unity of Mathematics*, vol. 244, pp. 525–596. Birkhäuser, Boston (2006). [arXiv:hep-th/0306238](https://arxiv.org/abs/hep-th/0306238)
40. Witten, E.: Topological quantum field theory. *Commun. Math. Phys.* **117**(3), 353–386 (1988)
41. Aganagic, M., Shakhov, S.: Knot homology and refined Chern–Simons index. *Commun. Math. Phys.* **333**(1), 187–228 (2015). [arXiv:1105.5117](https://arxiv.org/abs/1105.5117)
42. Witten, E.: Supersymmetry and Morse theory. *J. Differ. Geom.* **17**(4), 661–692 (1982)
43. Dimofte, T., Gaiotto, D., Gukov, S.: Gauge theories labelled by three-manifolds. *Commun. Math. Phys.* **325**, 367–419 (2014). [arXiv:1108.4389](https://arxiv.org/abs/1108.4389)
44. Terashima, Y., Yamazaki, M.: $SL(2, \mathbb{R})$ Chern-Simons, Liouville, and gauge theory on duality walls. *JHEP* **08**, 135 (2011). [arXiv:1103.5748](https://arxiv.org/abs/1103.5748)
45. Fuji, H., Gukov, S., Sulkowski, P.: Super-A-polynomial for knots and BPS states. *Nucl. Phys. B* **867**, 506–546 (2013). [arXiv:1205.1515](https://arxiv.org/abs/1205.1515)
46. Aharony, O., Hanany, A., Intriligator, K.A., Seiberg, N., Strassler, M.J.: Aspects of $N = 2$ supersymmetric gauge theories in three dimensions. *Nucl. Phys. B* **499**, 67–99 (1997). [arXiv:hep-th/9703110](https://arxiv.org/abs/hep-th/9703110)
47. Eliashberg, Y., Givental, A., Hofer, H.: Introduction to symplectic field theory. In: *Visions in Mathematics*, vol. Special Volume, Part II, pp. 560–673. Birkhäuser, Basel (2000)
48. Strominger, A.: Open p-branes. *Phys. Lett. B* **383**, 44–47 (1996). [arXiv:hep-th/9512059](https://arxiv.org/abs/hep-th/9512059)
49. Witten, E.: Chern-Simons gauge theory as a string theory. *Prog. Math.* **133**, 637–678 (1995). [arXiv:hep-th/9207094](https://arxiv.org/abs/hep-th/9207094)
50. Gaiotto, D., Moore, G.W., Neitzke, A.: Framed BPS States. *Adv. Theor. Math. Phys.* **17**(2), 241–397 (2013). [arXiv:1006.0146](https://arxiv.org/abs/1006.0146)
51. Jankowski, J., Kucharski, P., Larraguivel, H., Noshchenko, D., Sulkowski, P.: Permutohedra for knots and quivers. *Phys. Rev. D* **104**(8), 086017 (2021). [arXiv:2105.11806](https://arxiv.org/abs/2105.11806)
52. Kac, V., Cheung, P.: *Quantum Calculus*. Springer Science & Business Media, Berlin (2001)
53. Gorsky, E., Gukov, S., Stosic, M.: Quadruply-graded colored homology of knots. [arXiv:1304.3481](https://arxiv.org/abs/1304.3481)
54. Stosic, M.: Private communication (2021)

Publisher's Note Springer Nature remains neutral with regard to jurisdictional claims in published maps and institutional affiliations.